

Supporting Information

Biocatalytic Access to Piperazines from Diamines and Dicarboxylic Acids

Niels Borlinghaus, Sebastian Gergel and Bettina M. Nestl*

Institute of Biochemistry and Technical Biochemistry, Chair of Technical Biochemistry,
Universitaet Stuttgart, Allmandring 31, 70569 Stuttgart, Germany.

*Corresponding author: bettina.nestl@itb.uni-stuttgart.de

Content

1	Materials and methods	S2
2	Supporting figures and tables.....	S4
	Figure S1: Postulated reaction pathways for the formation of piperazines	S4
	Figure S2: Identification of an enamine tautomer.....	S5
	Figure S3: NADPH-depletion assay for activity testing.	S5
	Figure S4/Table S1: Analysis of the selectivity in the formation of 2,5-dimethylpiperazine	S6
	Figure S5: pH profile of <i>R</i> -IRED- <i>Ms</i> for the formation of piperazine	S7
3	General procedures	S8
4	GC chromatograms	S10
5	HPLC chromatograms	S55
6	Chemical syntheses	S56
7	NMR analysis of acetylated and extracted products from up-scaled biotransformationsS.....	S58
8	NMR spectra.....	S59
9	References	S70

1 Materials and methods

(A) Chemicals: Except otherwise noted, all solvents, buffer components and chemicals were obtained from Sigma-Aldrich and Fluka (Steinheim, Germany), Carl Roth GmbH (Karlsruhe, Germany), Acros Organics (Geel, Belgium), VWR (Darmstadt, Germany), abcr GmbH (Karlsruhe, Germany) and Alfa Aesar (Karlsruhe, Germany). NADPH was obtained from Prozomix (Haltwhistle, UK).

(B) Enzymes: Glucose-6-phosphate dehydrogenase from *Leuconostoc mesenteroides* and DNase I from bovine pancreas were purchased from Alfa Aesar (Karlsruhe, Germany) and Sigma-Aldrich (Steinheim, Germany), respectively.

(C) DNA-Sequences:

R-IRED_{Ms-his₆}

```
ATGGGCAGCA GCCATCATCA TCATCATCAC AGCAGCGGCC TGGTGCCGCG CGGCAGCCAT ATGAAACCGA
CCCTGACCGT TATTGGCGCT GGCCGTATGG GCTCCGCACT GATTAAAGCA TTCCTGCAAT CTGGCTACAC
GACCACGGTG TGGAAACCGTA CCAAAGCCAA AAGCGAACCG CTGGCAAAAC TGGGCGCACA TCTGGCTGAT
ACGGTGCGTG ACGCCGTTAA ACGCAGCGAT ATTATCGTGG TTAATGTGCT GGATTATGAC ACCTCTGATC
AGCTCTGCG CCAAGACGAA GTGACGCGTG AACTGCGCGG CAAACTGCTG GTTCAGCTGA CCAGCGGTTT
TCCGCGACTG GCTCGTGAAC AGGAAACGTG GGC GCGCCAA CATGGCATTG ATTATCTGGA CGGTGCGATC
ATGGCCACCC CGGATTTTAT TGGCCAGGCA GAATGCGCTC TGCTGTACAG TGGTTCCGCG GCCCTGTTTC
AAAAACACCG TGCTGTCCTG AATGTGCTGG GCGGTGCCAC CAGCCATGTC GGCGAAGATG TTGGTCATGC
CTCAGCACTG GACAGCGCCC TGCTGTTTCA GATGTGGGGC ACCCTGTTTC GTACGCTGCA AGCACTGGCT
ATTTCTCGCG CAGAAGGCAT CCCGCTGGAA AAAACACCG CGTTTATCAA ACTGACCGAA CCGGTCAACC
AGGTGCGCTG TGCAGATGTC CTGACCCGTG TTCAGCAAAA TCGCCTGACC GCAGACGCTC AGACGCTGGC
AAGTCTGGAA GCTCATAACG TGGCGTTCCA ACACCTGCTG GCCCTGTGTG AAGAACGTAA TATCCATCGC
GGTGTGCGG ATGCCATGTA CTCGCTTATT CGTGAAGCGG TCAAAGCCGG CCACGGTAA GATGACTTTG
CAATTCTGAC CCGCTTCCTG AAATAA
```

R-IRED_{Sr-his₆}

```
ATGGGCAGCA GCCATCATCA TCATCATCAC AGCAGCGGCC TGGTGCCGCG CGGCAGCCAT ATGCGTGATA
CCGATGTCAC CGTTCTGGGT CTGGGTCTGA TGGGTCAAGC ACTGGCTGGC GCGTTCCTGA AAGATGGTCA
TGCGACGACC GTCTGGAACC GTTCAGAAGG CAAAGCCGGT CAGCTGGCAG AACAAGGCGC TGTGCTGGCG
AGCTCTGCCC GCGATGCCGC GGAAGCCAGC CCGCTGGTTG TGGTCTGCGT GTCCGACCAT GCAGCTGTTT
GTGCGGTTCT GGATCCGCTG GGTGATGTTT TGGCAGGTCG TGTCTGGTG AATCTGACCA GCGGCACGTC
TGAACAGGCA CGTGCTACCG CCGAATGGGC CGCAGAACGT GGTATTACGT ATCTGGATGG TGCAATTATG
GCTATCCCGC AGGTGGTTTG CACCGCCGAC GCATTTCTGC TGTATTACAG TCCGGAAGCA GCTTACGAAG
CCCATGAACC GACCTGCGT AGCCTGGGTG CAGGTACCAC CTATCTGGGT GCAGATCAGC GTCTGAGTTT
CCTGTACGAC GTTGCGCTGC TGGGCATTAT GTGGGGTACC CTGAACTCCT TTCTGCATGG TGCCGCACTG
CTGGGTACCG CTAAAGTGGA AGCGACCACG TTTGCGCCGT TCGCCAATCG CTGGATCGAA GCCGTCACCG
GCTTCGTGAG CGCTTATGCG GGCCAGGTTG ATCAAGGTGC ATACCCGGCT CTGGATGCGA CCATTGACAC
GCAGCTGGCG ACCGTTGATC ATCTGATCCA CGAATCTGAA GCAGCTGGCG TTAACACCGA ACTGCCGCGT
CTGGTTTCGA CCCTGGCAGA TCGTGCACTG GCAGGCGGTC AGGGCGGTCT GGGTTATGCC GCAATGATCG
AACAAATCCG CTCACCGTCG GCGTAA
```

S-IRED_{Pe-his₆}

```
ATGGGCAGCA GCCATCATCA TCATCATCAC AGCAGCGGCC TGGTGCCGCG CGGCAGCCAT ATGAACTCCA
GCAATCCGAA AGACAACATC TCAGTGGGCT CCGCAAGCAC CGCAACCAAT CGCAAAAGCG TCACCGTTAT
GGGCTGGGC CCGATGGGTC AGGCAATGGC TGGCGTGTTT CTGGAAAGCG GTTATGAAGT GACCGTTTGG
AACCGTACCG CATCTAAAGC TGATGAACTG GTCGCGAAAG GCGCCATTCT CGCAAGTACC GTGGACGAAG
CACTGGCGCG CAATGAACTG GTTATTCTGT CCTGACGGA TTATGACGCT ATGTACGCGA TCCTGGAACC
GAGCTCTGCG AACCTGAGCG GCAAAGTCTT GGTGAATCTG AGTTCCGATA CCCCAGAAAA AGTCCGTGAA
GCAGCTAAAT GGCTGGCGGA CCGTGGTGCA CGTCATGTGA CCGGCGGTGT TCAAGTCCCG CCGTCAGGCA
TTGGTAAACC GGAATCATAT ACGTATTACT CCGGCCCGCG TGAAGTTTTT GAAGCCCACC GCGAATCGCT
GGAATCCTG ACCGGTACGG ATTACCGCGG CGAAGACCCG GGCTCTGGCA TGCTGTACTA CCAGATCCAA
ATGGATATCT TTTGGACCA CATGCTGTCT TATCTGCATG CGCTGGCCGT GGCAAAAGCT AACGGCATTG
CCGCCAAACA GTTCTGCGG TATGCGAGCG CCACGCTGTC ATCGCTGCCG CAATTTGTTG AATTCTACAC
CCCGCGTCTG GATGAAGGCA AACACCCGGG TGATGTGAC CGCCTGGCTA TGGGCTGGC GTCTGTGGAA
CATATTGTTT ACACCACGGA AGATGCCGGT ATTGACACCA CCCTGCCGGC CGCAGTTCTG GAAATCTTTA
AACGTGGTAT GGAAAACGGC CATGCCGGTG ATAGTTTTAC CAGCTGATT GAAATCTTCA AAAATCCGGT
GCGCAGCTAA
```

(D) GC analysis: Gas chromatography analysis for the quantification of product formations was conducted on a Shimadzu GC-2010 instrument equipped with a flame ionization detector using an Agilent HP-1ms UI column (30 m × 250 µm × 0.25 µm) with hydrogen as carrier gas (30 cm s⁻¹). Injector temperature: 250°C. Split mode with a split ratio of 5. Detector temperature: 330°C. Three different oven temperature programmes were used depending on the analyte.

<u>Program A for compounds 1a, 1b, 1c, 1e, 1g, 1i, 1j, 2a, 2b, 4a</u>			<u>Program B for compounds 3a and 3c</u>			<u>Program C for compound 1d</u>		
rate °C min ⁻¹	final temp. °C	hold min	rate °C min ⁻¹	final temp. °C	hold min	rate °C min ⁻¹	final temp. °C	hold min
-	100	1	-	100	1	-	50	2
40	150	-	40	260	-	20	90	-
2,5	170	-	4	290	-	50	320	2
20	200	-	50	320	2			
50	260	2						

(E) Chiral GC analysis: Chiral gas chromatography analysis was performed on a Shimadzu GC-2010 instrument equipped with a flame ionization detector using an Agilent Chirasil Dex-CB column (30 m × 250 µm × 0.25 µm) with hydrogen as carrier gas (30 cm s⁻¹). Injector temperature: 225°C. Split mode with a split ratio of 10 or 40. Detector temperature: 230°C.

(F) GC-MS analysis: Gas chromatography-mass spectrometry was carried out on an Agilent GC 7890A instrument coupled with an Agilent 5975 Series mass selective detector (MSD) and an additional flame ionization detector. An Agilent DB-5 column (30 m × 250 µm × 0.25 µm) was operated with hydrogen as carrier gas (30 cm s⁻¹). Injector temperature: 250°C. Split mode with a split ratio of 5. Detector temperature: 320°C. Electron ionization of the analyte with 70 eV acceleration voltage.

<u>Program D for all compounds</u>			<u>Program E for compounds 1d-5d</u>		
rate °C min ⁻¹	final temp. °C	hold min	rate °C min ⁻¹	finale temp. °C	hold min
-	100	1	-	50	2
25	310	2.5	20	150	-
			50	310	2,5

(G) Chiral HPLC analysis: Chiral high-performance liquid chromatography was conducted on an Agilent 1200 Series system with autosampler using a Daicel Chiralpak IB column (150 × 4.6 mm, 5 µm) or a Daicel Chiralpak IC column (250 × 4.6 mm, 5 µm) at a temperature of 20°C. Analytes were detected by using a diode array detector (DAD) at a wavelength of 261 nm. A binary solvent mixture of cyclohexane and ethanol (0.2% v/v diethylamine added) in a ratio of 75/25 was used for the isocratic separation within 25 min with a flow rate of (0.7 mL/min).¹

(H) NMR spectroscopy: ¹H and ¹³C NMR spectra were recorded on a Bruker Avance spectrometer working at a frequency of 500 MHz (protons) using CDCl₃, D₂O or DMSO-d₆ as solvents. Chemical shifts (δ) are given in ppm referenced to tetramethylsilane. Coupling constants (Hz) and signal multiplicity (s = singlet, d = doublet, dd = doublet of doublets, t = triplet, m = multiplet) are as well noted in the conventional form.

2 Supporting figures and tables

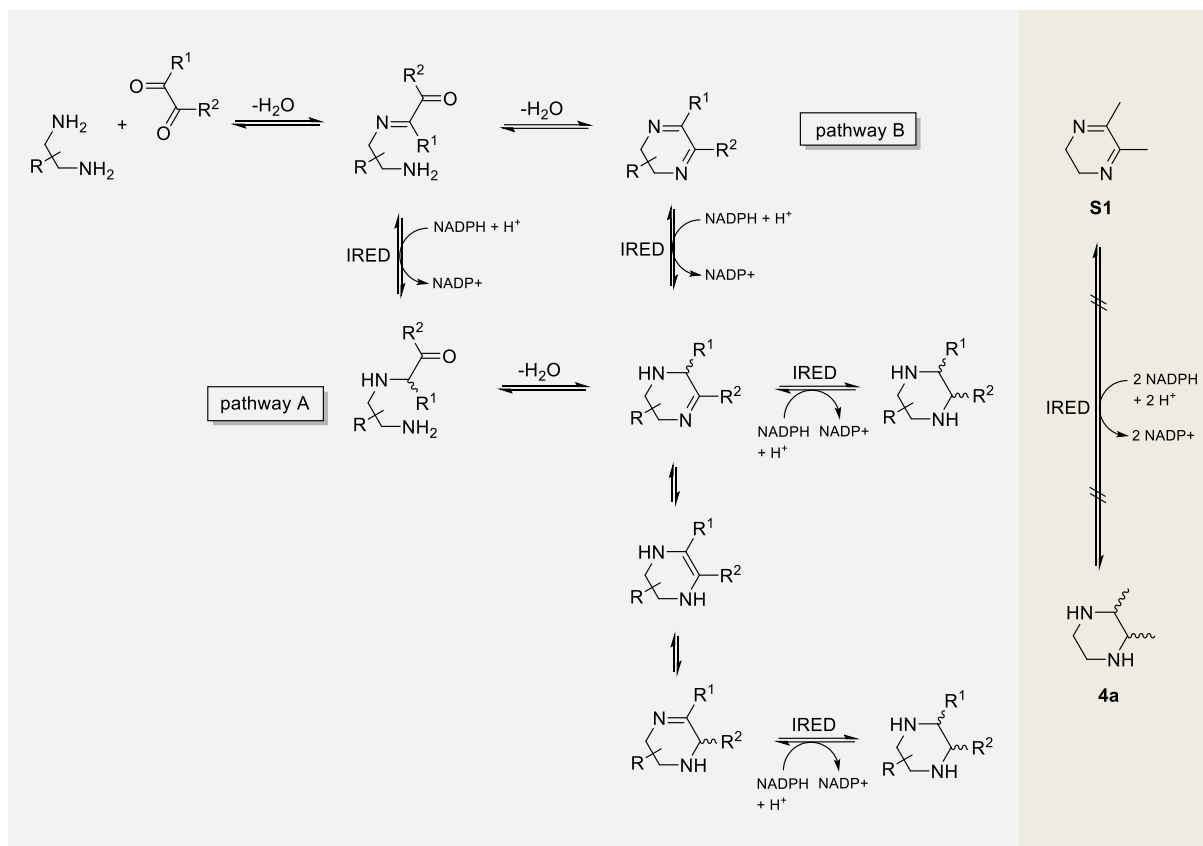


Figure S1: Postulated reaction pathways for the formation of piperazines (left, grey background). In pathway A, IRED reduces the first imine intermediate from the reaction of the diamine and dicarbonyl prior to cyclization and further reduction to the piperazine. In pathway B, IRED reduces the 2,3-dihydropyrazine diamine reaction intermediate over two steps to the final piperazine product. No activity was observed when 5,6-dimethyl-2,3-dihydropyrazine (**S1**) was used as substrate (right, light green background). This result indicates that the piperazine synthesis most likely occurs via pathway A.

Tautomerization of the partially reduced intermediate (equals intermediate **III**) may lead to the racemization of the already induced stereocenter. However, the final reduction step allows the control of at least one stereocenter. This hypothesis is underlined by finding enantiopure monosubstituted piperazines but both diastereomers for 2,3-disubstituted piperazines.

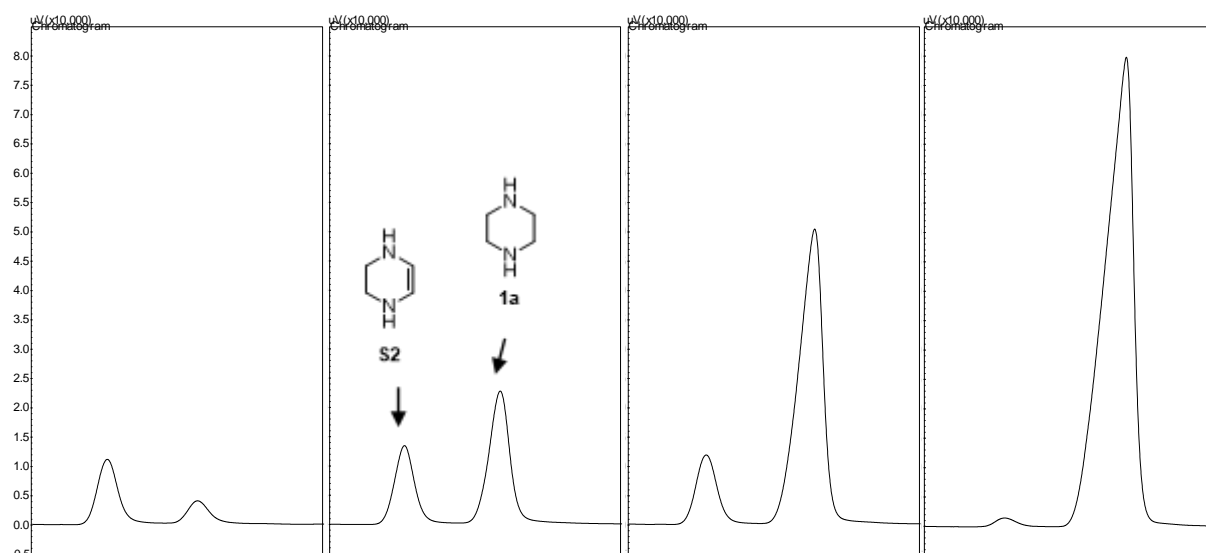


Figure S2: The composition of the reaction mixture over time showed that 1,2,3, 6-tetrahydropyrazine (equals intermediate **III**) is formed in the first couple of minutes during the biotransformation forming **1a** and is able to undergo tautomerization. The occurrence of the enamine tautomer 1,2,3,4-tetrahydropyrazine (**S2**) in its acetylated form was confirmed by GC-MS.

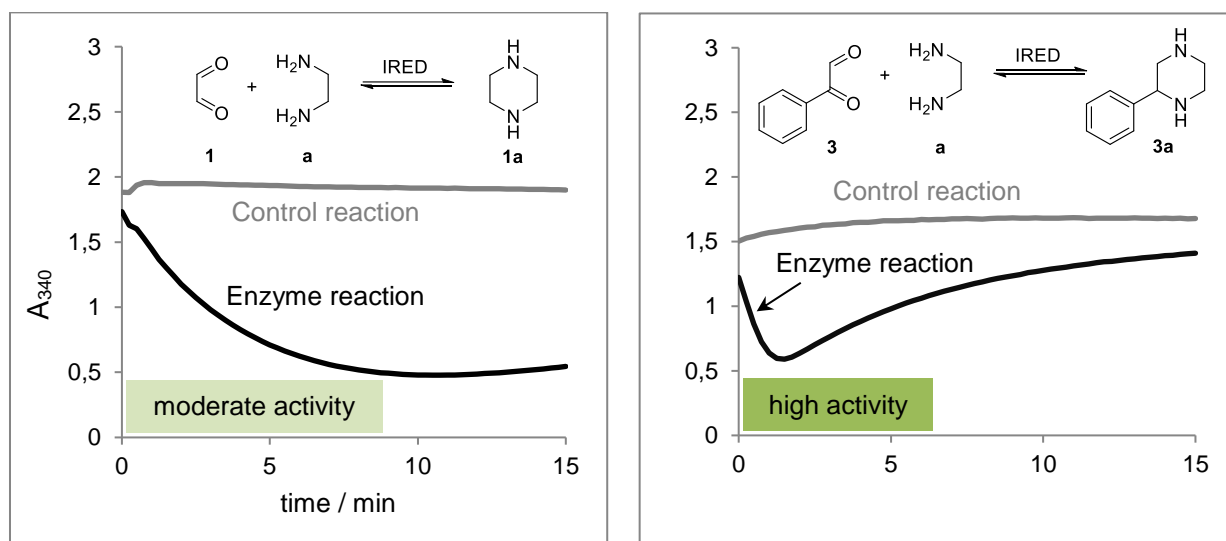
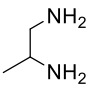
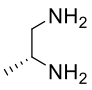
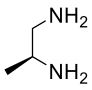
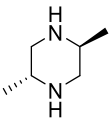
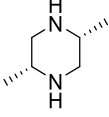
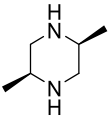


Figure S3: NADPH-depletion assay for activity testing.

Measured rates of piperazine formation of **1a** (left) and **3a** (right) using a NADPH depletion assay. The absorbance at 340 nm was measured for 15 minutes at room temperature. 10 μ M of purified enzyme was mixed with 5 mM diamine, 5 mM dicarbonyl and 0.5 mM NADPH. Both reactions show a clear decrease in absorbance due to NADPH consumption (black). In the formation of **1a** NADPH was completely consumed after 10 minutes (moderate activity). An even faster consumption of NADPH was observed in the formation of **3a** with no NADPH left after one minute reaction time (high activity). In contrast, the control reactions without enzyme (grey) show no decrease in absorbance. In the case of **3a**, an increase in absorbance could be monitored after NADPH was consumed. This might be due to the formation of condensation products including absorptive components.

Table S1: Analysis of the selectivity in the formation of 2,5-dimethylpiperazine (**2b**), using racemic or enantiopure 1,2-diaminopropane (**b**) and methylglyoxal (**2**).

	 <i>(rac)</i> - b	 <i>(R)</i> - b	 <i>(S)</i> - b
	product / %	product / %	product / %
 <i>(2R,5S)</i> - 2b	21 ± 1	2.6 ± 0.1	42 ± 1
 <i>(2R,5R)</i> - 2b	19 ± 1	36 ± 1	0
 <i>(2S,5S)</i> - 2b	0	0	0

R-IRED_*Ms* is highly selective for the formation of *R*-stereocenters, which is independent from other stereocenters. The utilization of enantiopure (*R*)-1,2-diaminopropane as well as (*S*)-1,2-diaminopropane resulted in the formation of (*2R,5R*)-dimethylpiperazine (87% ee) and (*2R,5S*)-dimethylpiperazine (> 99% ee), respectively. In consequence, a mixture of (*2R,5R*)-dimethylpiperazine and (*2R,5S*)-dimethylpiperazine was obtained when the racemic mixture was used. No (*2S,5S*)-dimethylpiperazine was formed, which confirmed the excellent enantioselectivity.

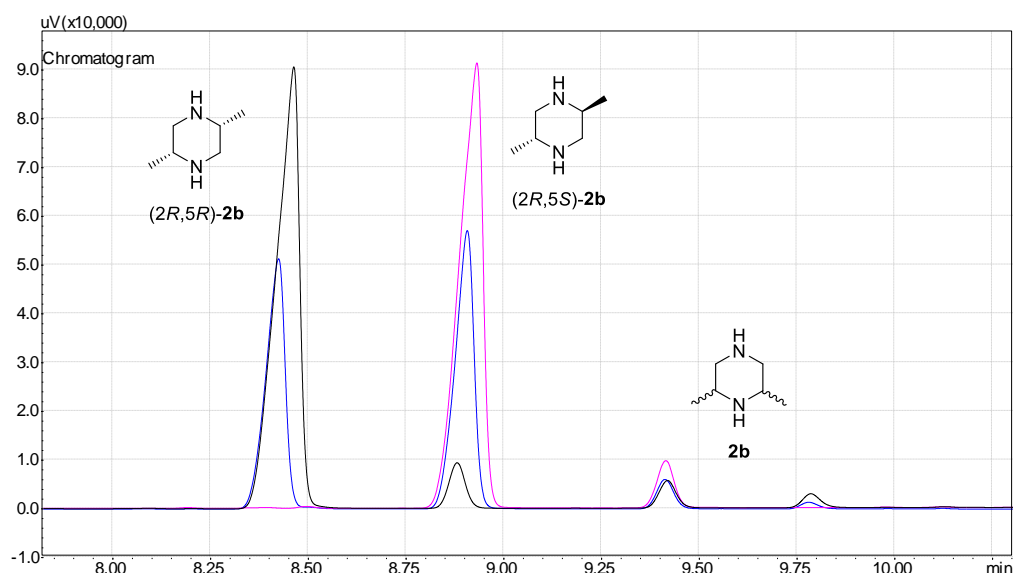


Figure S4: Products observed in the biotransformation of 1,2-diaminopropane (**b**) with methylglyoxal (**2**) to 2,5-dimethylpiperazine (**2b**). Main products (*2R,5R*)-dimethylpiperazine and (*2R,5S*)-dimethylpiperazine were formed with 2,6-dimethylpiperazine as a minor product. The following diamines were used in the shown scenarios: blue, (*rac*)-**b**; black, (*R*)-**b**; pink, (*S*)-**b**.

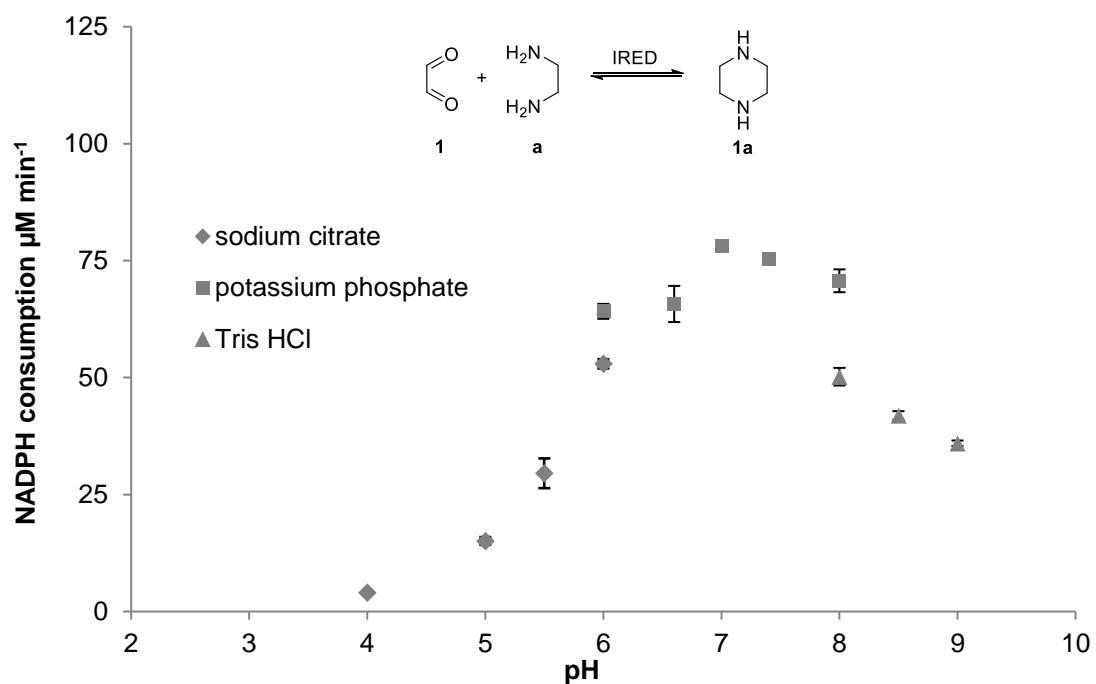


Figure S5: pH profile of *R*-IRED-*Ms* for the formation of **1a** in sodium citrate buffer (pH 4.0 - 6.0), potassium phosphate buffer (pH 6.0 - 8.0) and Tris HCl buffer (pH 8.0 - 9.0). Determined NADPH consumptions were measured in triplicates using 5 mM of glyoxale (**1**), 5 mM ethylenediamine (**a**), 5 μM *R*-IRED-*Ms* and 2.5 mM of NADPH. The error bars show the standard deviation.

3 General procedures

(A) Protein expression, and purification:

The gene of *R*-IRED_*Ms* was cloned into a pBAD33 plasmid and fused with an *N*-terminal his6-tag. For gene expression, *E. coli* JW5510 cells were transformed with the vector and grown over night at 37°C. Terrific broth (TB) culture medium containing 34 $\mu\text{g mL}^{-1}$ chloramphenicol was inoculated using 0.25% v/v of preculture. After 2-3 h of incubation at 37°C and reaching an optical density of $\text{OD}_{600} = 0.8\text{-}1.0$, the protein expression was induced with the addition of arabinose (final concentration 0.02%). The cultures were incubated for about 20 h at 25°C. After harvesting and lysing the cells, protein purification was performed with cobalt His-Trap columns (His-GraviTrap-TALON, GE Healthcare) using buffer A (50 mM potassium phosphate buffer pH 7.0, 300 mM KCl) for binding, buffer B (50 mM potassium phosphate buffer pH 7.0, 300 mM KCl, 5 mM imidazole) for washing and buffer C (50 mM potassium phosphate buffer pH 7.0, 300 mM KCl, 500 mM imidazole) for eluting the enzyme. After purification, the buffer was changed via dialysis (two times for 2 h in 5 L, 50 mM potassium phosphate buffer pH 7.0, MWCO = 6-8 kDa). Purity and size was verified by SDS-PAGE. The protein concentration was determined using the BCA Protein Assay Kit (Thermo Scientific).

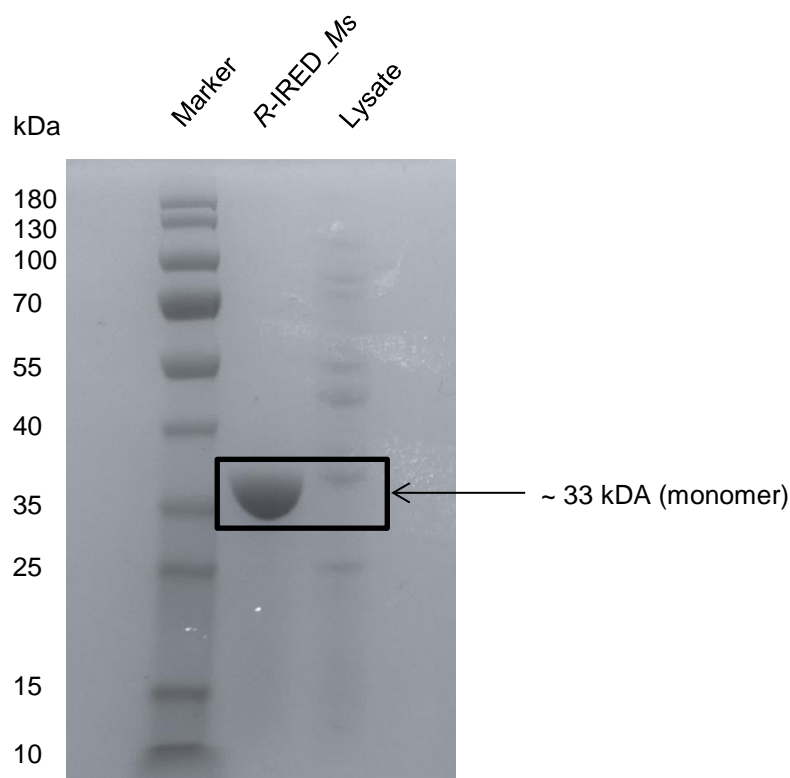


Figure S6: SDS-PAGE analysis of purified *R*-IRED_*Ms* compared to the lysate.

(B) Biotransformations:

Batch biotransformations:

Biotransformations were performed on a 350 μL scale in glass vials with 30 μM purified IRED (1 mg L^{-1} , protein purity > 90%), 5 mM diamine, 5 mM dicarbonyl, 2 mM NADPH, 2.5 mM MgCl_2 , 40 mM glucose-6-phosphate, 5 U mL^{-1} glucose-6-phosphate dehydrogenase, buffer system: 50 mM potassium

phosphate buffer pH 7.0. After 4 h incubation at 25°C an internal standard (10 µL, 5 mM final concentration) was added and the reaction was stopped with 10 M aqueous NaOH (35 µL).

Fed-batch biotransformations:

Biotransformations were performed on a 350 µL scale in glass vials with 30 µM purified IRED (1 mg L⁻¹, protein purity > 90%), 5 mM diamine, 6.25 mM dicarbonyl (continuous addition over 5 h with a syringe pump), 2 mM NADPH, 2.5 mM MgCl₂, 40 mM glucose-6-phosphate, 5 U mL⁻¹ glucose-6-phosphate dehydrogenase, buffer system: 50 mM potassium phosphate buffer pH 7.0. For the upscaling experiments, the substrate concentration was increased to 50 mM and the buffer strength was increased to 100 mM. After 6 h incubation at 25°C an internal standard (10 µL, 5 mM final concentration) was added and the reaction was stopped with 10 M aqueous NaOH (35 µL).

(C) Sample preparation and derivatization for (chiral) GC and GC-MS analysis:

The samples were extracted and derivatized simultaneously by adding 2.5 parts derivatization mix (250 µL, 0.6 M acetic anhydride in dichloromethane) on one part of sample (100 µL) and vortexing for 2 min. The organic phase was analyzed by gas chromatography.

Table S2: Added internal standards for the determination of product formations. The corresponding piperazine compounds and the applied temperature programs are assigned.

Analyte	Internal Standard	Temperature program
1a, 1b, 1g, 1i, 1j, 2a, 2b, 4a	1c	A
1d, 1e	1a	A
3c	3a	B
3a	3c	B
1d	1e	C

(D) Sample preparation and derivatization for chiral HPLC analysis:

Proteins and particles were removed from the sample through microfiltration. Then 0.1 parts of 10 M aqueous NaOH (10 µL) and 2 parts of derivatization mix (200 µL, 50 mM 1-fluoro-2,4-dinitrobenzene in dichloromethane) were added to the sample (100 µL) and the mixture was shaken for 20 h at room temperature. An excess amount of 1-fluoro-2,4-dinitrobenzene was quenched by the addition of 0.05 parts diethylamine (5 µL). The organic phase was washed with dH₂O (100 µL) and analyzed via chiral HPLC chromatography.

(E) Sample preparation for the determination of isolated yields

Fed-batch biotransformations were performed on a 1 mL scale using the substrates at a concentration of 50 mM as described in 3(B). The samples were extracted and derivatized simultaneously by adding 2.5 parts derivatization mix (2.5 mL, 0.6 M acetic anhydride in dichloromethane) on one part of sample and vortexing for 2 min. After separating the organic phase, the solvent was removed under reduced pressure. The residue was dissolved in 1 M aqueous NaOH (1 mL) and incubated at 37°C overnight. The solution was extracted with dichloromethane (3 x 4 mL) and the combined extracts were dried over MgSO₄. Finally, the solvent was removed and the isolated yield was determined gravimetrically.

4 GC chromatograms

(A) GC-MS analysis for product identification:

Table S3: Retention times (min) of detected piperazine products in their acetylated form using GC-MS with temperature program D.

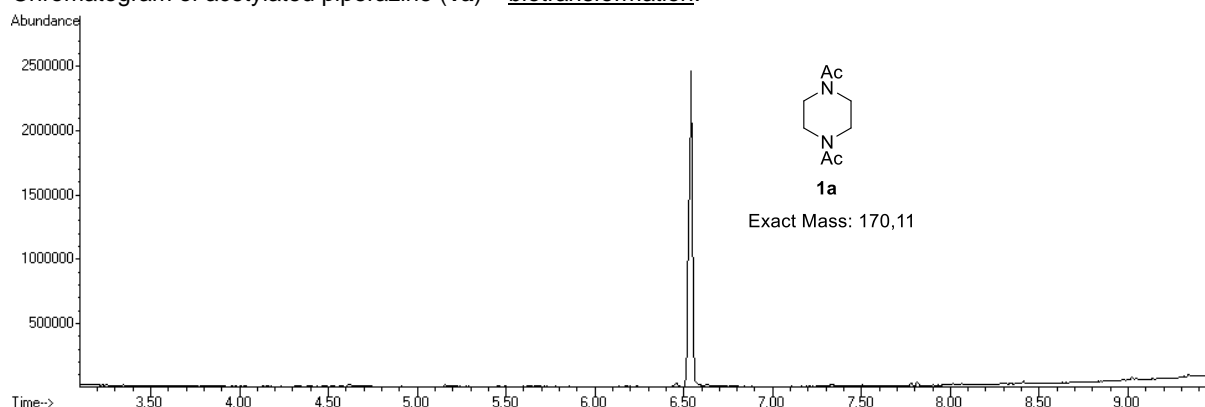
1a	6.55	1r	7.19	3c	7.19	4f	7.85, 7.97	5i	7.91
1b	6.63	2a	6.63	3d*	8.71	4g	6.51, 6.65, 6.90	6a	6.92, 7.10
1c	4.38	2b	6.53, 6.68	3e	7.45	4h	8.00	7a	7.17, 7.28
1d*	4.52	2c	4.57	3f**	5.33	4i	6.72	8a	7.32, 7.48
1e	4.88	2d*	5.23	3g	8.44, 8.66	5a	7.77, 8.17	9a	8.65, 8.78
1f	7.60	2e	5.00	3h	9.66	5b	7.87, 8.09	10a	8.61
1g	6.15	2f	7.62, 7.77	3i	8.84	5c	6.45, 6.47	11a	8.84
1h	7.77	2g	6.33	4a	6.66	5d	8.03, 8.06	12a**	9.16
1i	6.79	2h	7.91	4b	6.63, 6.79	5e	6.82	13a**	10.37
1j	5.31	2i	6.80	4c	4.98, 5.11	5f**	7.49		
1n	6.74	3a	8.73,	4d*	6.06	5g	7.77, 7.80		
1q	8.73	3b	8.58, 8.72, 8.83	4e	5.31, 5.52	5h**	6.22, 6.28, 6.48		

*temperature program E was used.

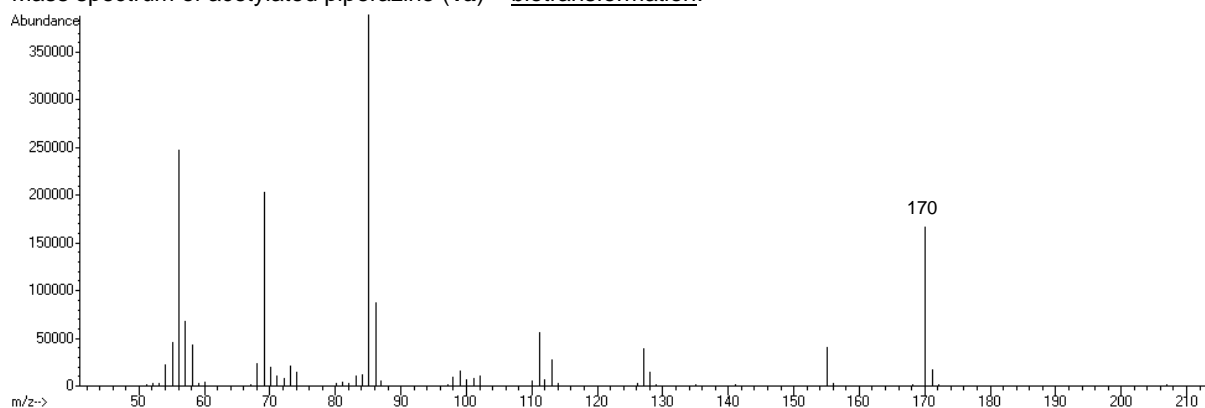
**derivatization was omitted

(B) Chromatograms and mass spectra for all piperazine products listed in table 3, compared to analytical standards.

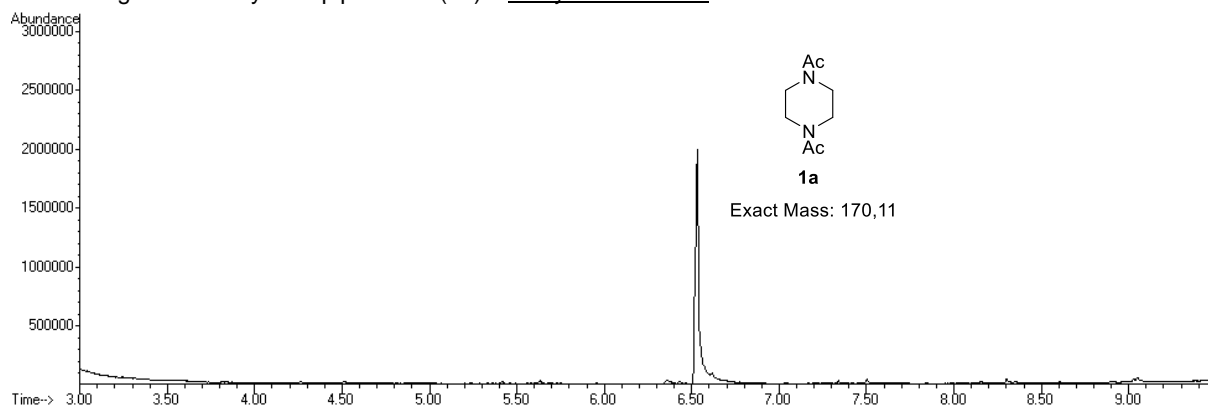
Chromatogram of acetylated piperazine (**1a**) – biotransformation:



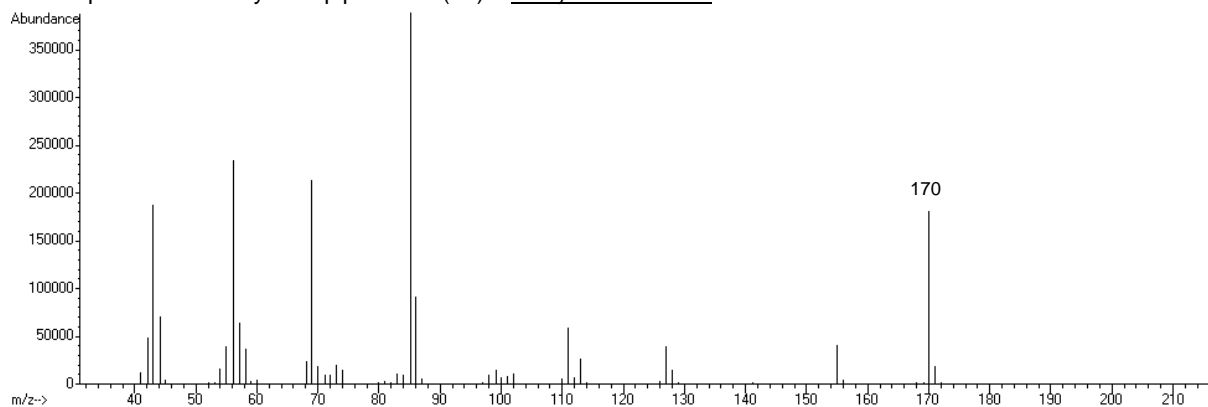
Mass spectrum of acetylated piperazine (**1a**) – biotransformation:



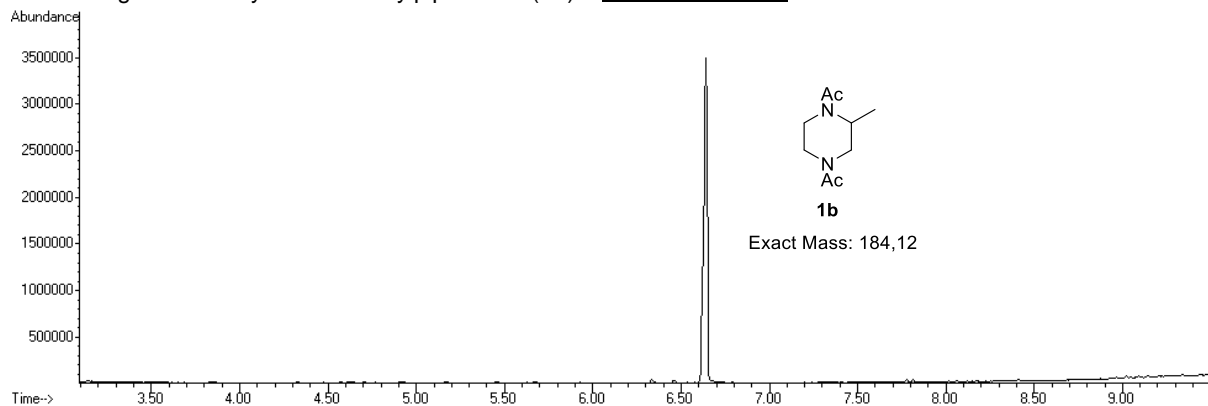
Chromatogram of acetylated piperazine (**1a**) – analytical standard:



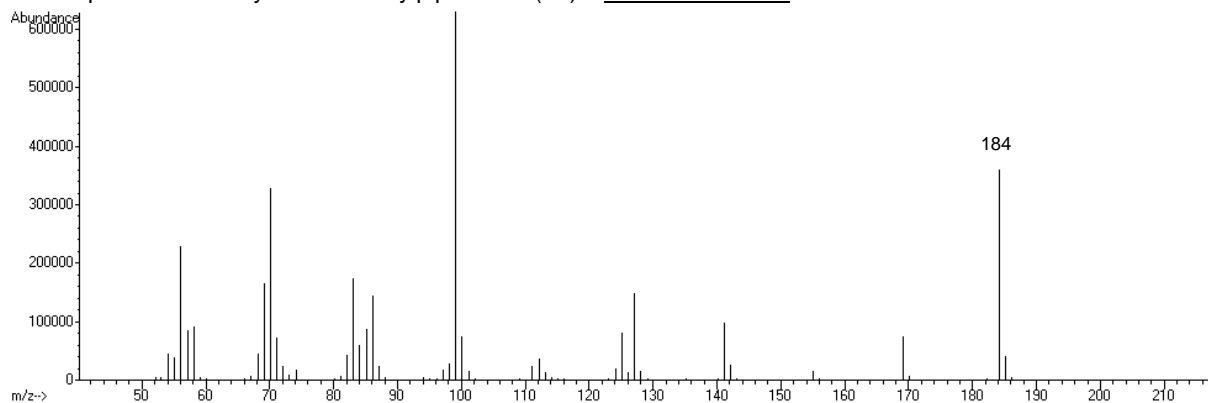
Mass spectrum of acetylated piperazine (**1a**) – analytical standard:



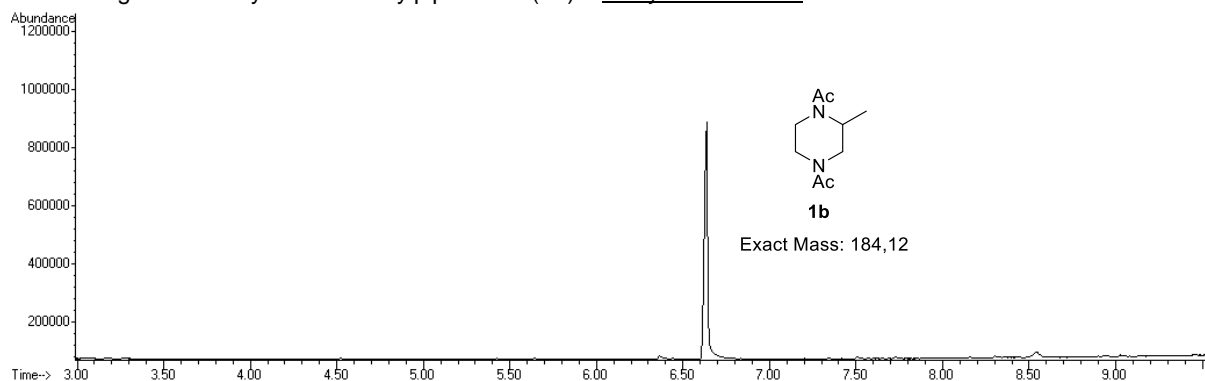
Chromatogram of acetylated 2-methylpiperazine (**1b**) – biotransformation:



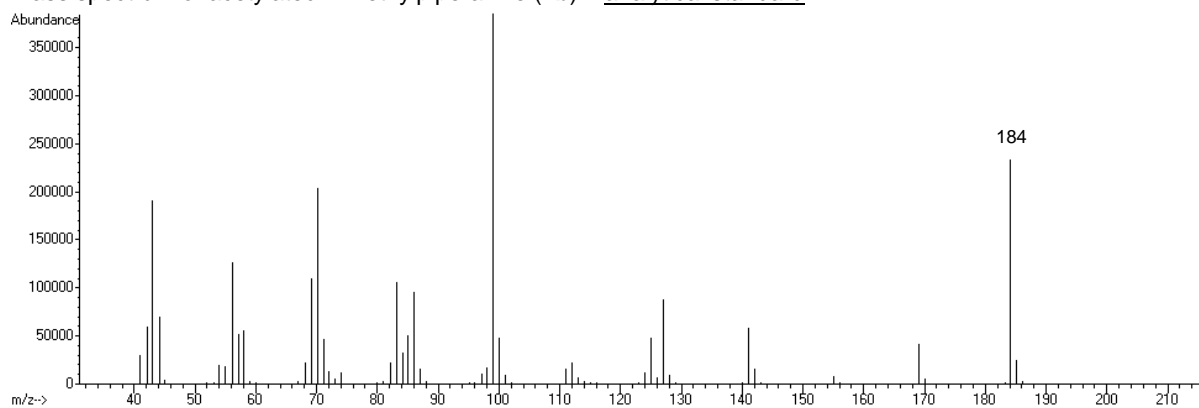
Mass spectrum of acetylated 2-methylpiperazine (**1b**) – biotransformation:



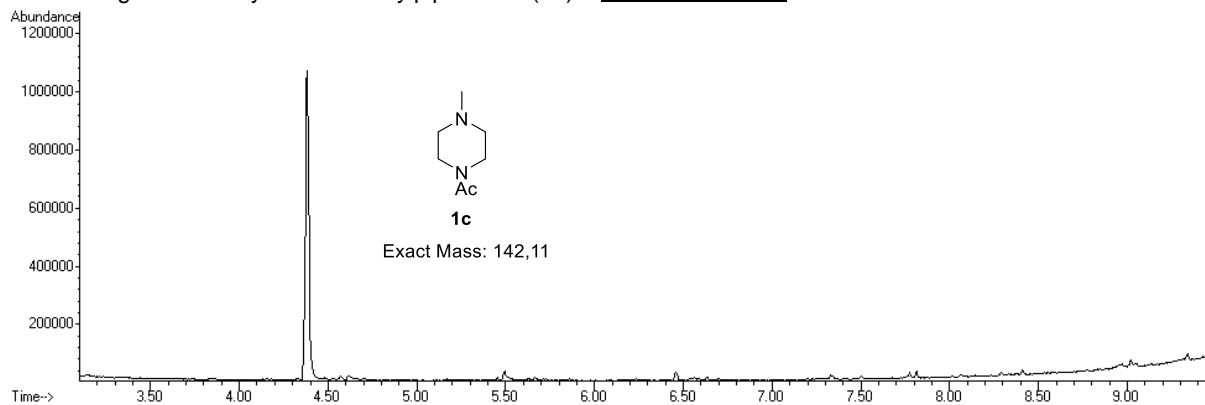
Chromatogram of acetylated 2-methylpiperazine (**1b**) – analytical standard:



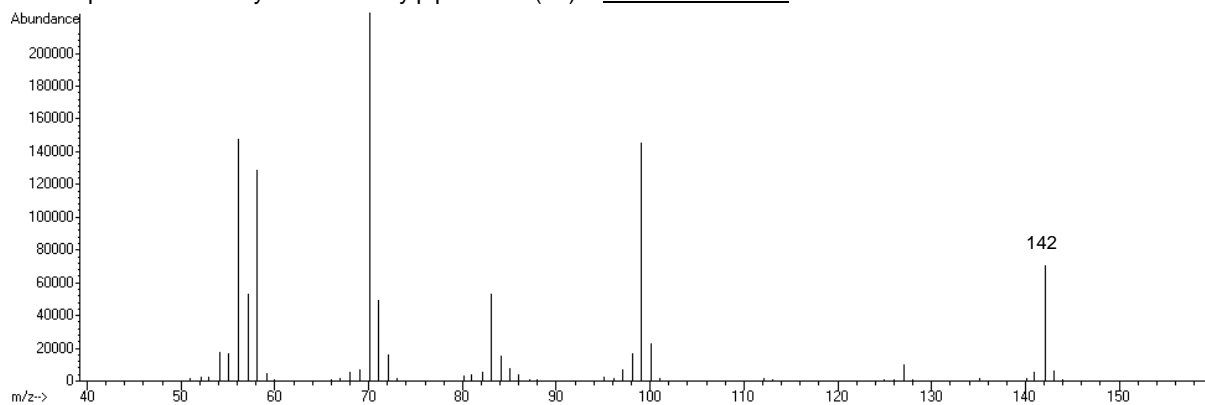
Mass spectrum of acetylated 2-methylpiperazine (**1b**) – analytical standard:



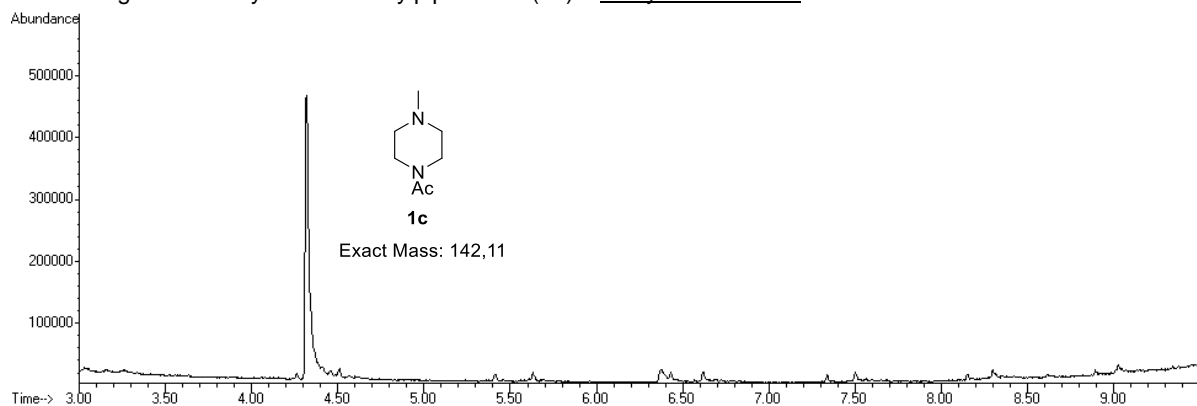
Chromatogram of acetylated 1-methylpiperazine (**1c**) – biotransformation:



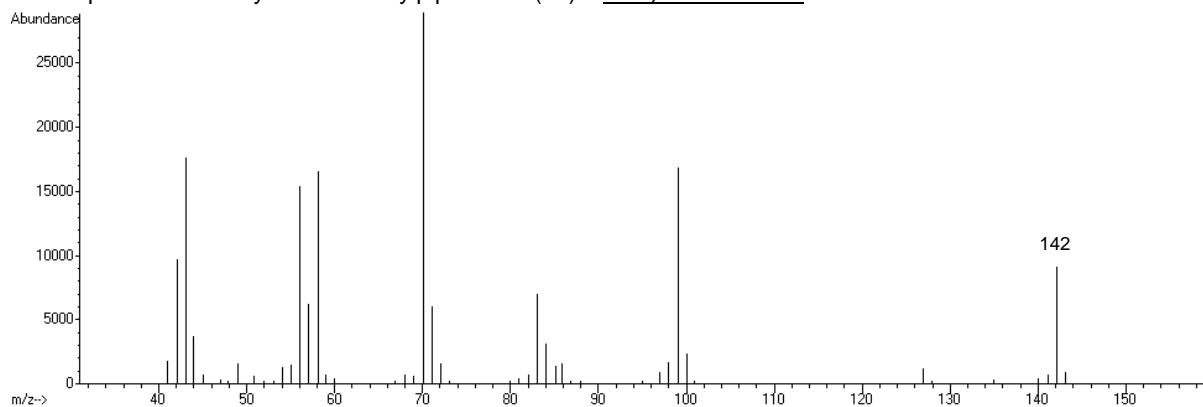
Mass spectrum of acetylated 1-methylpiperazine (**1c**) – biotransformation:



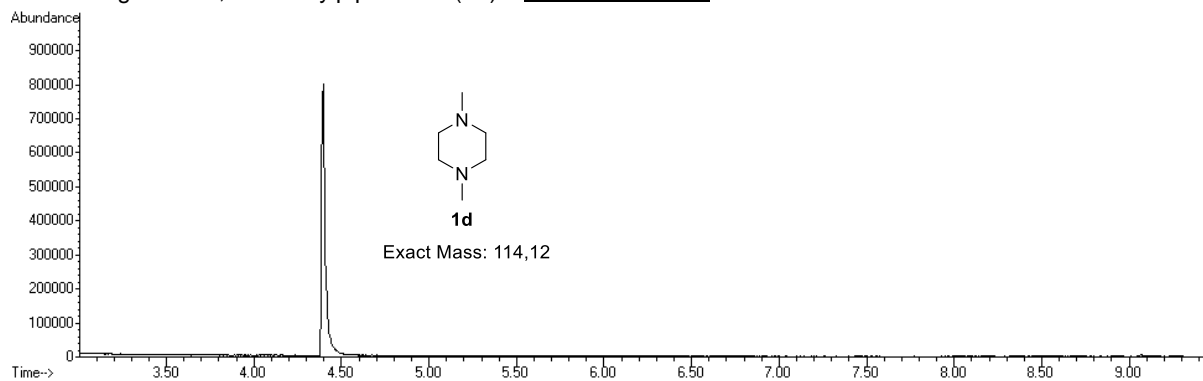
Chromatogram of acetylated 1-methylpiperazine (**1c**) – analytical standard:



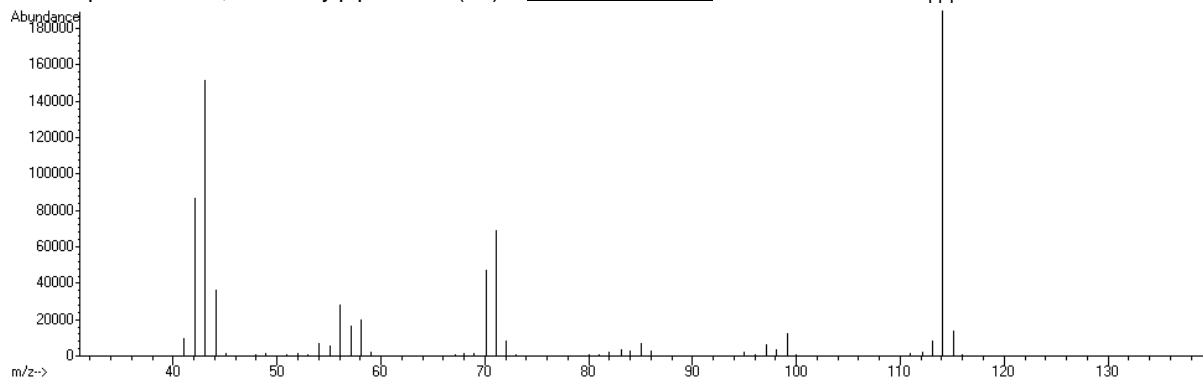
Mass spectrum of acetylated 1-methylpiperazine (**1c**) – analytical standard:



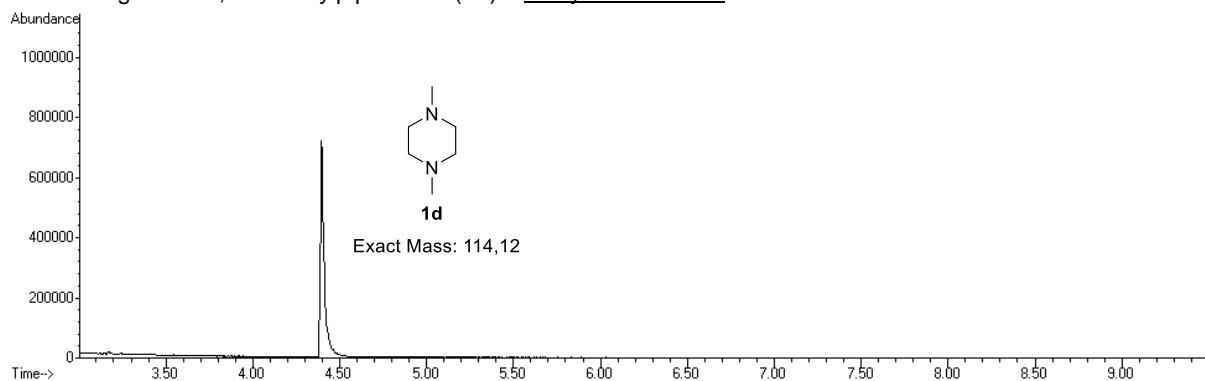
Chromatogram of 1,4-dimethylpiperazine (**1d**) – biotransformation:



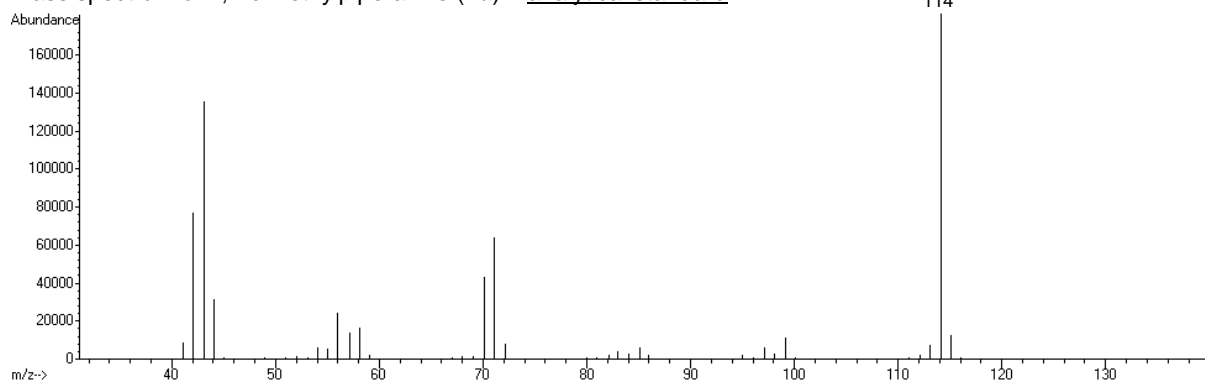
Mass spectrum of 1,4-dimethylpiperazine (**1d**) – biotransformation:



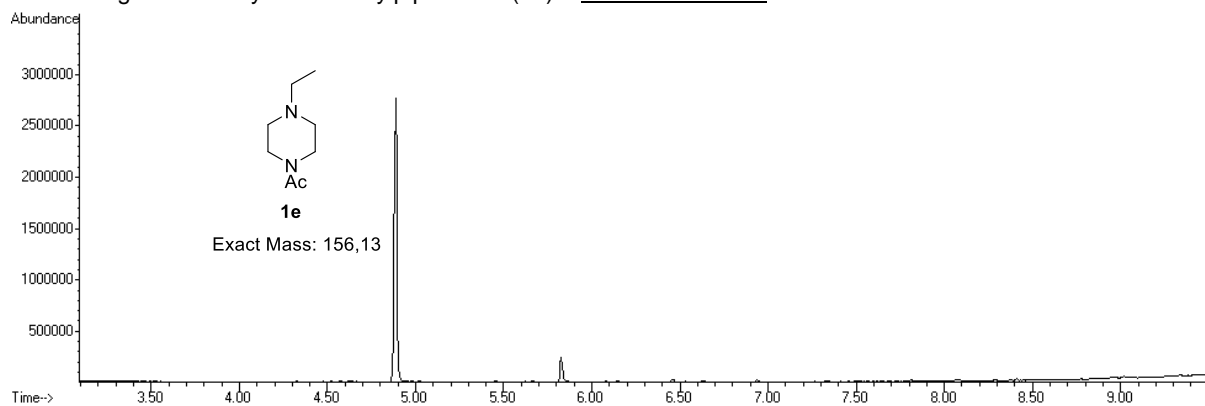
Chromatogram of 1,4-dimethylpiperazine (**1d**) – analytical standard:



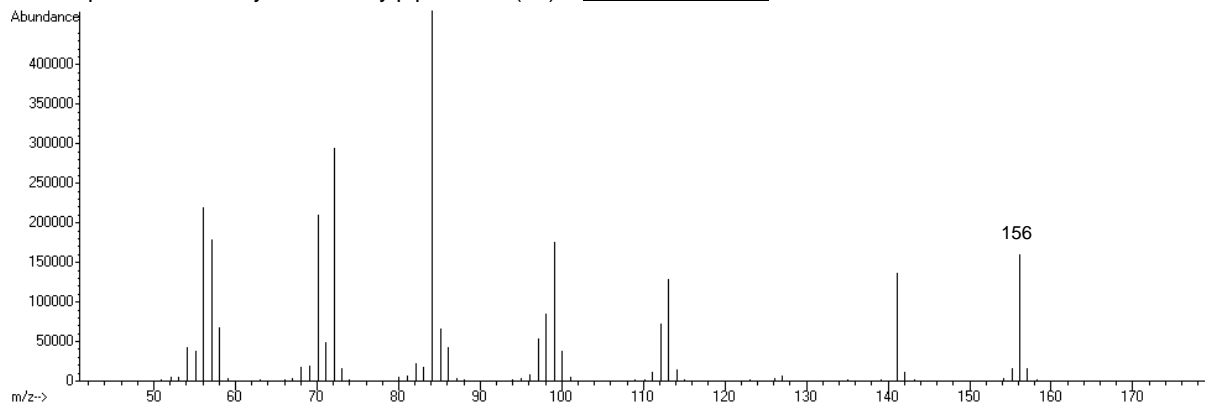
Mass spectrum of 1,4-dimethylpiperazine (**1d**) – analytical standard:



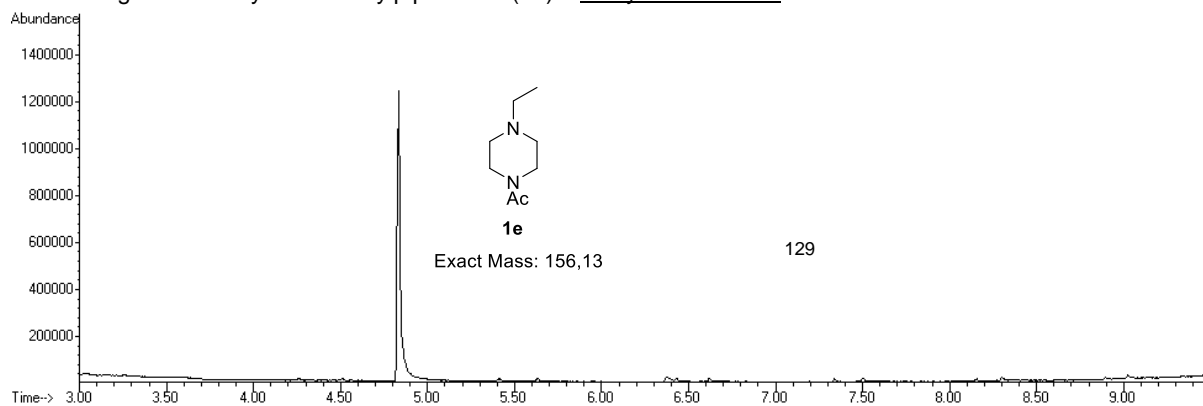
Chromatogram of acetylated 1-ethylpiperazine (**1e**) – biotransformation:



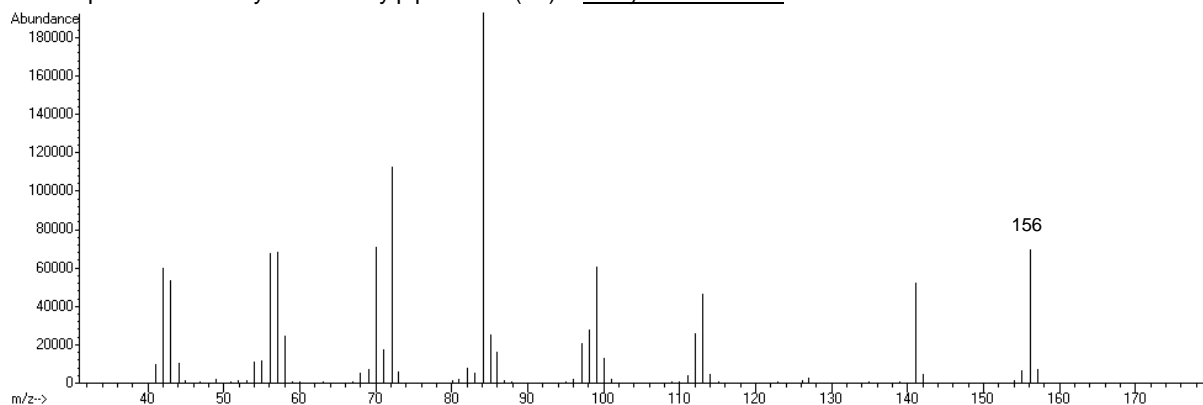
Mass spectrum of acetylated 1-ethylpiperazine (**1e**) – biotransformation:



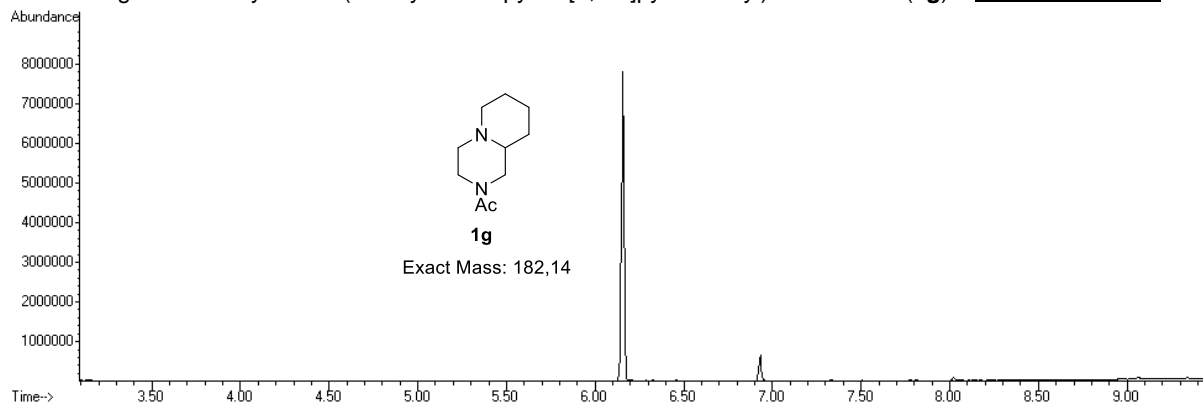
Chromatogram of acetylated 1-ethylpiperazine (**1e**) – analytical standard:



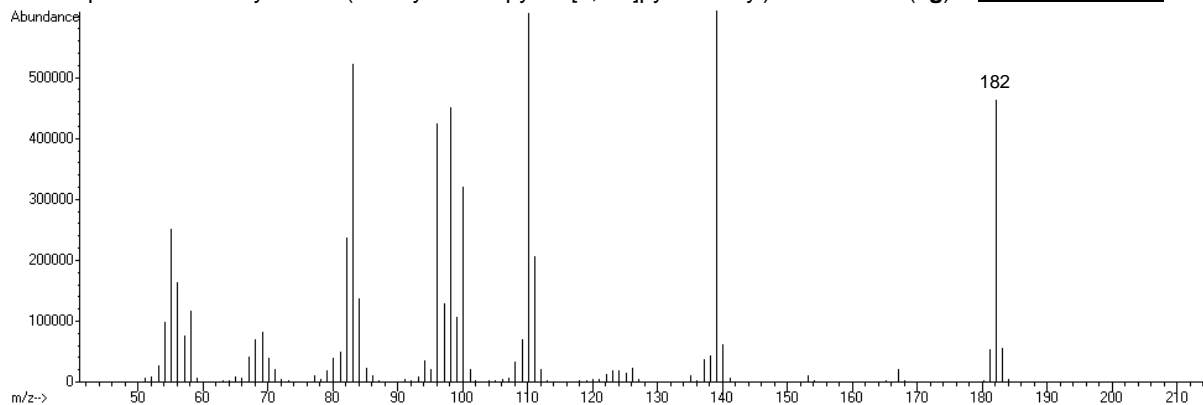
Mass spectrum of acetylated 1-ethylpiperazine (**1e**) – analytical standard:



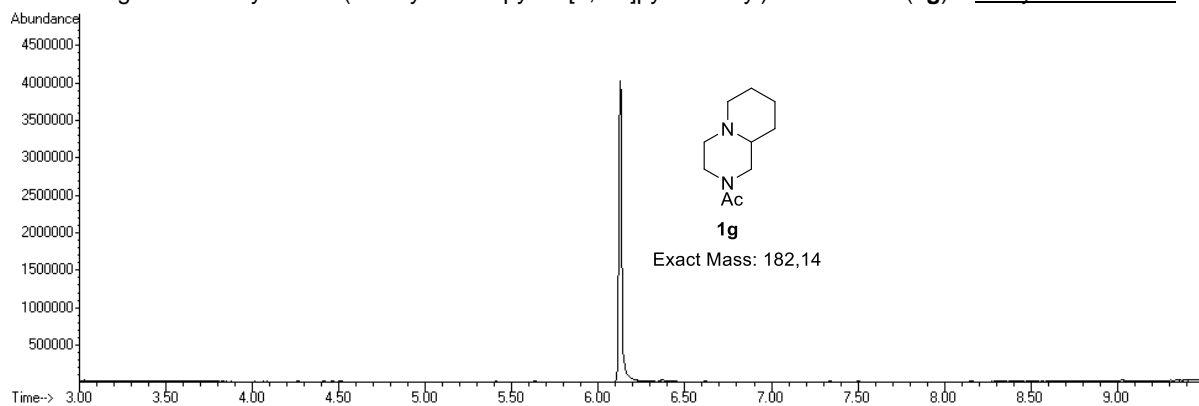
Chromatogram of acetylated 1-(octahydro-2H-pyrido[1,2-a]pyrazin-2-yl)ethan-1-one (**1g**) – biotransformation:



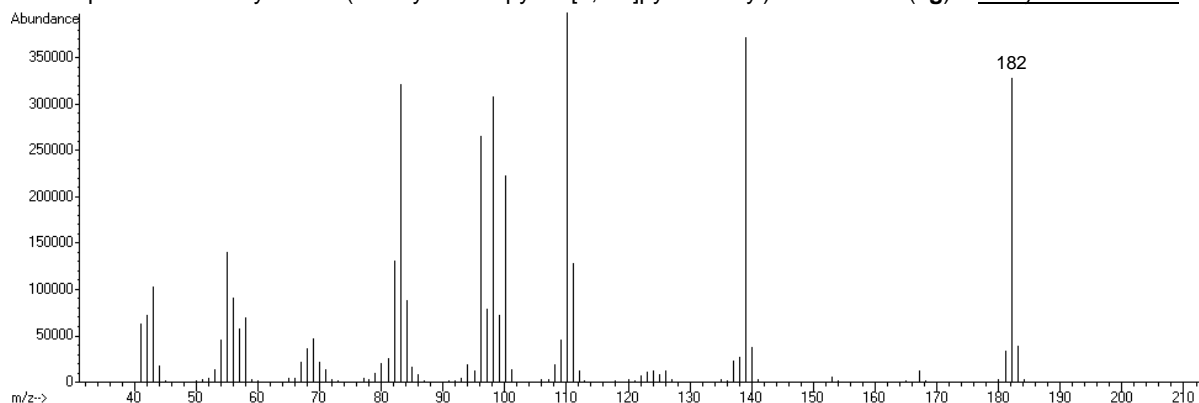
Mass spectrum of acetylated 1-(octahydro-2H-pyrido[1,2-a]pyrazin-2-yl)ethan-1-one (**1g**) – biotransformation:



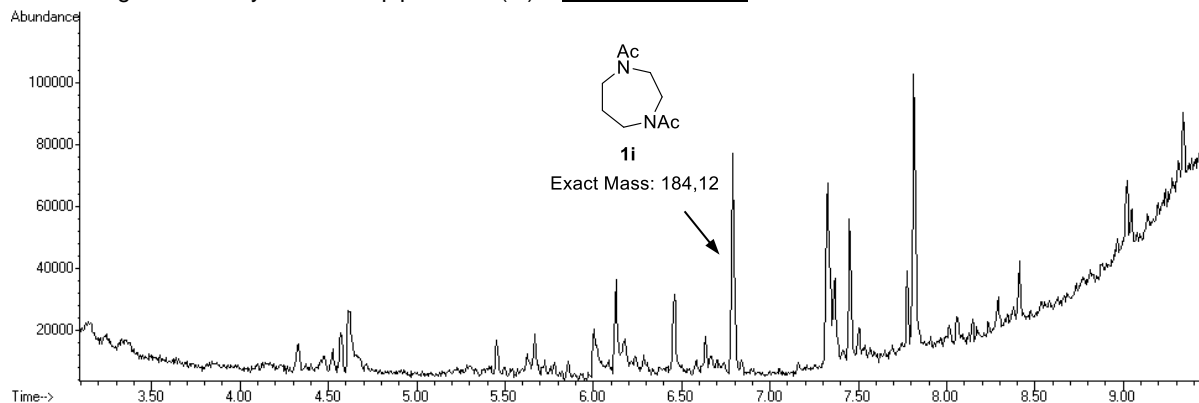
Chromatogram of acetylated 1-(octahydro-2H-pyrido[1,2-a]pyrazin-2-yl)ethan-1-one (**1g**) – analytical standard:



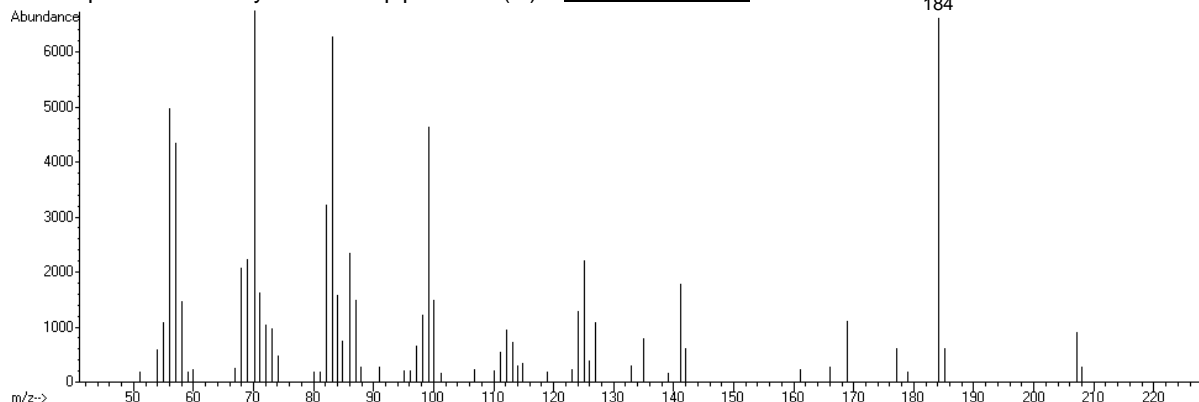
Mass spectrum of acetylated 1-(octahydro-2H-pyrido[1,2-a]pyrazin-2-yl)ethan-1-one (**1g**) – analytical standard:



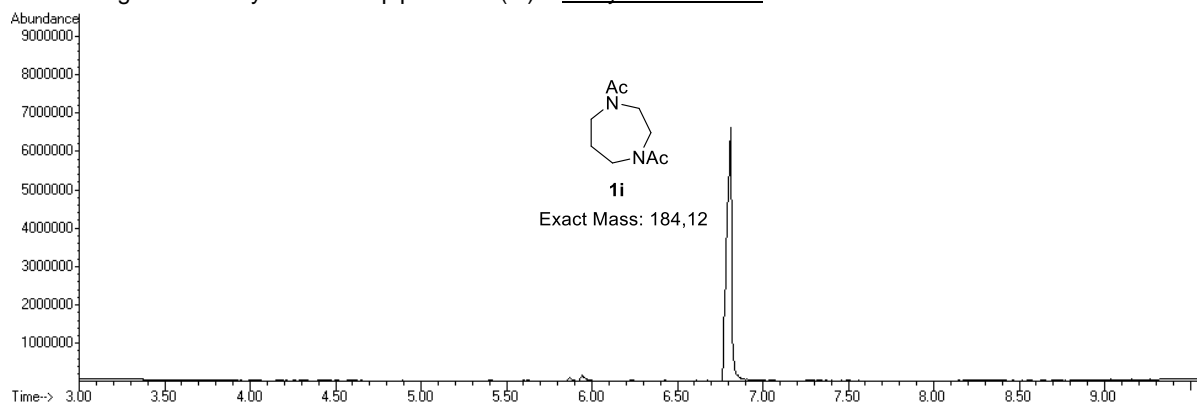
Chromatogram of acetylated homopiperazine (**1i**) – biotransformation:



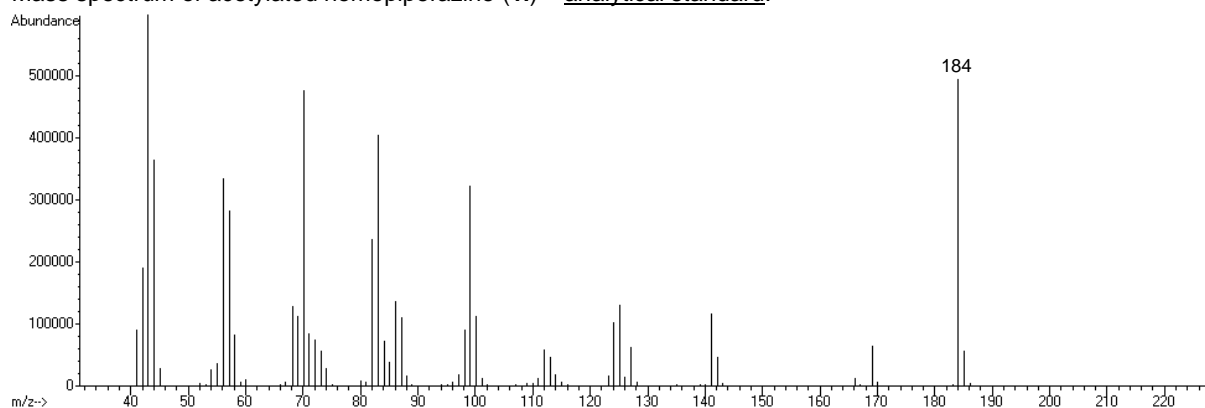
Mass spectrum of acetylated homopiperazine (**1i**) – biotransformation:



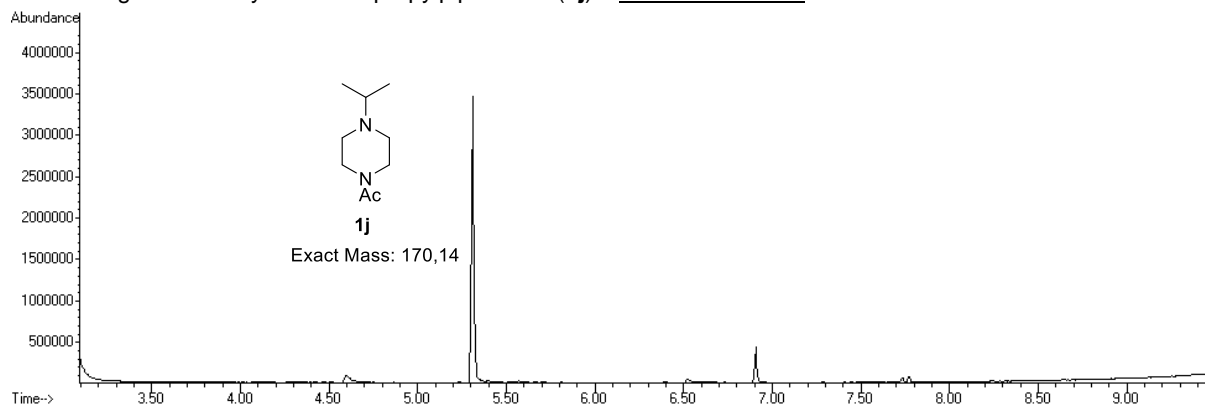
Chromatogram of acetylated homopiperazine (**1i**) – analytical standard:



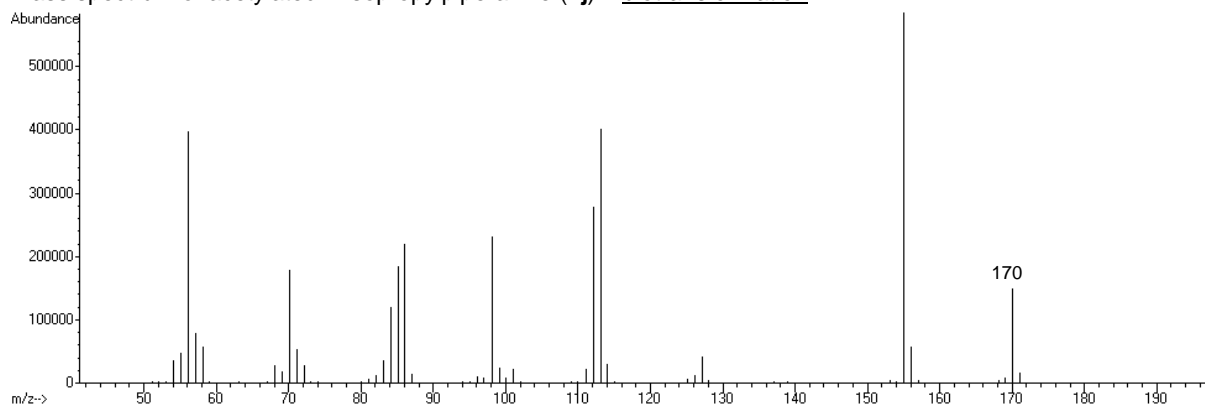
Mass spectrum of acetylated homopiperazine (**1i**) – analytical standard:



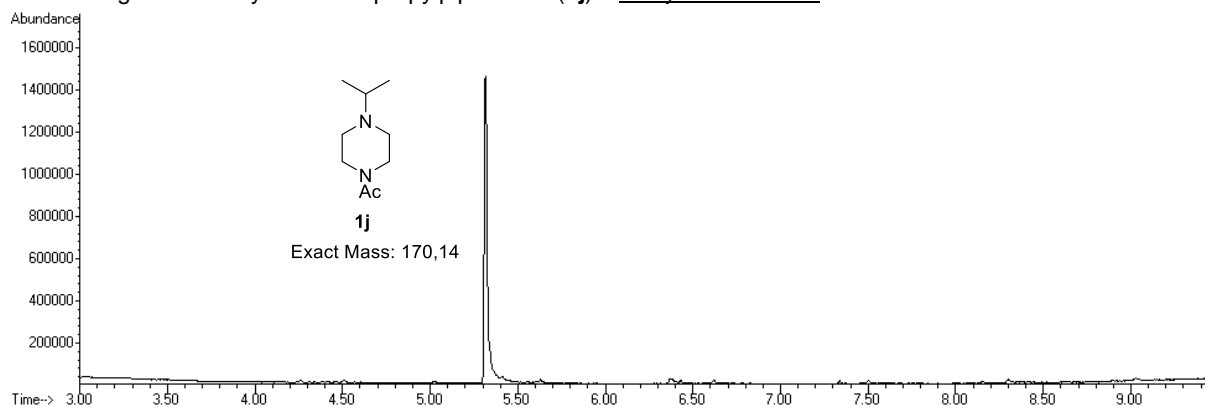
Chromatogram of acetylated 1-isopropylpiperazine (**1j**) – biotransformation:



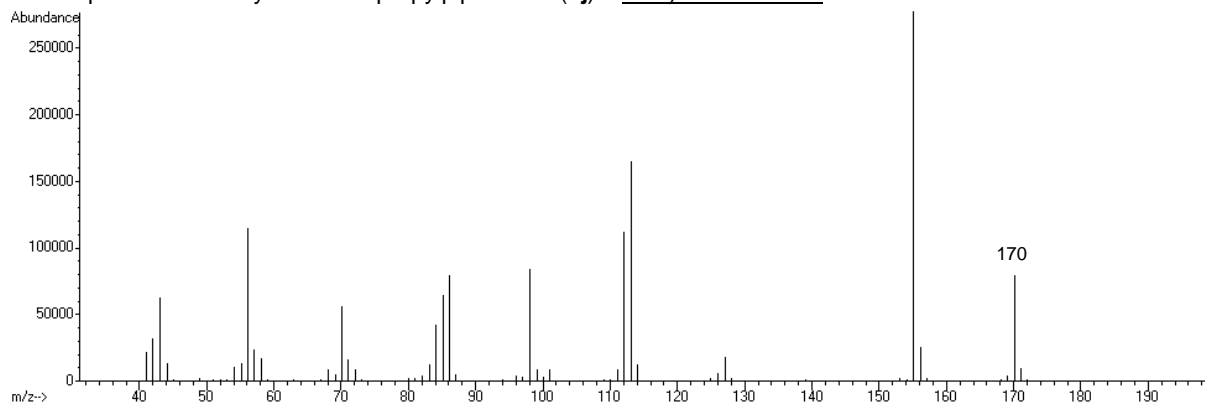
Mass spectrum of acetylated 1-isopropylpiperazine (**1j**) – biotransformation:



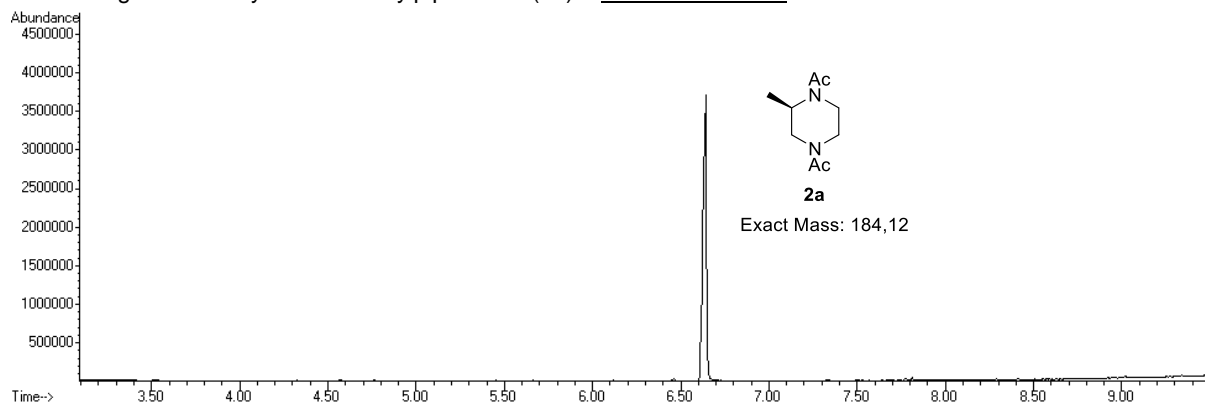
Chromatogram of acetylated 1-isopropylpiperazine (**1j**) – analytical standard:



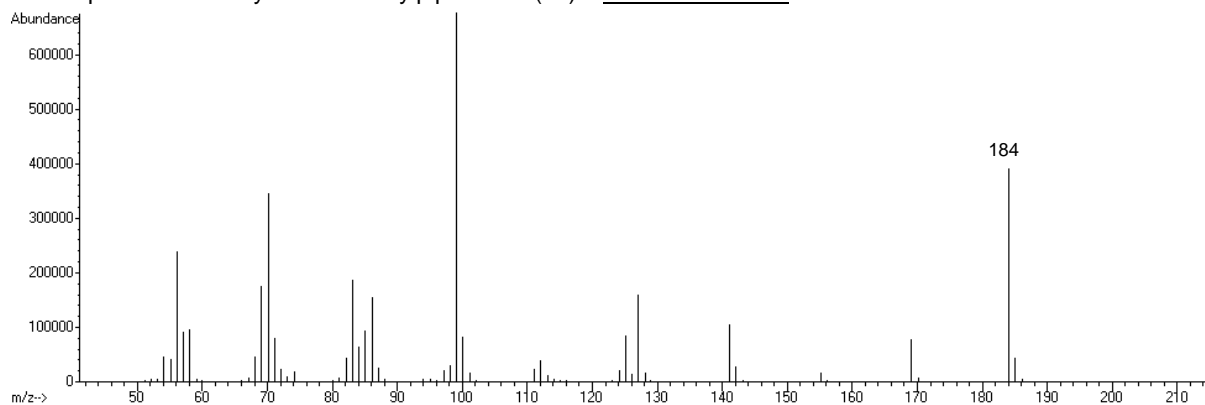
Mass spectrum of acetylated 1-isopropylpiperazine (**1j**) – analytical standard:



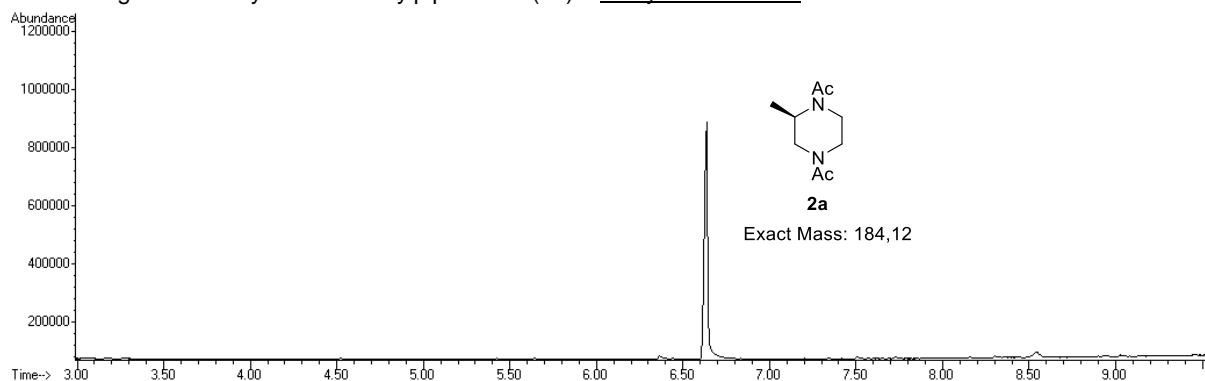
Chromatogram of acetylated 2-methylpiperazine (**2a**) – biotransformation:



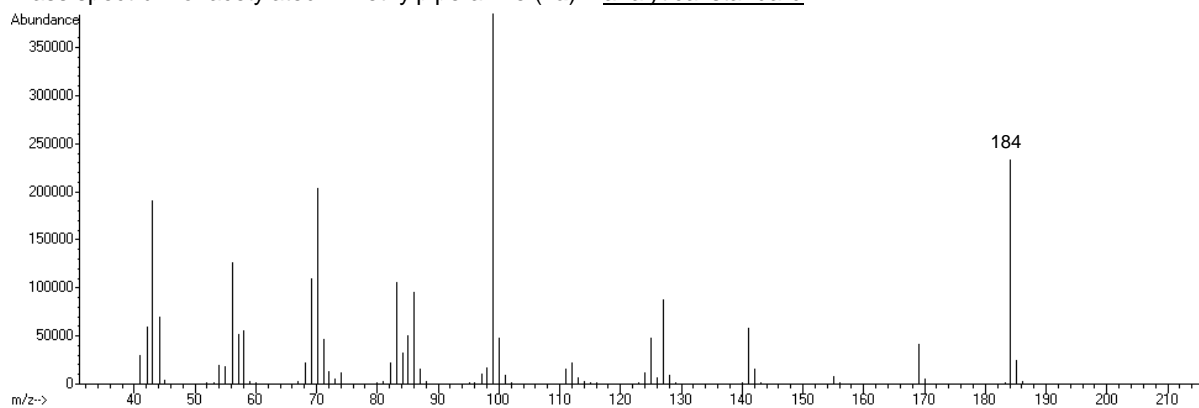
Mass spectrum of acetylated 2-methylpiperazine (**2a**) – biotransformation:



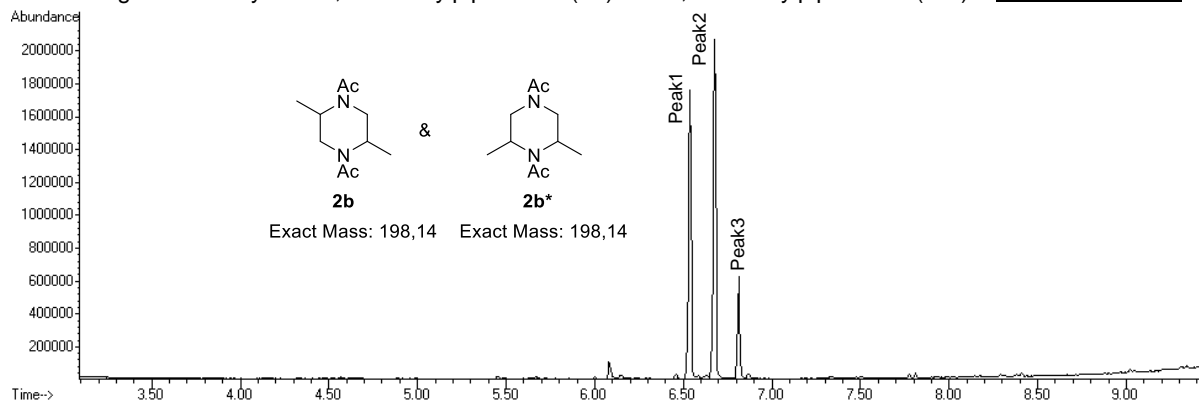
Chromatogram of acetylated 2-methylpiperazine (**2a**) – analytical standard:



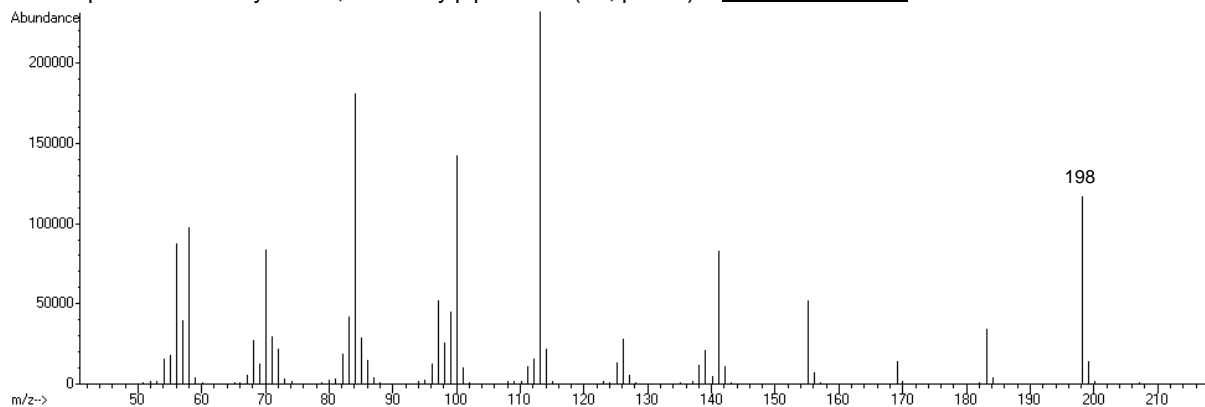
Mass spectrum of acetylated 2-methylpiperazine (**2a**) – analytical standard:



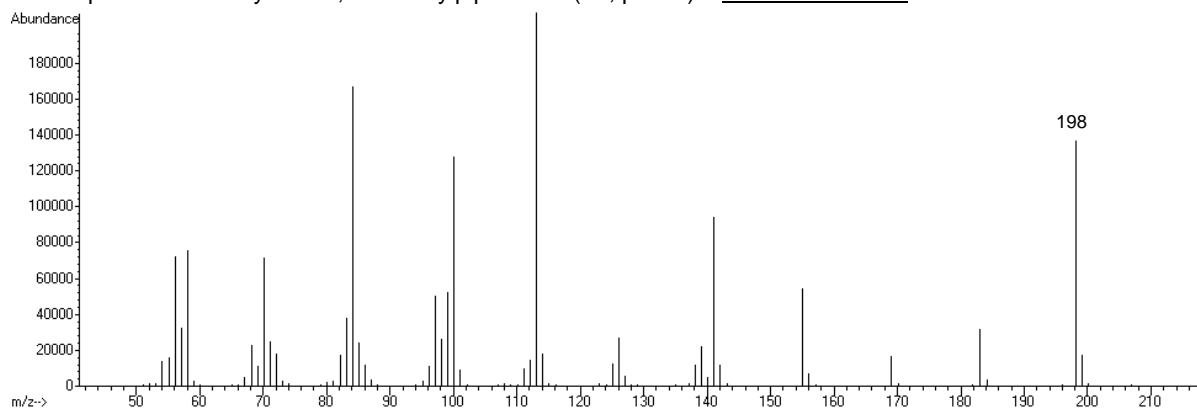
Chromatogram of acetylated 2,5-dimethylpiperazine (**2b**) and 2,6-dimethylpiperazine (**2b***) – biotransformation:



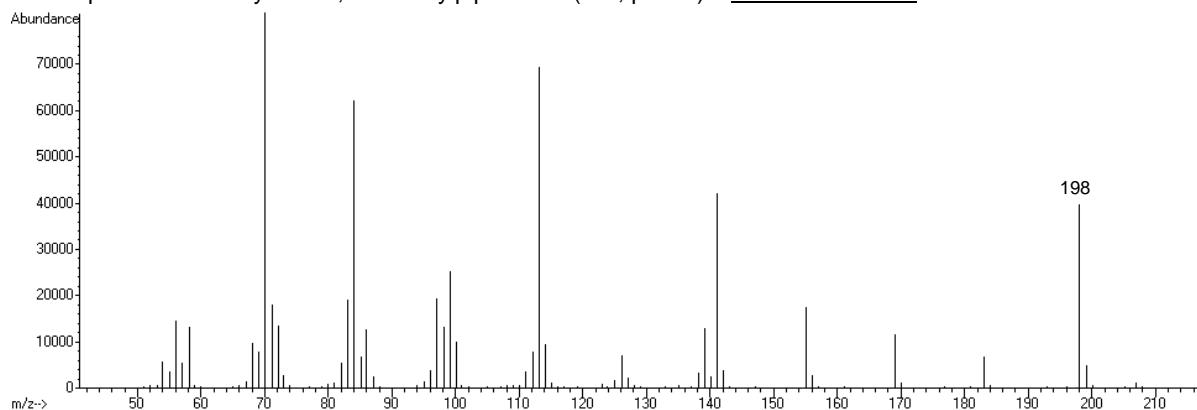
Mass spectrum of acetylated 2,5-dimethylpiperazine (**2b**, peak1) – biotransformation:



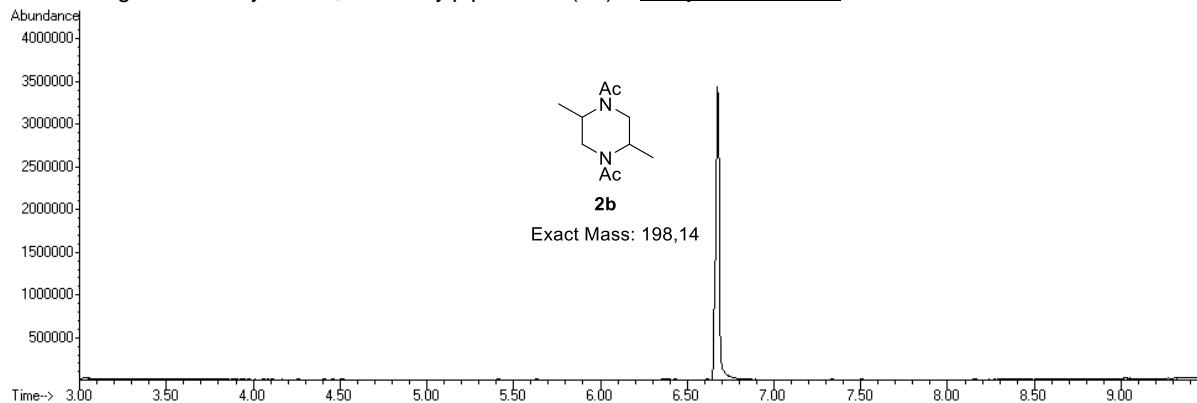
Mass spectrum of acetylated 2,5-dimethylpiperazine (**2b**, peak2) – biotransformation:



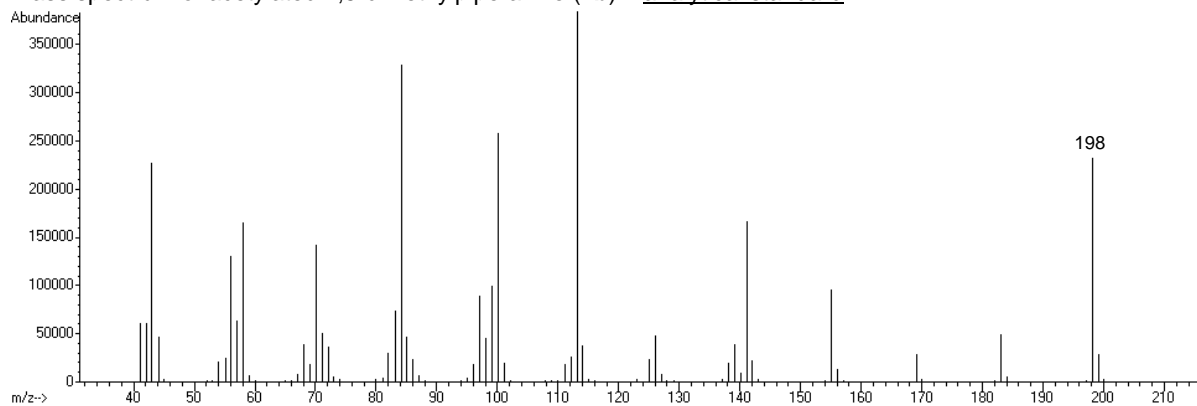
Mass spectrum of acetylated 2,6-dimethylpiperazine (**2b***, peak3) – biotransformation:



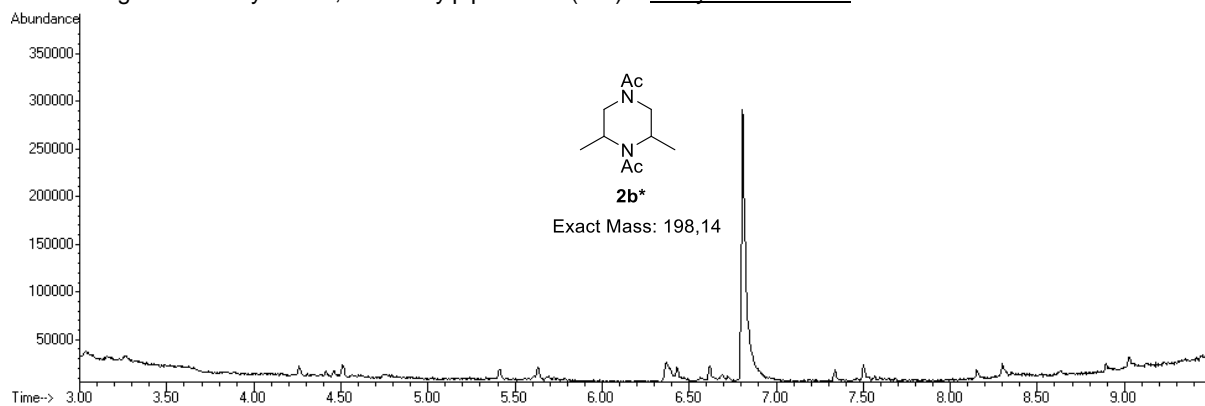
Chromatogram of acetylated 2,5-dimethylpiperazine (**2b**) – analytical standard:



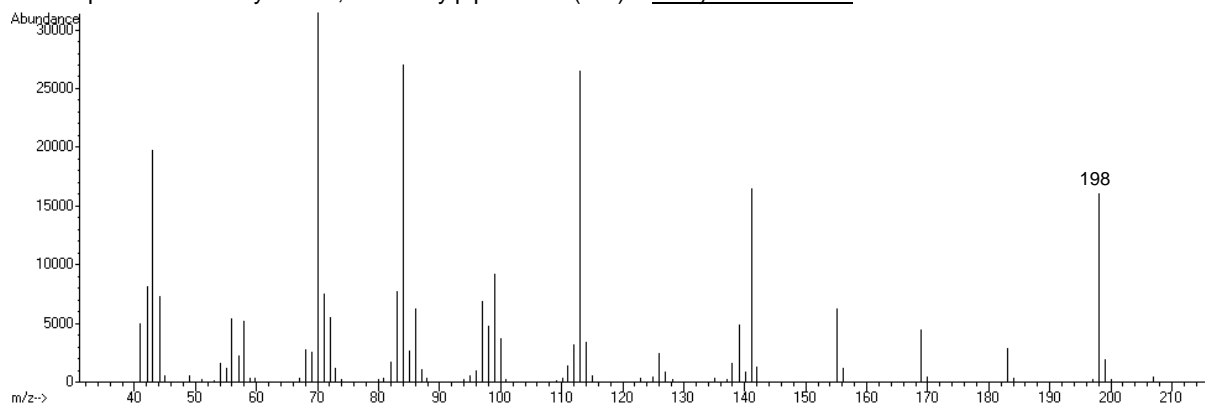
Mass spectrum of acetylated 2,5-dimethylpiperazine (**2b**) – analytical standard:



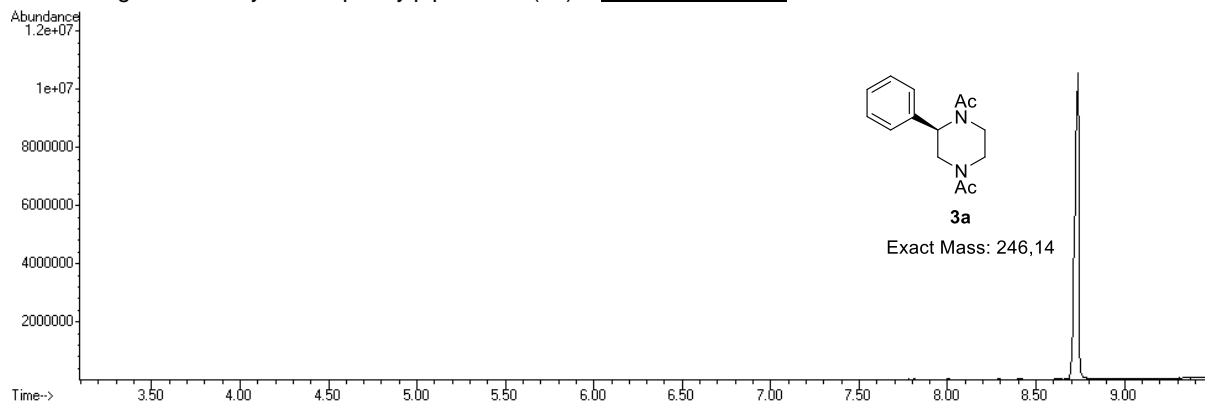
Chromatogram of acetylated 2,6-dimethylpiperazine (**2b***) – analytical standard:



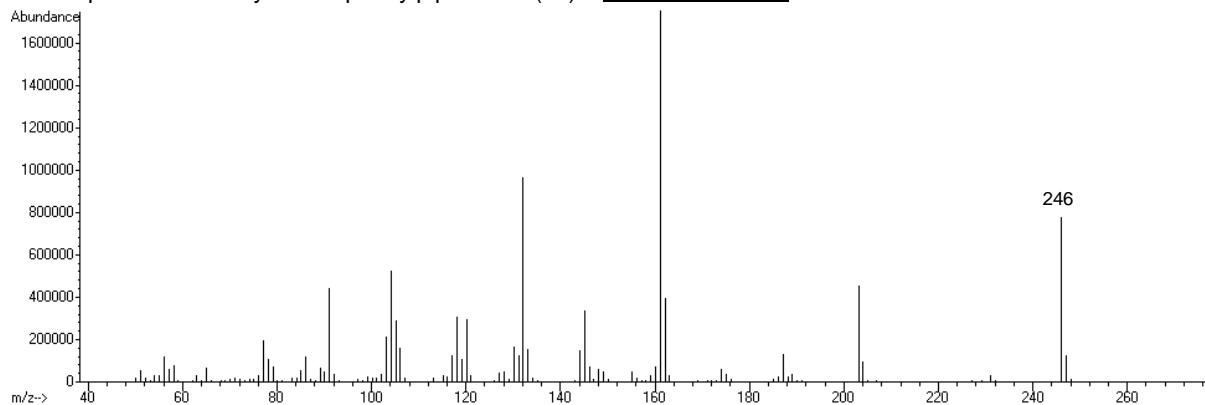
Mass spectrum of acetylated 2,6-dimethylpiperazine (**2b***) – analytical standard:



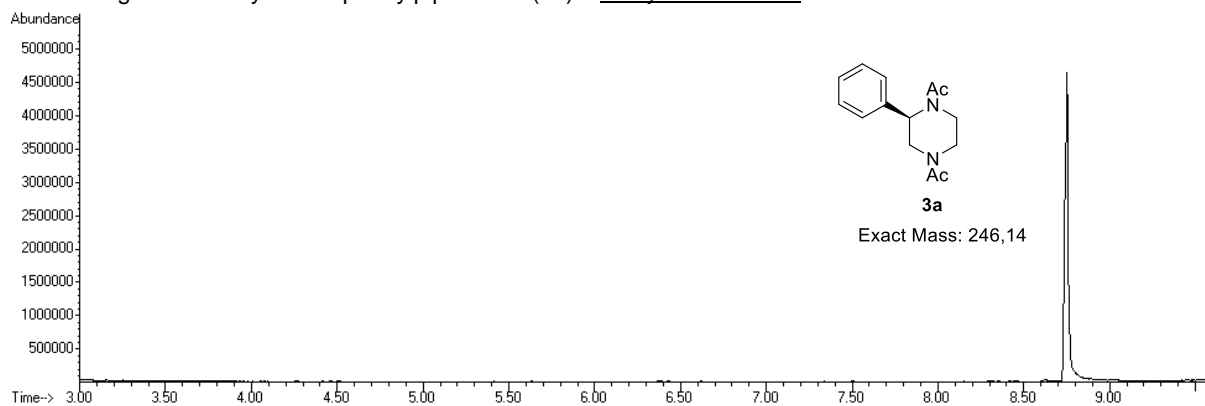
Chromatogram of acetylated 2-phenylpiperazine (**3a**) – biotransformation:



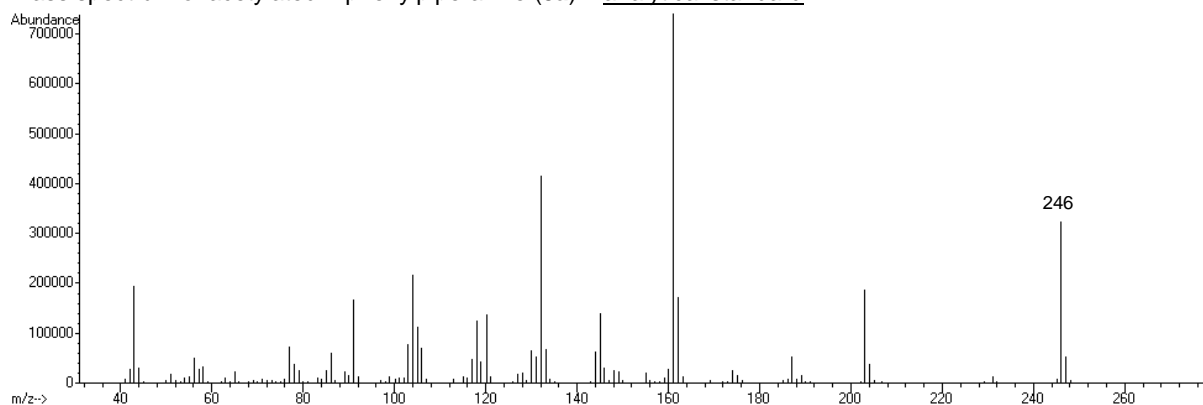
Mass spectrum of acetylated 2-phenylpiperazine (**3a**) – biotransformation:



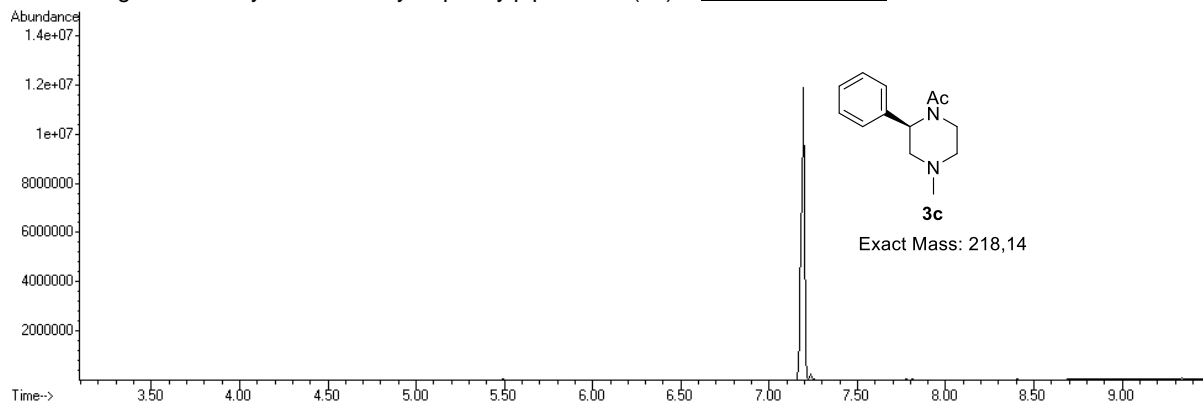
Chromatogram of acetylated 2-phenylpiperazine (**3a**) – analytical standard:



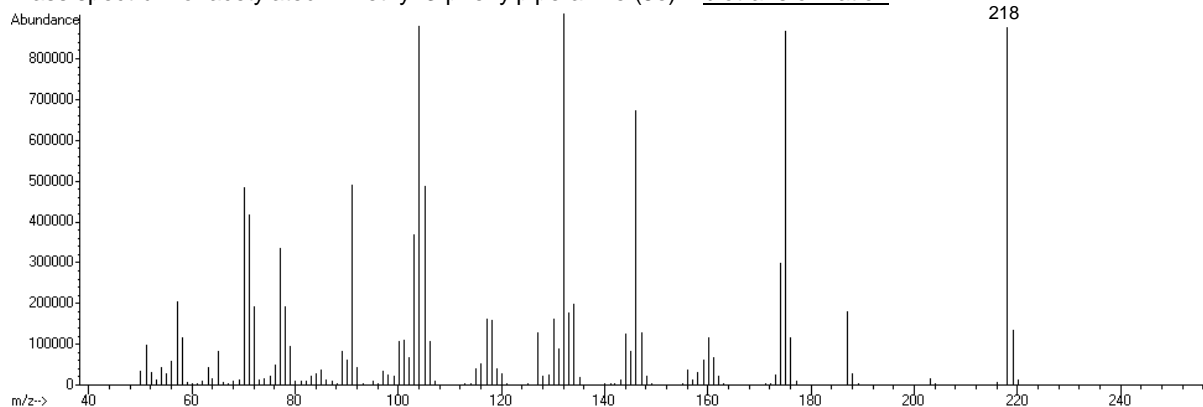
Mass spectrum of acetylated 2-phenylpiperazine (**3a**) – analytical standard:



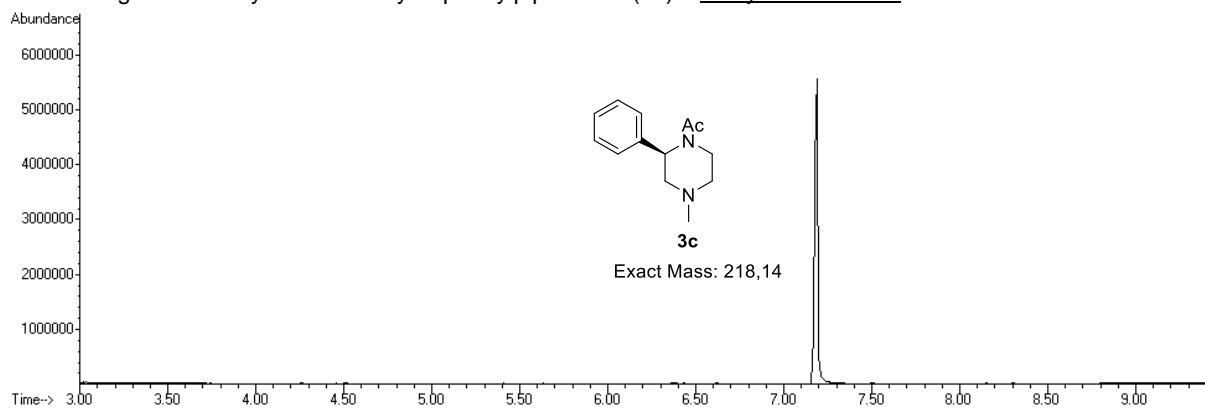
Chromatogram of acetylated 1-methyl-3-phenylpiperazine (**3c**) – biotransformation:



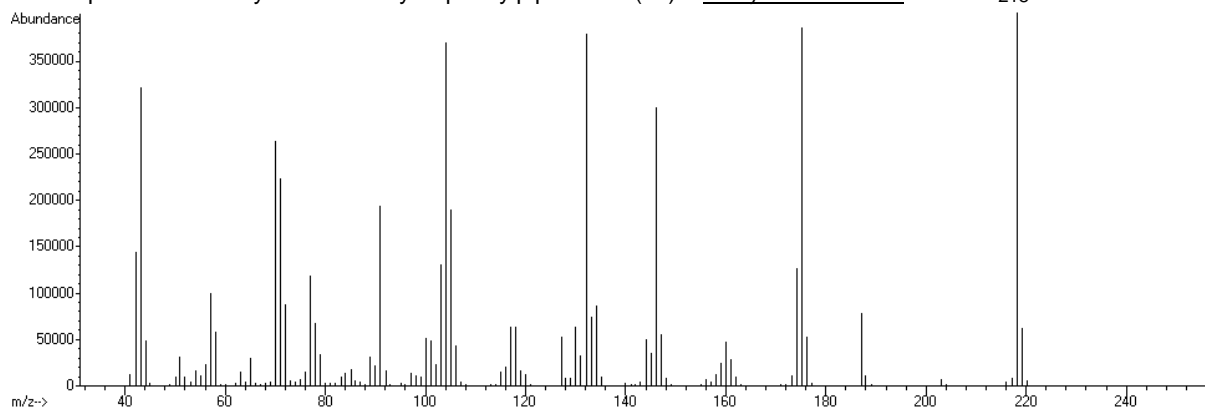
Mass spectrum of acetylated 1-methyl-3-phenylpiperazine (**3c**) – biotransformation:



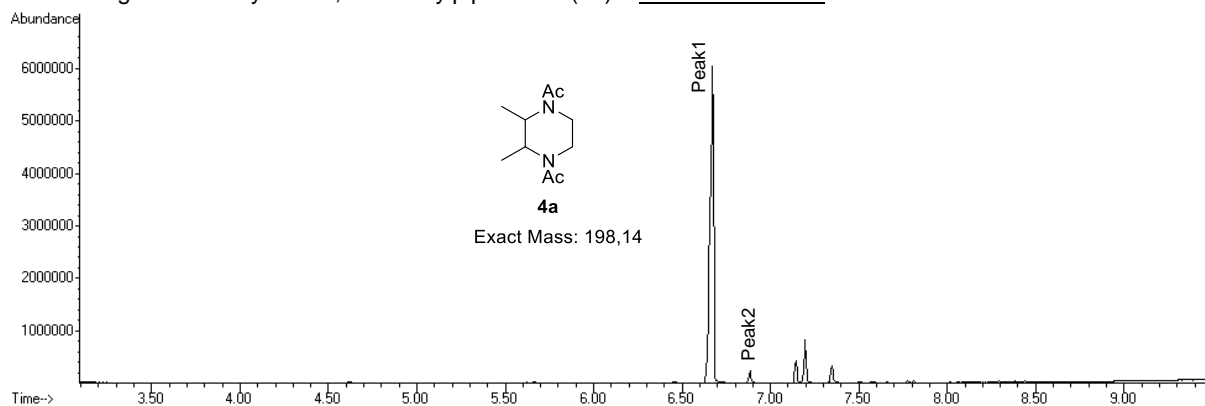
Chromatogram of acetylated 1-methyl-3-phenylpiperazine (**3c**) – analytical standard:



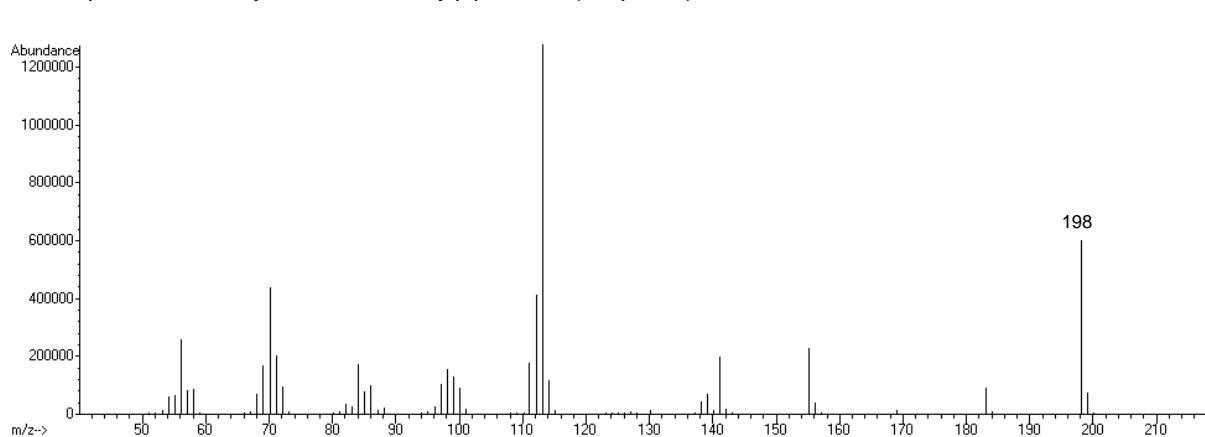
Mass spectrum of acetylated 1-methyl-3-phenylpiperazine (**3c**) – analytical standard:



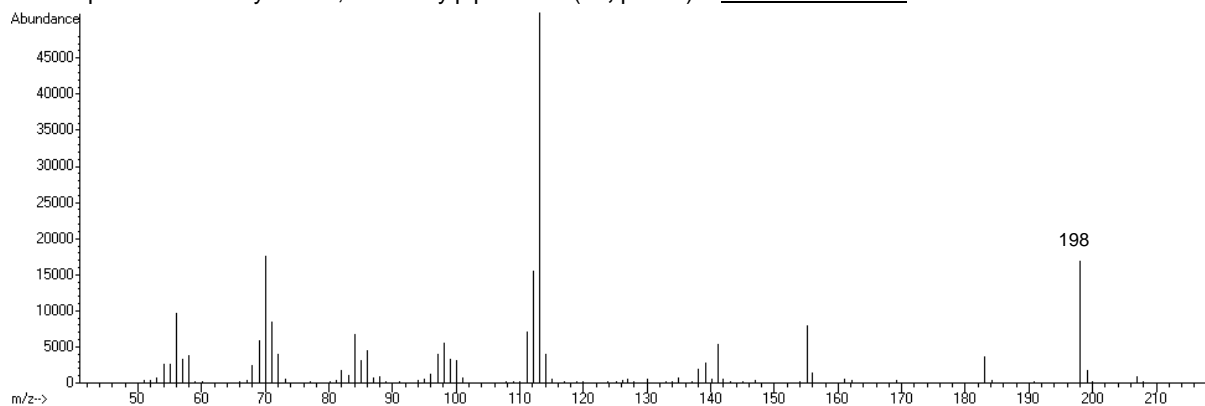
Chromatogram of acetylated 2,3-dimethylpiperazine (**4a**) – biotransformation:



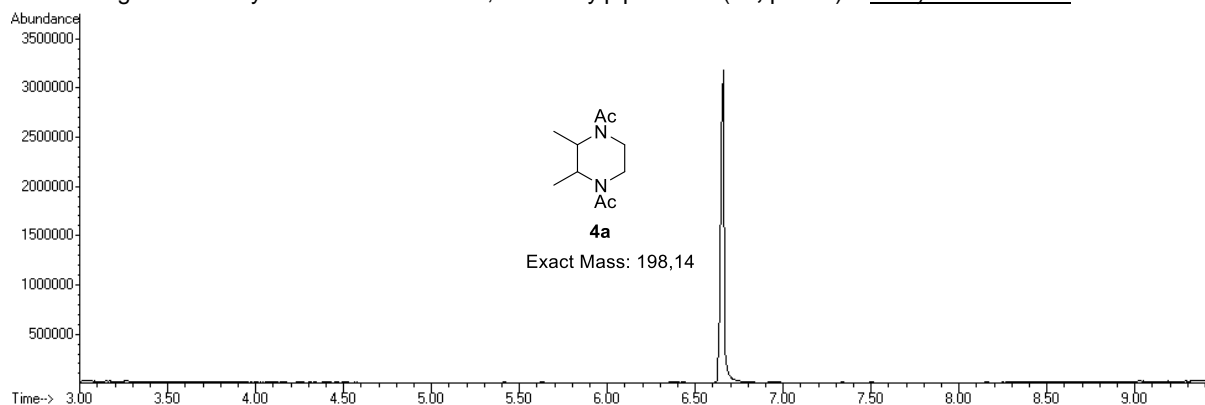
Mass spectrum of acetylated 2,3-dimethylpiperazine (**4a**, peak1) – biotransformation:



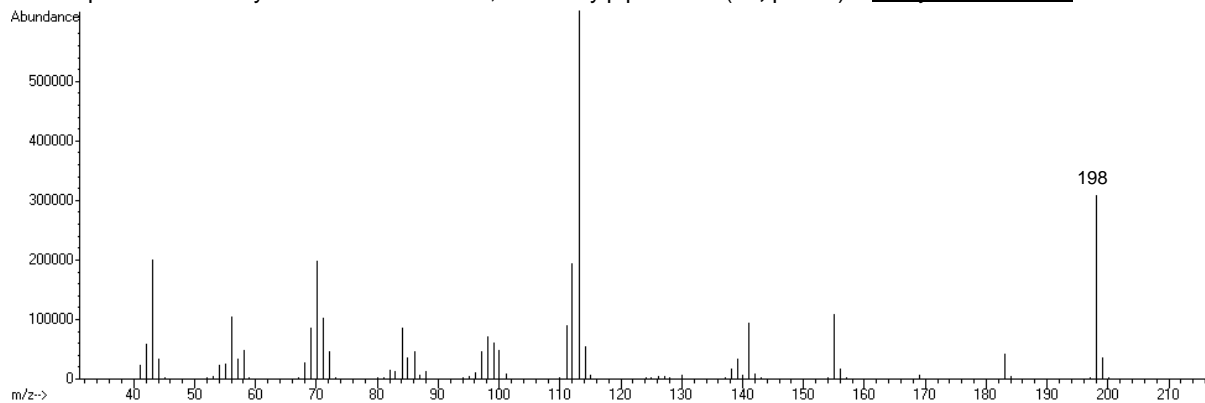
Mass spectrum of acetylated 2,3-dimethylpiperazine (**4a**, peak2) – biotransformation:



Chromatogram of acetylated racemic *trans*-2,3-dimethylpiperazine (**4a**, peak2) – analytical standard:

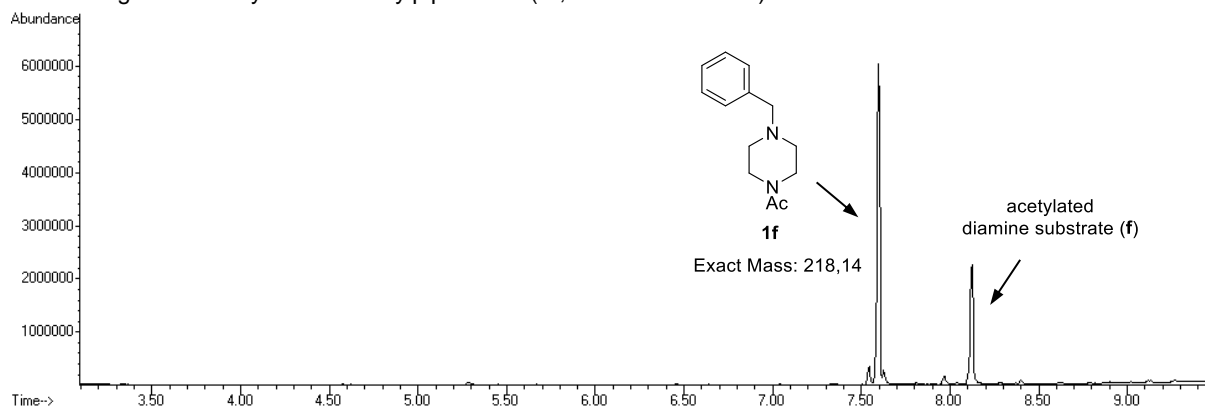


Mass spectrum of acetylated racemic *trans*-2,3-dimethylpiperazine (**4a**, peak2) – analytical standard:

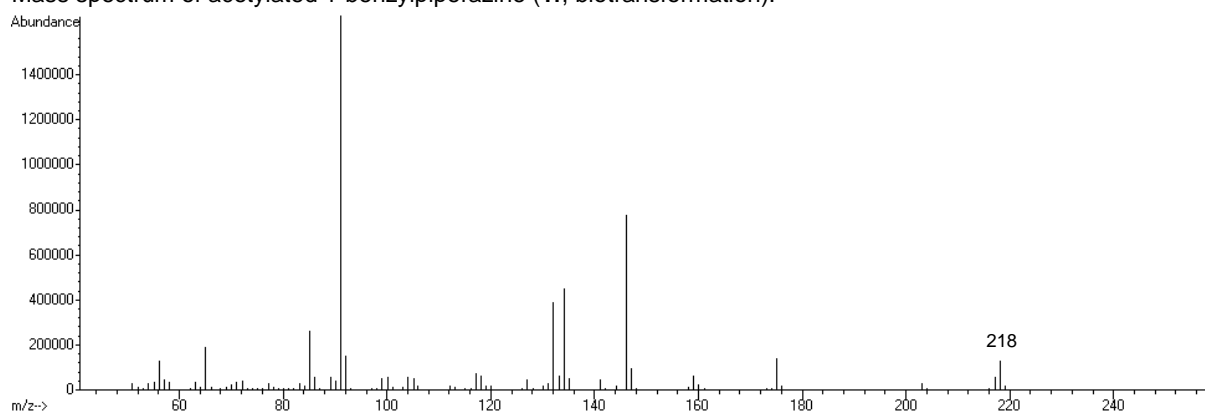


(C) Further Chromatograms and mass spectra for piperazine products listed in table 2.

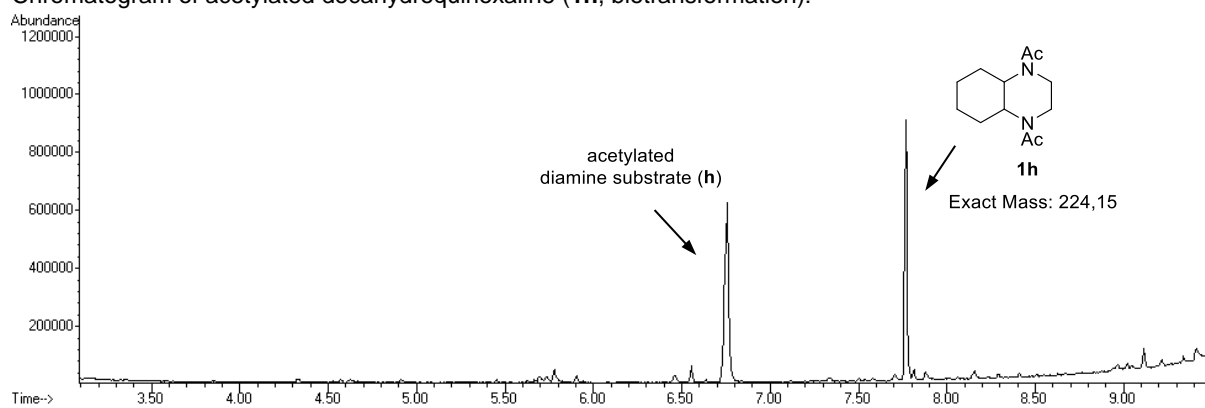
Chromatogram of acetylated 1-benzylpiperazine (**1f**, biotransformation):



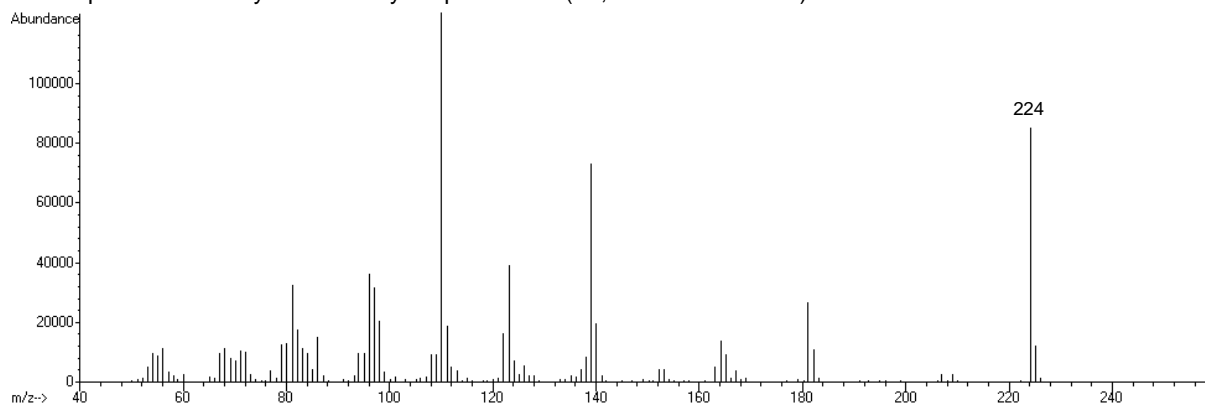
Mass spectrum of acetylated 1-benzylpiperazine (**1f**, biotransformation):



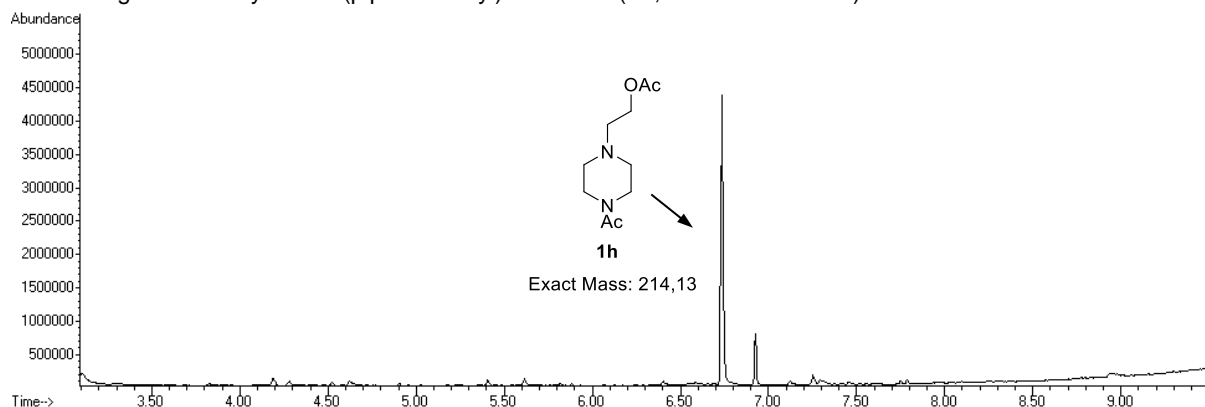
Chromatogram of acetylated decahydroquinoxaline (**1h**, biotransformation):



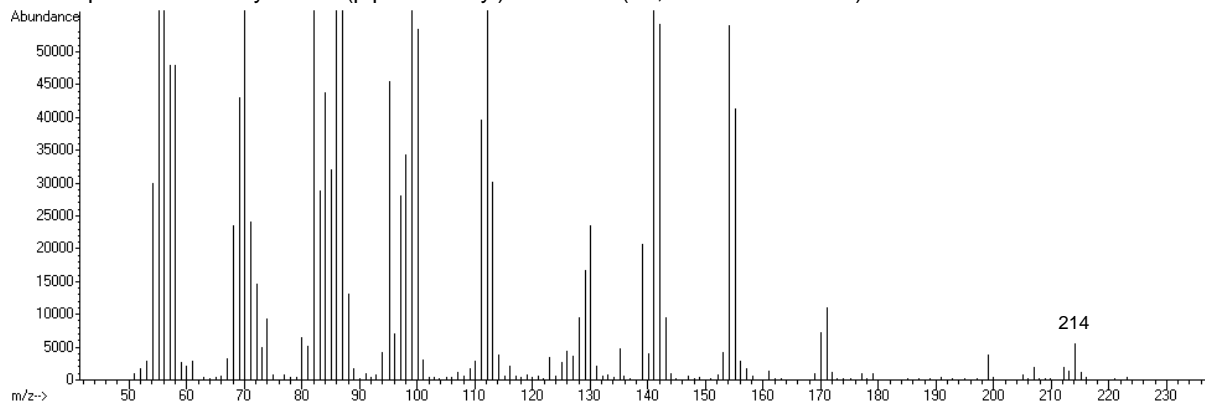
Mass spectrum of acetylated decahydroquinoxaline (**1h**, biotransformation):



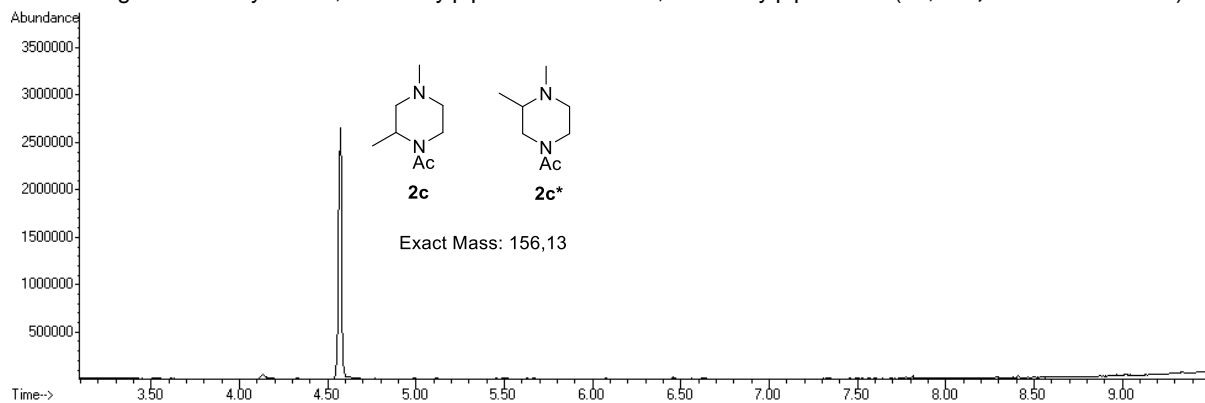
Chromatogram of acetylated 2-(piperazin-1-yl)ethan-1-ol (**1n**, biotransformation):



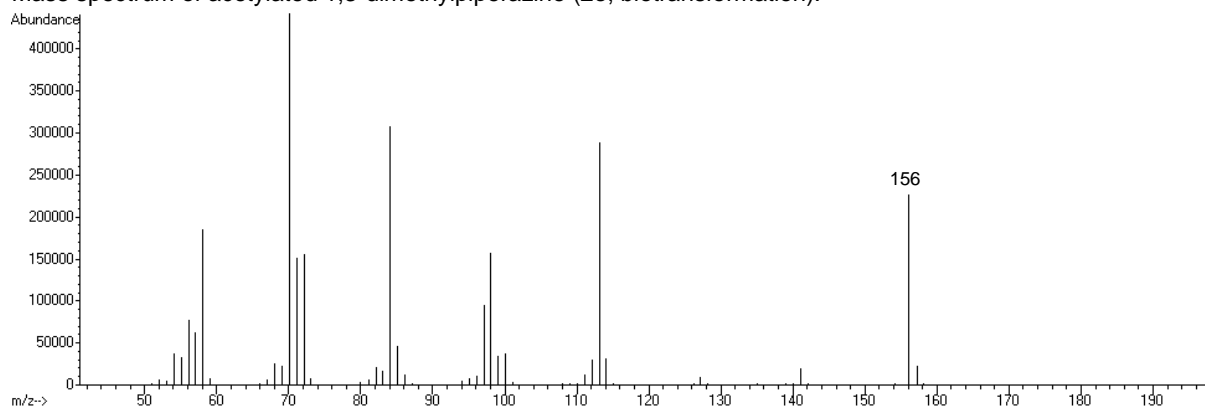
Mass spectrum of acetylated 2-(piperazin-1-yl)ethan-1-ol (**1n**, biotransformation):



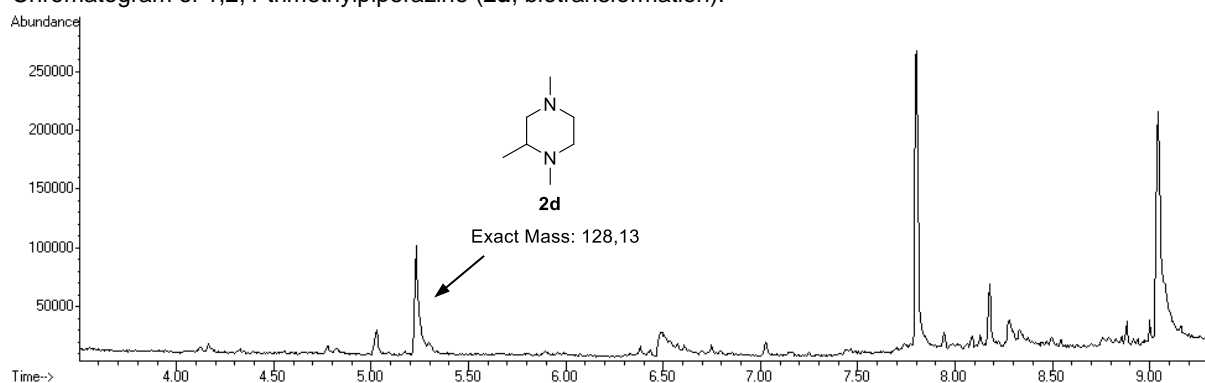
Chromatogram of acetylated 1,3-dimethylpiperazine and/or 1,2-dimethylpiperazine (**2c**, **2c***, biotransformation):



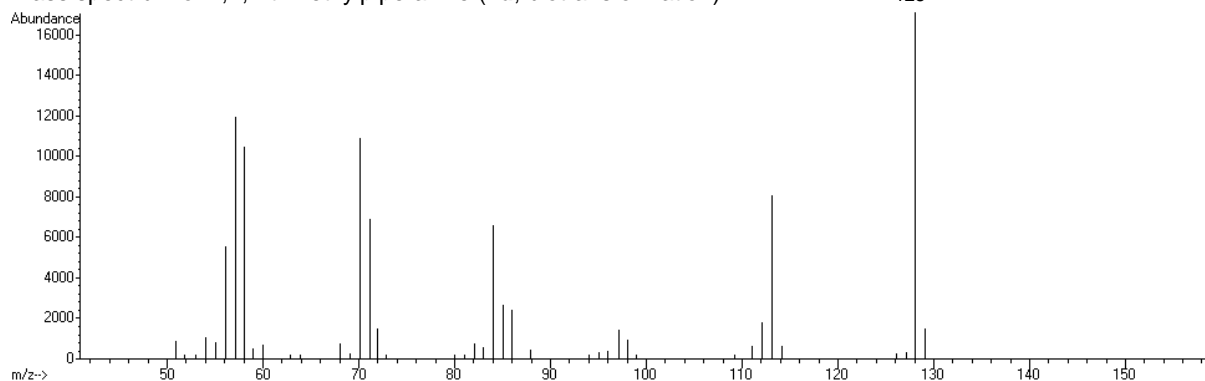
Mass spectrum of acetylated 1,3-dimethylpiperazine (**2c**, biotransformation):



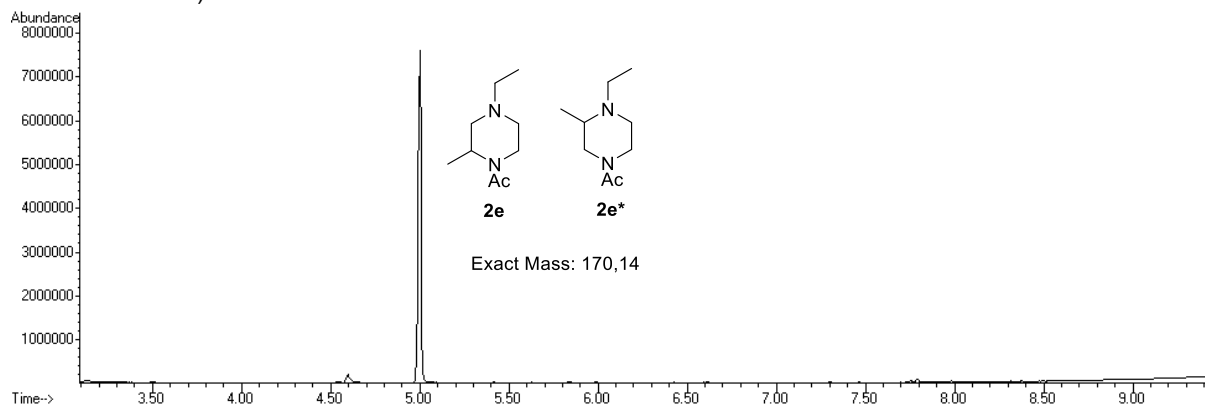
Chromatogram of 1,2,4-trimethylpiperazine (**2d**, biotransformation):



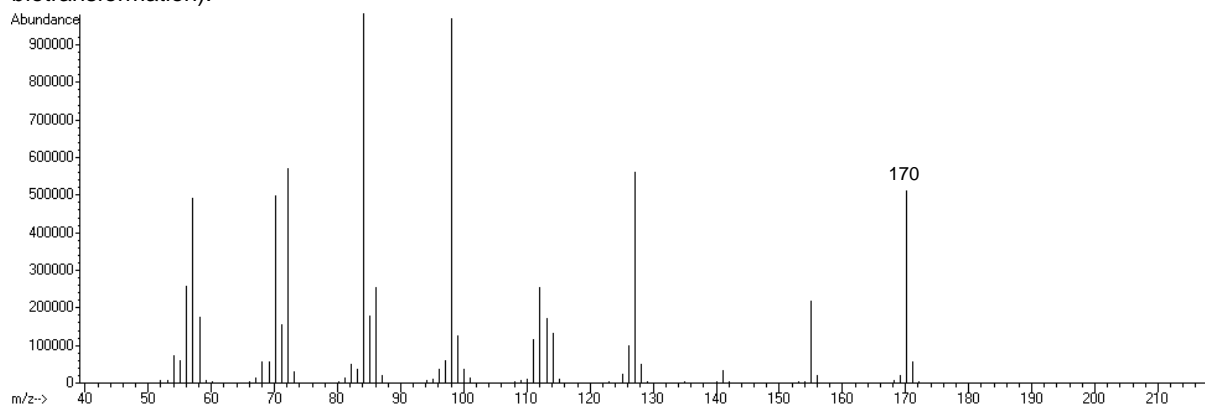
Mass spectrum of 1,2,4-trimethylpiperazine (**2d**, biotransformation):



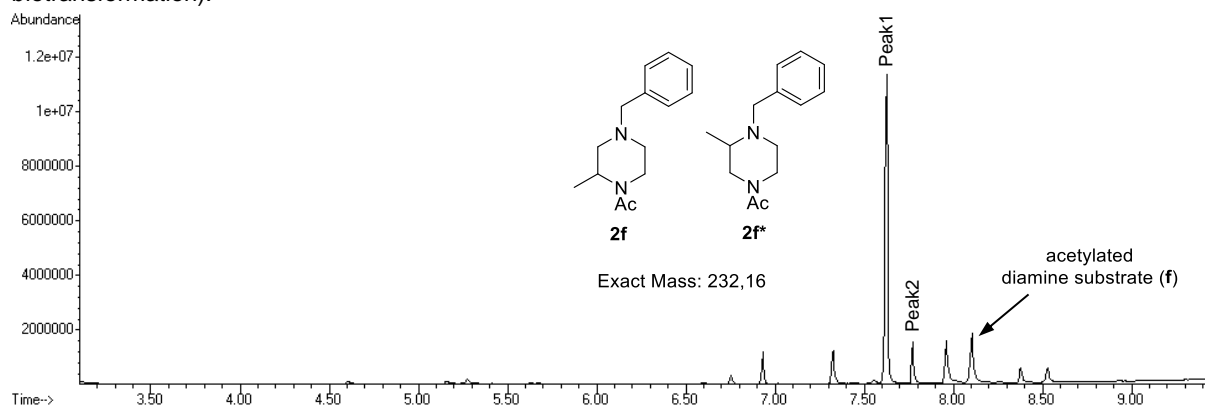
Chromatogram of acetylated 1-ethyl-3-methylpiperazine and/or 1-ethyl-2-methylpiperazine (**2e**, **2e***, biotransformation):



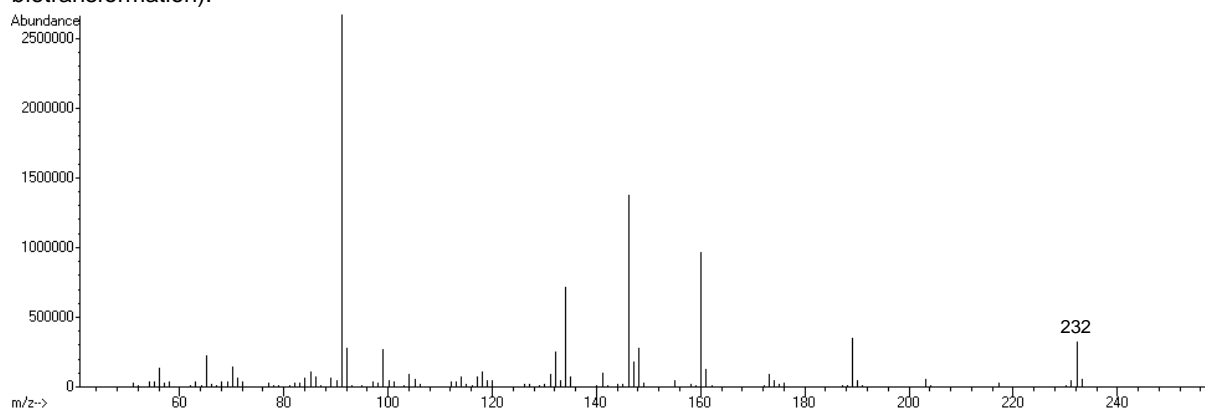
Mass spectrum of acetylated 1-ethyl-3-methylpiperazine and/or 1-ethyl-2-methylpiperazine (**2e**, **2e***, biotransformation):



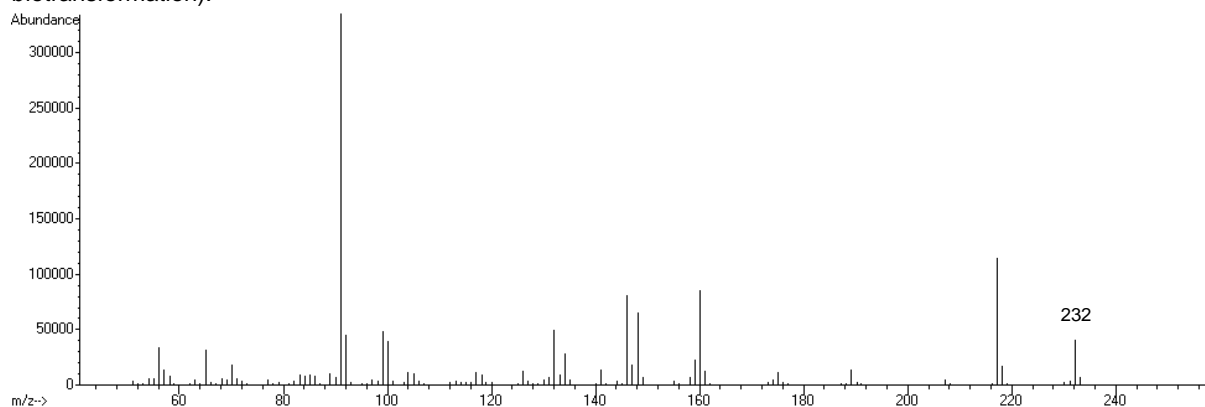
Chromatogram of acetylated 1-benzyl-3-methylpiperazine and/or 1-benzyl-2-methylpiperazine (**2f**, **2f***, biotransformation):



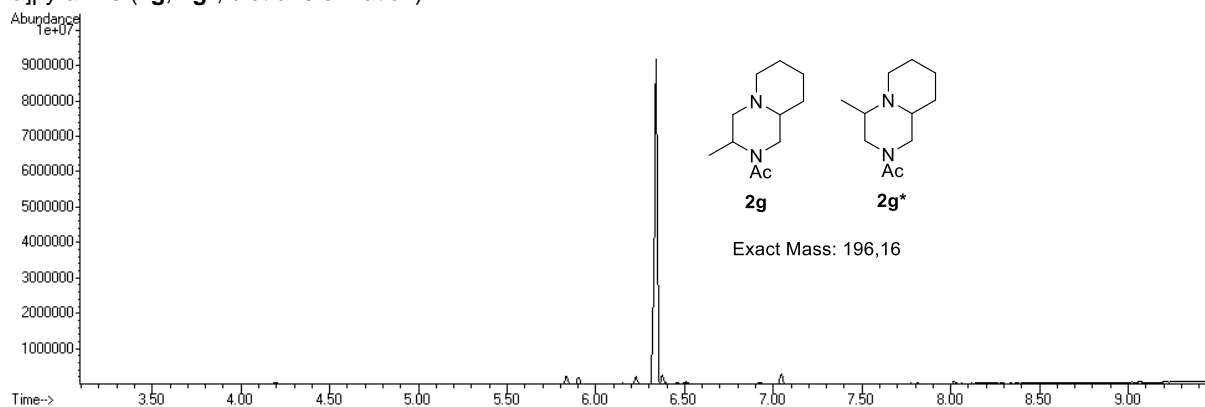
Mass spectrum of acetylated 1-benzyl-3-methylpiperazine and/or 1-benzyl-2-methylpiperazine (**2f**, **2f***, peak 1, biotransformation):



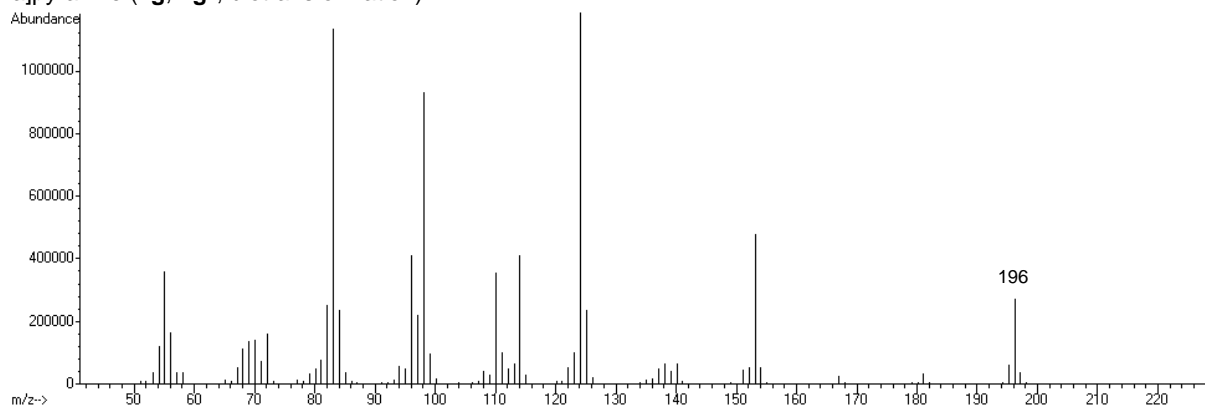
Mass spectrum of acetylated 1-benzyl-3-methylpiperazine and/or 1-benzyl-2-methylpiperazine (**2f**, **2f***, peak 2, biotransformation):



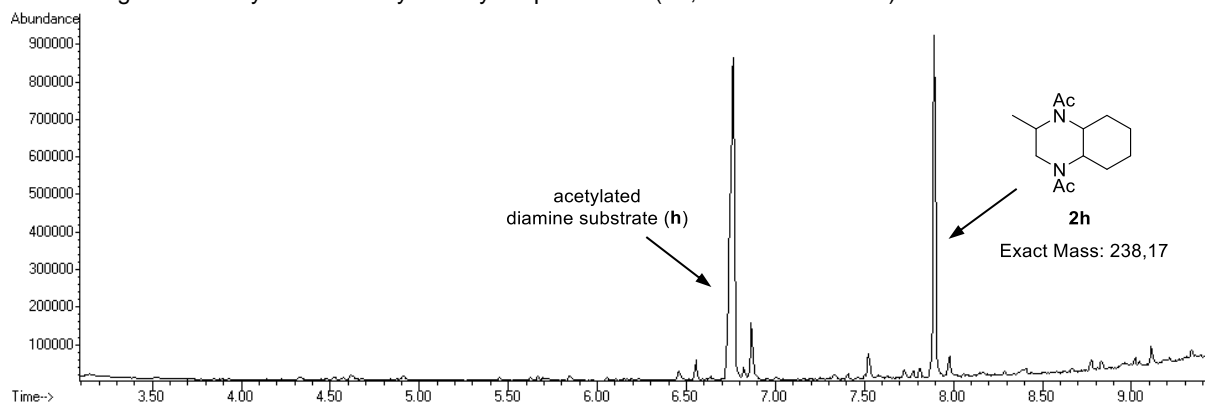
Chromatogram of acetylated 3-methyloctahydro-2H-pyrido[1,2-a]pyrazine and/or 4-methyloctahydro-2H-pyrido[1,2-a]pyrazine (**2g**, **2g***, biotransformation):



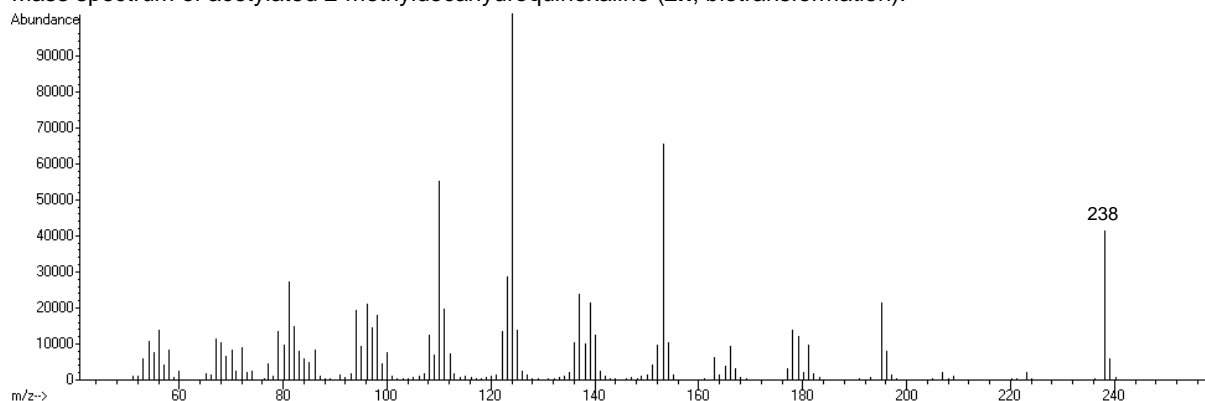
Mass spectrum of acetylated 3-methyloctahydro-2H-pyrido[1,2-a]pyrazine and/or 4-methyloctahydro-2H-pyrido[1,2-a]pyrazine (**2g**, **2g***, biotransformation):



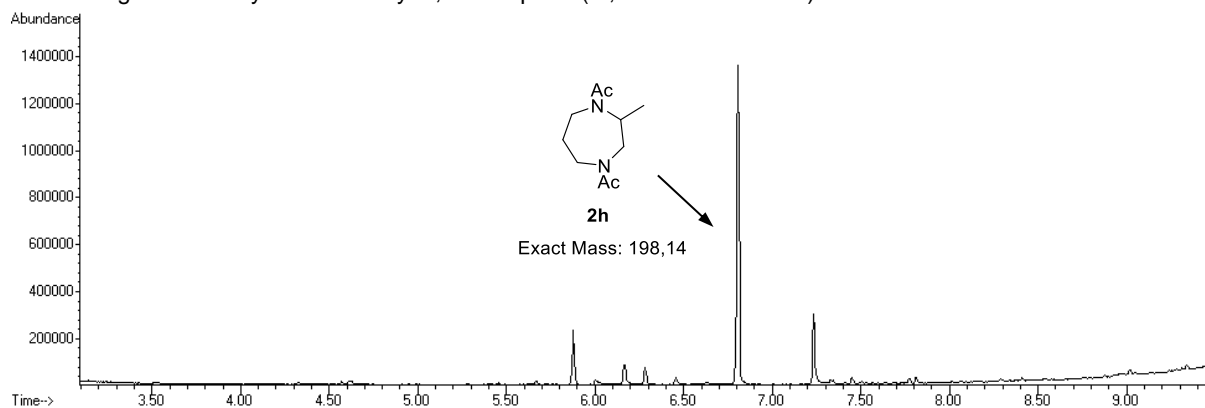
Chromatogram of acetylated 2-methyldecahydroquinoxaline (**2h**, biotransformation):



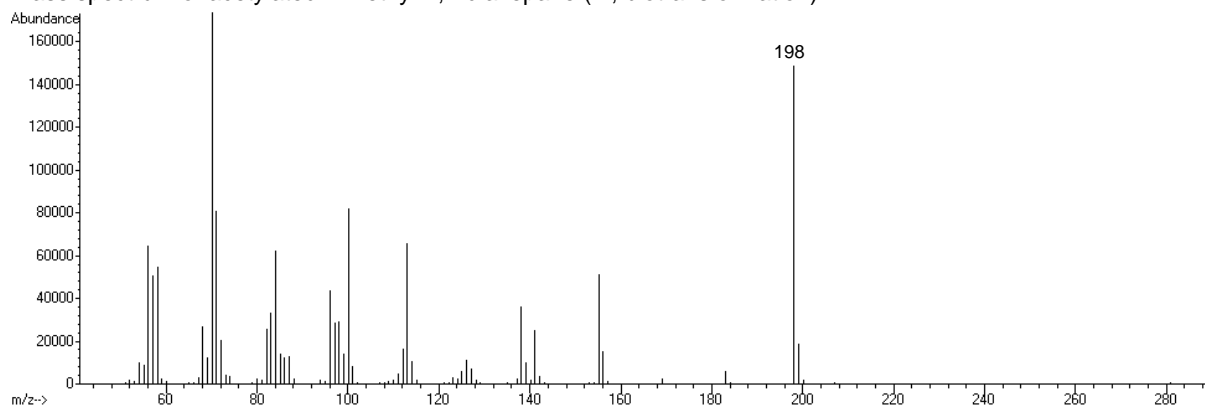
Mass spectrum of acetylated 2-methyldecahydroquinoxaline (**2h**, biotransformation):



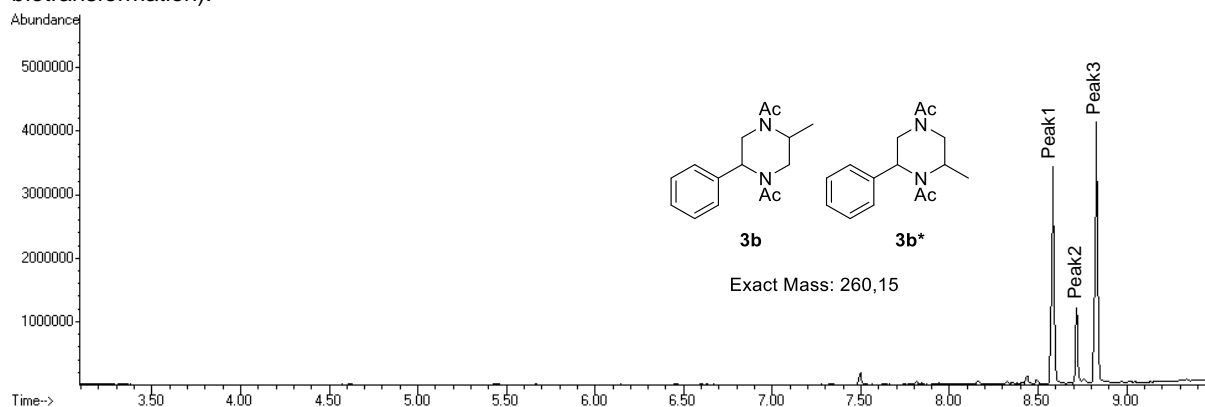
Chromatogram of acetylated 2-methyl-1,4-diazepane (**2i**, biotransformation):



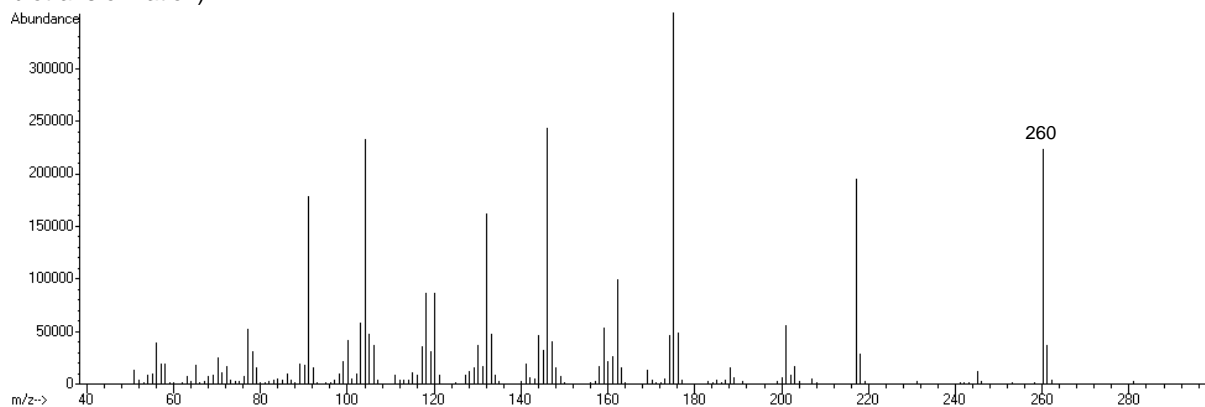
Mass spectrum of acetylated 2-methyl-1,4-diazepane (**2i**, biotransformation):



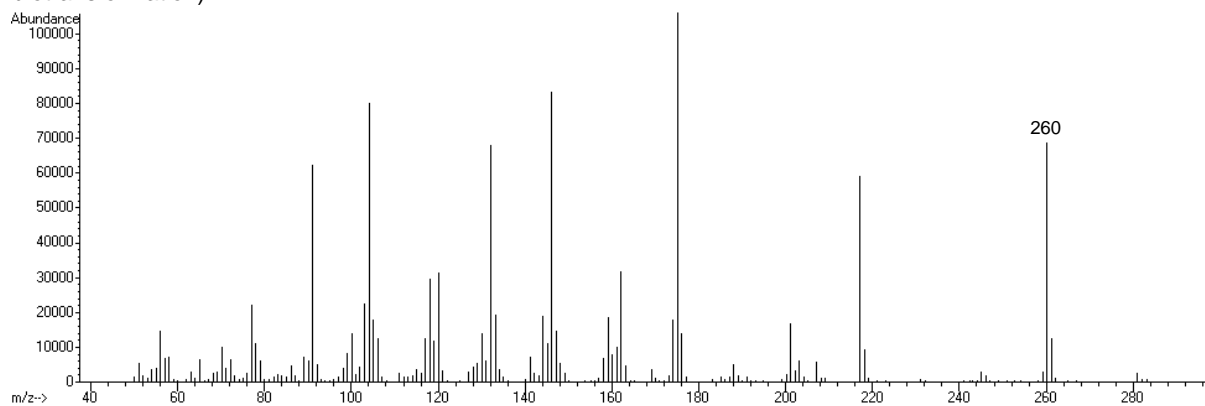
Chromatogram of acetylated 2-methyl-5-phenylpiperazine and/or 2-methyl-6-phenylpiperazine (**3b**, **3b***, biotransformation):



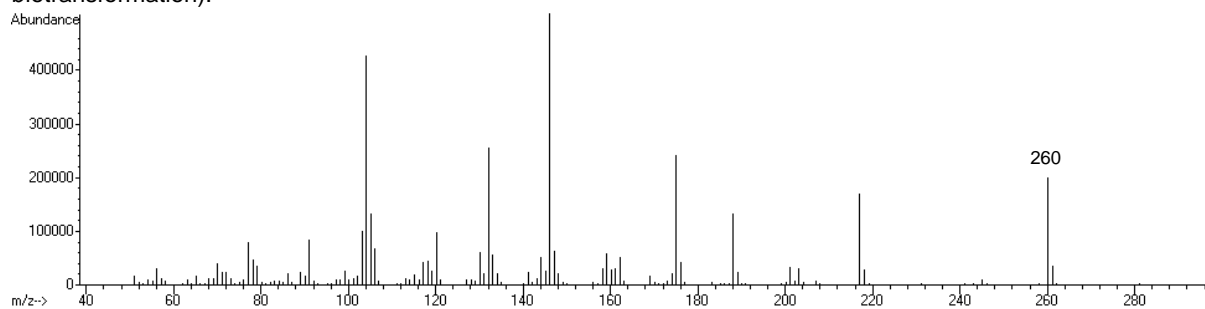
Mass spectrum of acetylated 2-methyl-5-phenylpiperazine and/or 2-methyl-6-phenylpiperazine (**3b**, **3b***, peak 1 biotransformation):



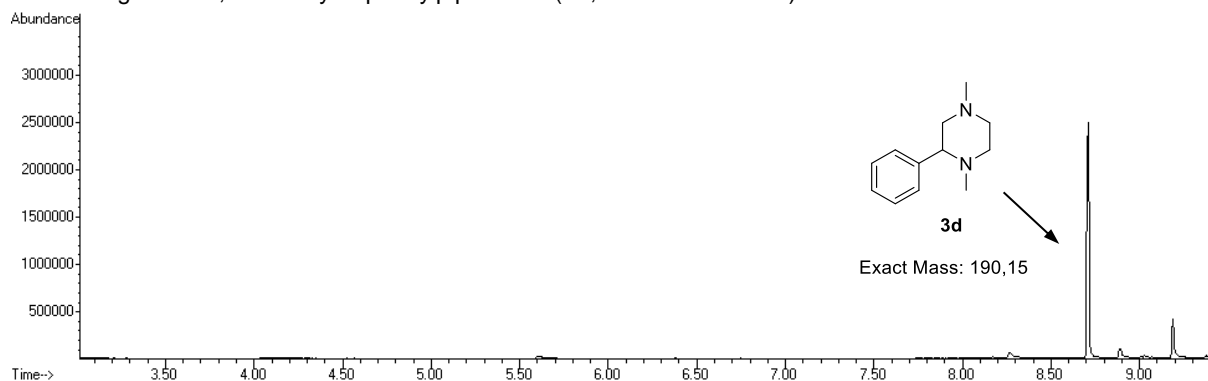
Mass spectrum of acetylated 2-methyl-5-phenylpiperazine and/or 2-methyl-6-phenylpiperazine (**3b**, **3b***, peak 2 biotransformation):



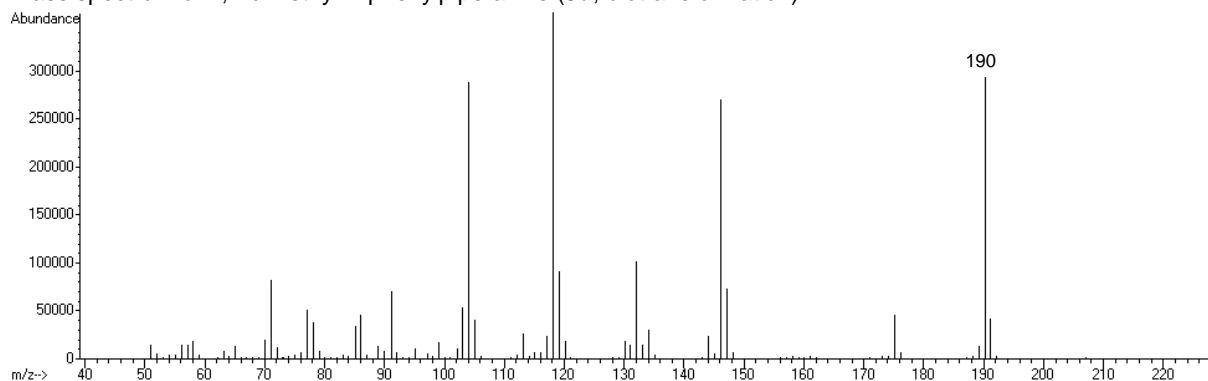
Mass spectrum of acetylated 2-methyl-5-phenylpiperazine and/or 2-methyl-6-phenylpiperazine (**3b**, **3b***, peak 3 biotransformation):



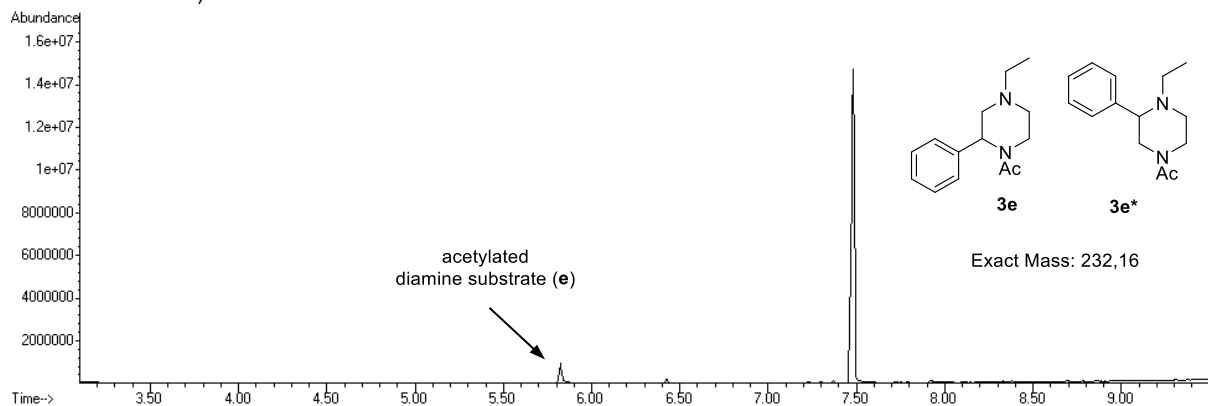
Chromatogram of 1,4-dimethyl-2-phenylpiperazine (**3d**, biotransformation):



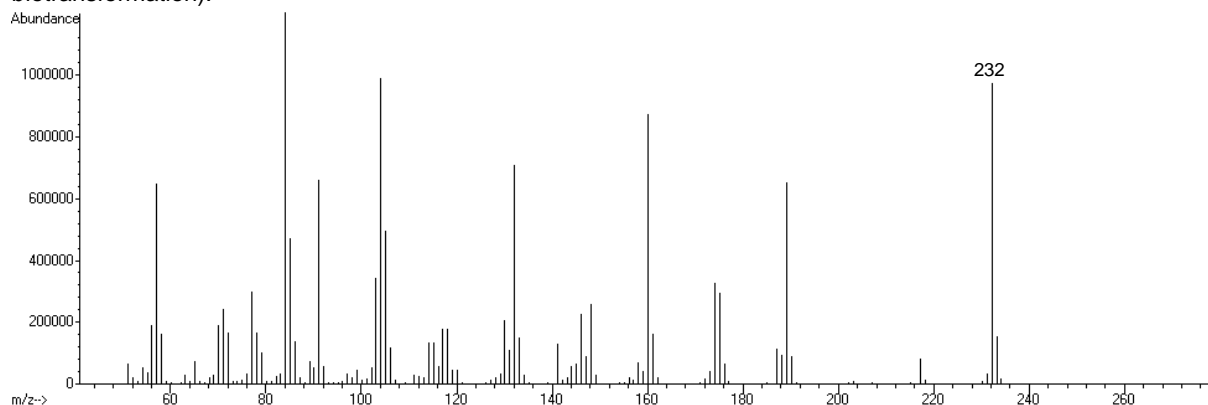
Mass spectrum of 1,4-dimethyl-2-phenylpiperazine (**3d**, biotransformation):



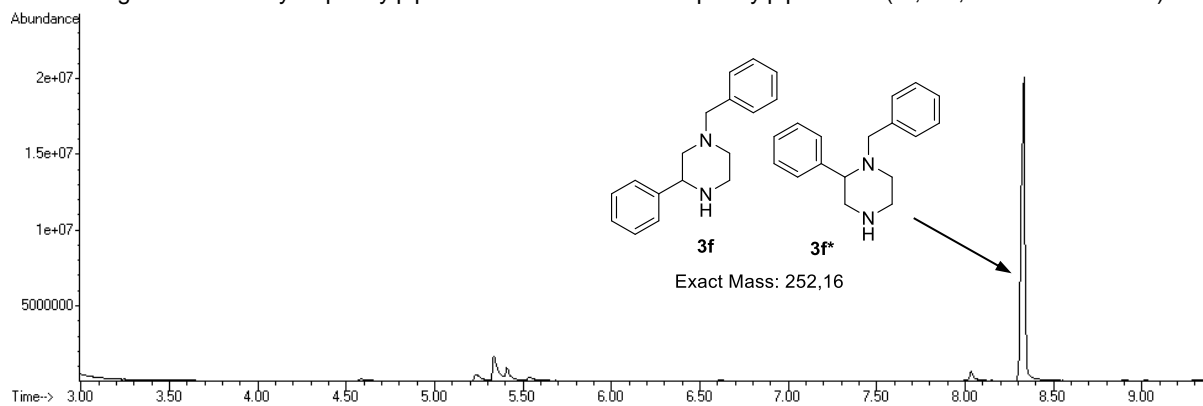
Chromatogram of acetylated 1-ethyl-3-phenylpiperazine and/or 1-ethyl-2-phenylpiperazine (**3e**, **3e***, biotransformation):



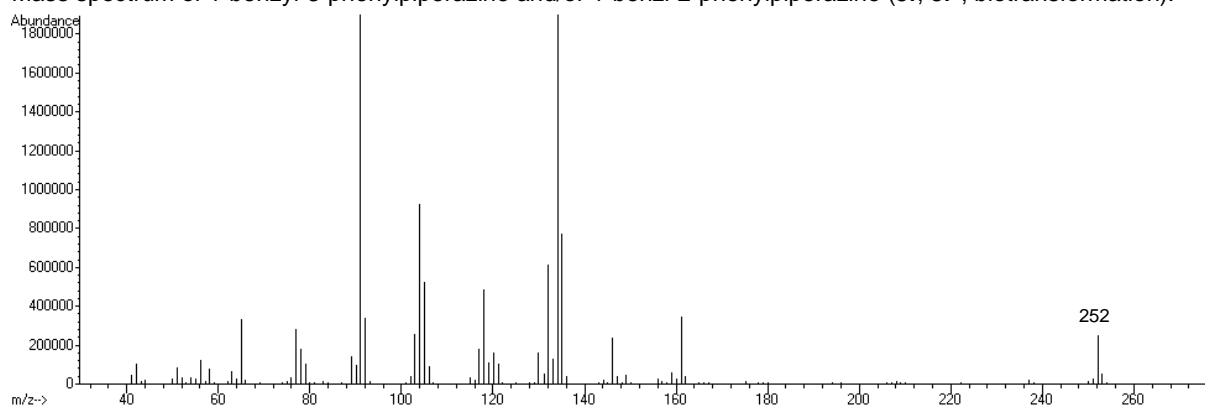
Mass spectrum of acetylated 1-ethyl-3-phenylpiperazine and/or 1-ethyl-2-phenylpiperazine (**3e**, **3e***, biotransformation):



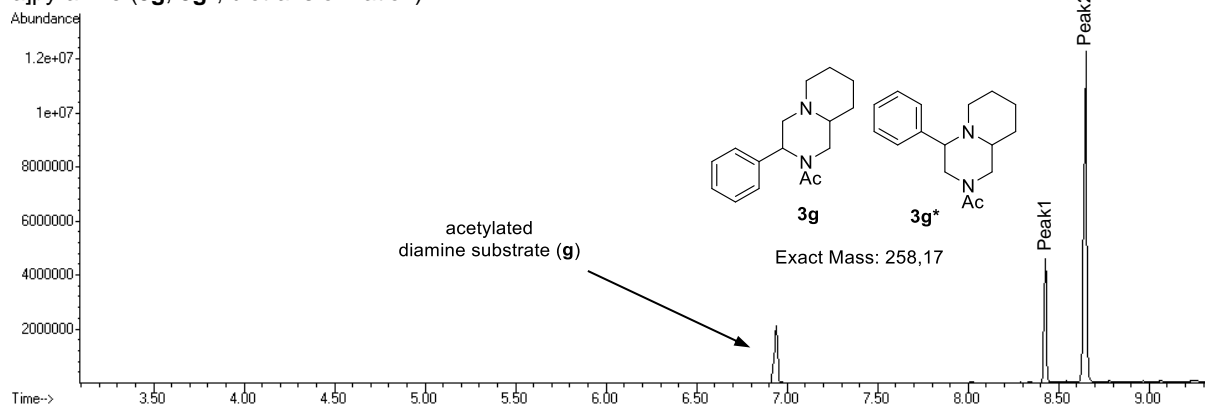
Chromatogram of 1-benzyl-3-phenylpiperazine and/or 1-benzyl-2-phenylpiperazine (**3f**, **3f***, biotransformation):



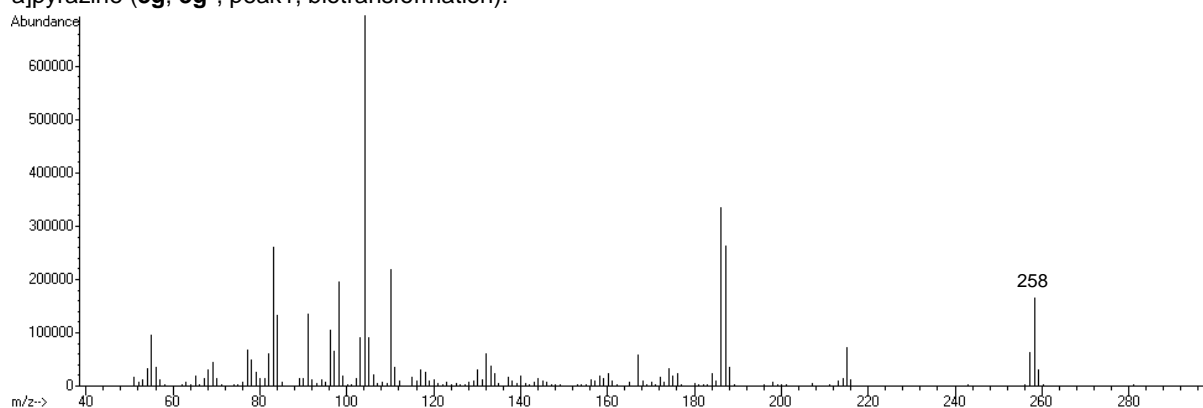
Mass spectrum of 1-benzyl-3-phenylpiperazine and/or 1-benzyl-2-phenylpiperazine (**3f**, **3f***, biotransformation):



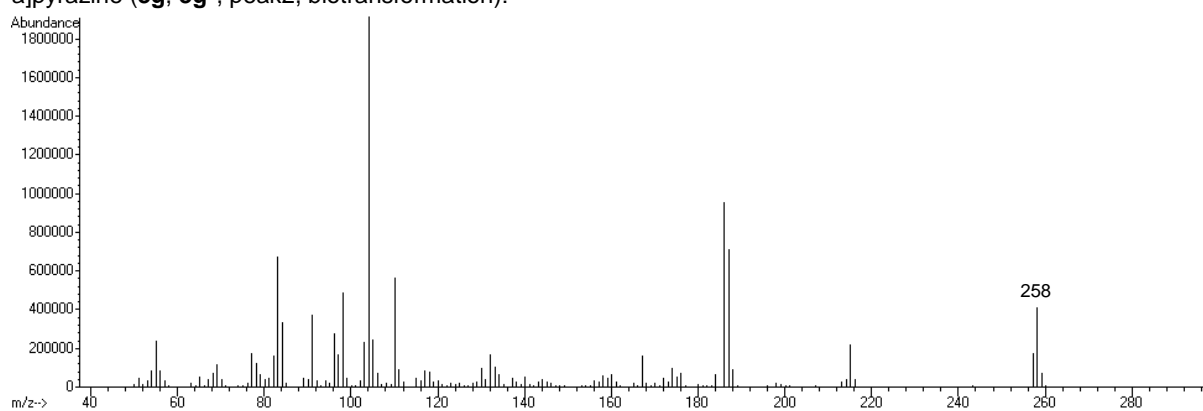
Chromatogram of acetylated 3-phenyloctahydro-2H-pyrido[1,2-a]pyrazine and/or 4-phenyloctahydro-2H-pyrido[1,2-a]pyrazine (**3g**, **3g***, biotransformation):



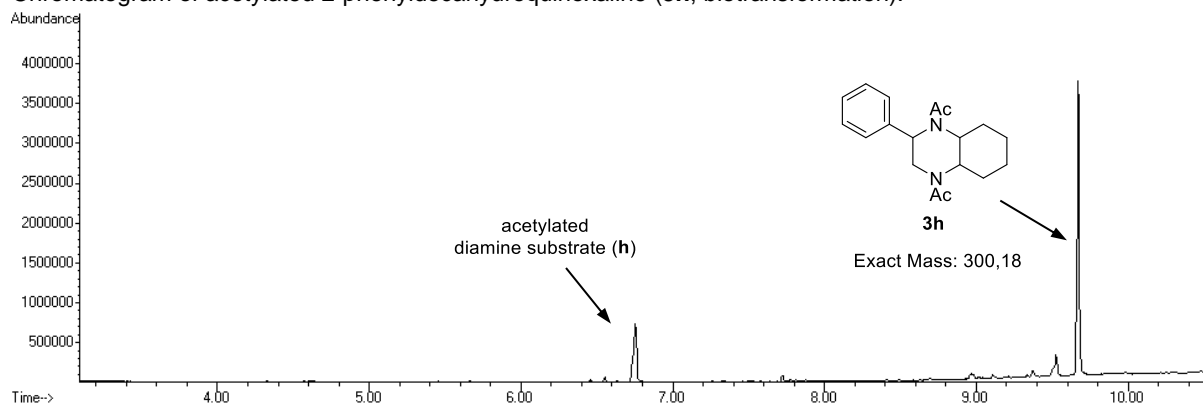
Mass spectrum of acetylated 3-phenyloctahydro-2H-pyrido[1,2-a]pyrazine and/or 4-phenyloctahydro-2H-pyrido[1,2-a]pyrazine (**3g**, **3g***, peak1, biotransformation):



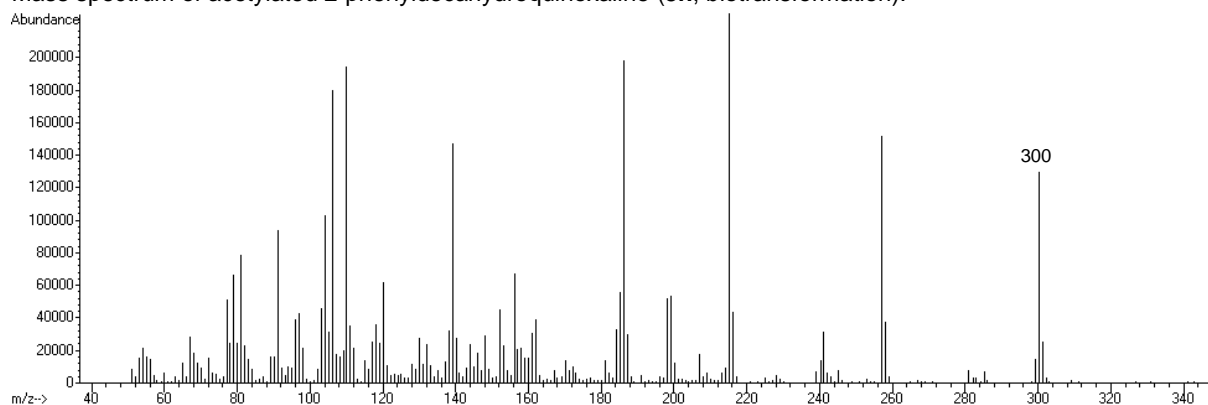
Mass spectrum of acetylated 3-phenyloctahydro-2H-pyrido[1,2-a]pyrazine and/or 4-phenyloctahydro-2H-pyrido[1,2-a]pyrazine (**3g**, **3g***, peak2, biotransformation):



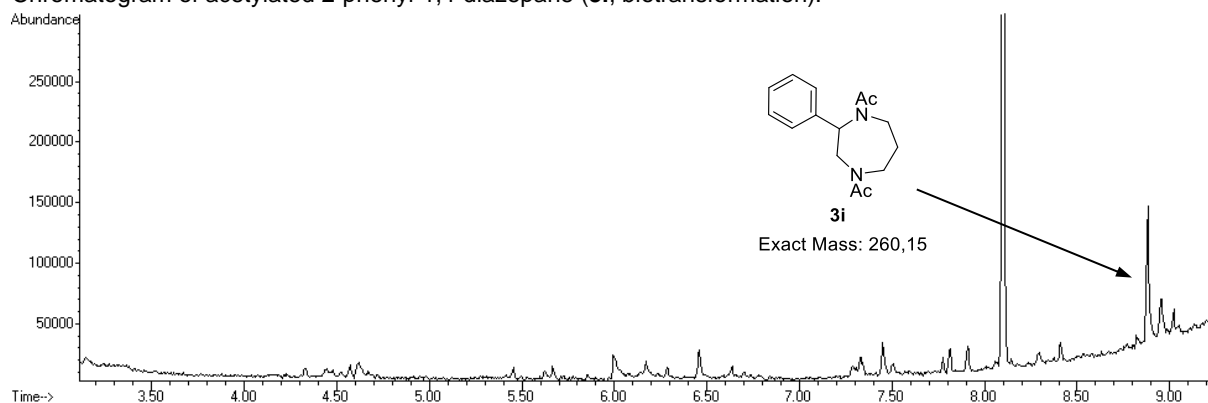
Chromatogram of acetylated 2-phenyldecahydroquinoxaline (**3h**, biotransformation):



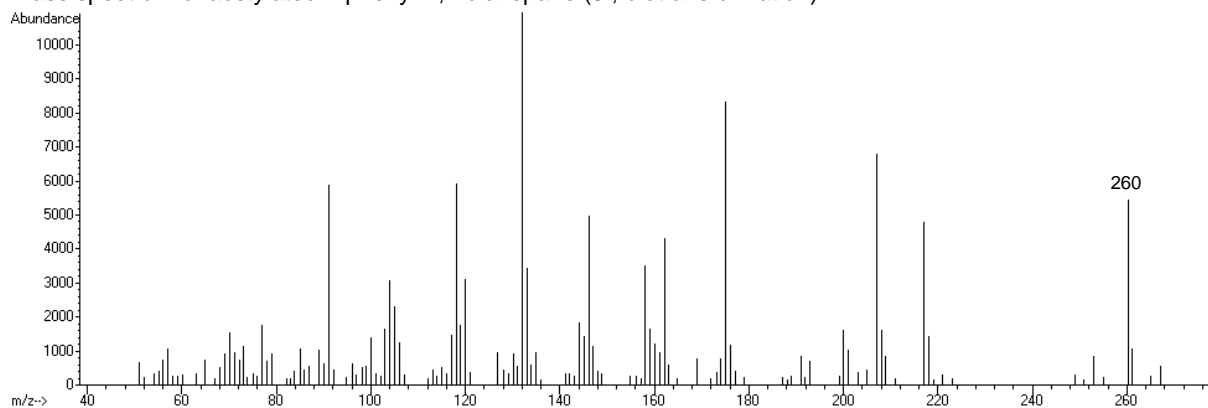
Mass spectrum of acetylated 2-phenyldecahydroquinoxaline (**3h**, biotransformation):



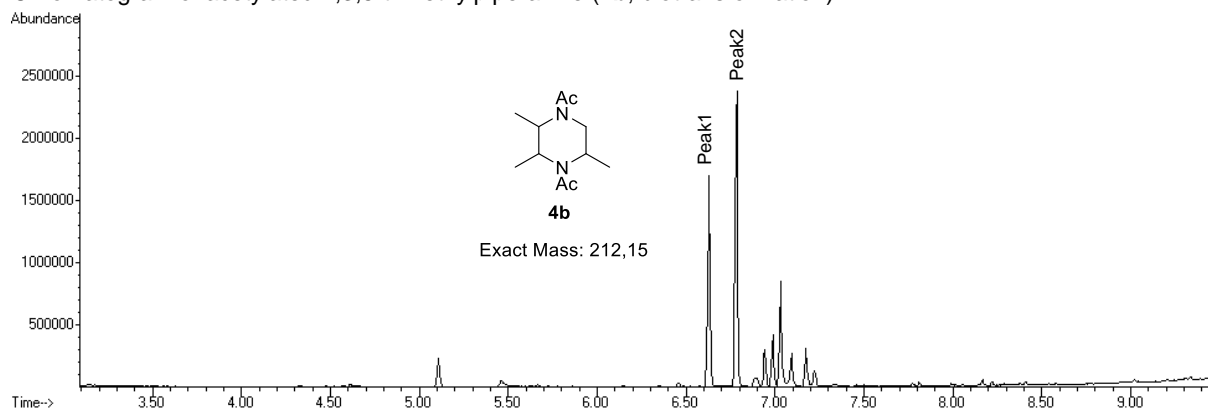
Chromatogram of acetylated 2-phenyl-1,4-diazepane (**3i**, biotransformation):



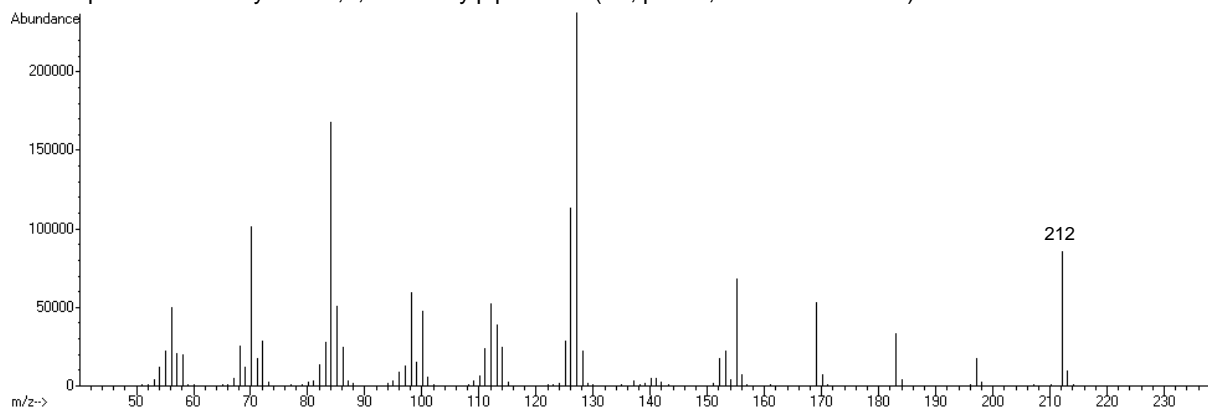
Mass spectrum of acetylated 2-phenyl-1,4-diazepane (**3i**, biotransformation):



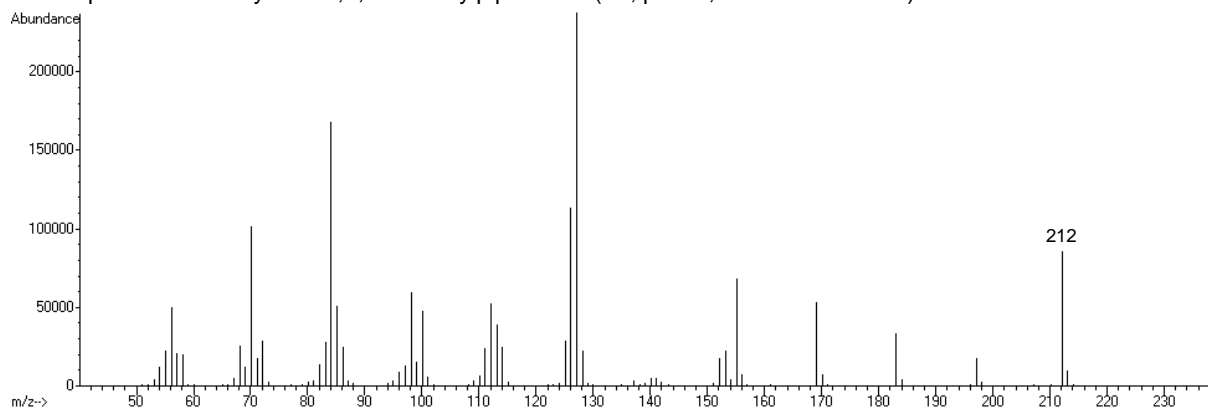
Chromatogram of acetylated 2,3,5-trimethylpiperazine (**4b**, biotransformation):



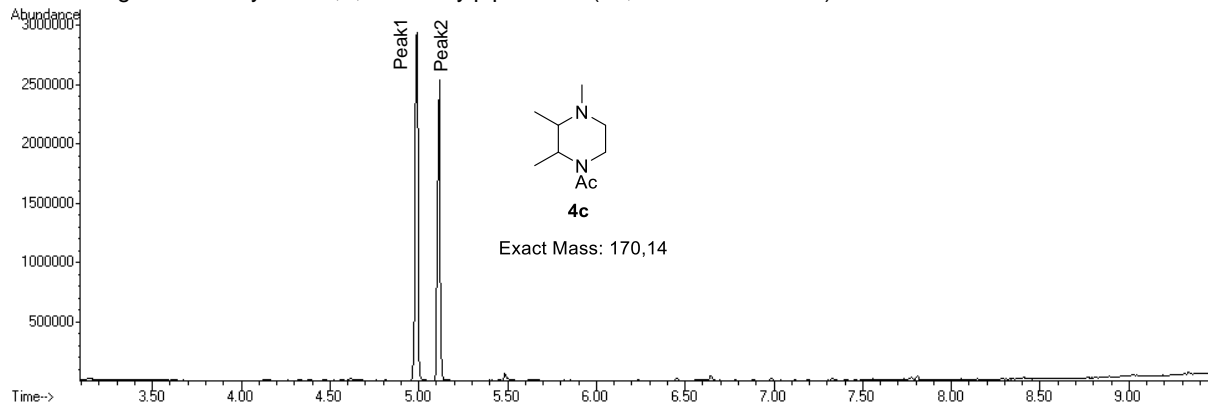
Mass spectrum of acetylated 2,3,5-trimethylpiperazine (**4b**, peak1, biotransformation):



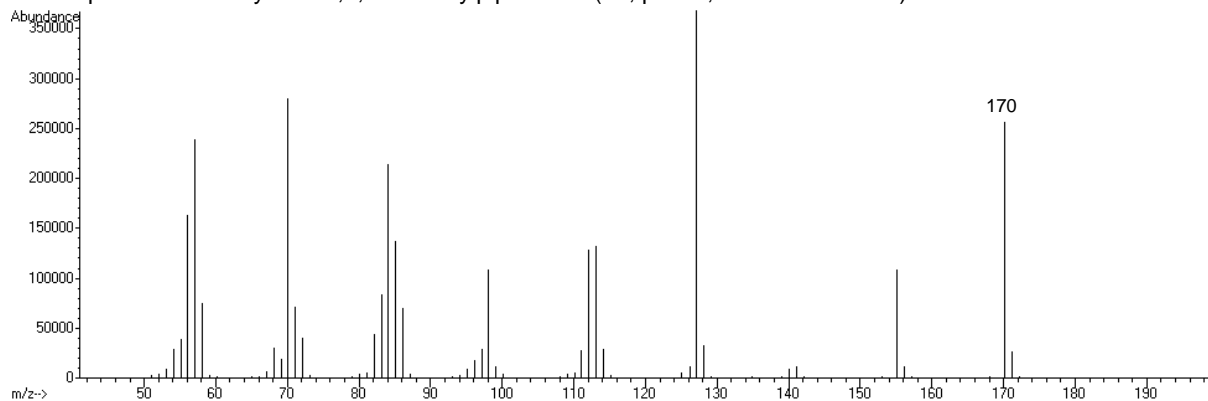
Mass spectrum of acetylated 2,3,5-trimethylpiperazine (**4b**, peak2, biotransformation):



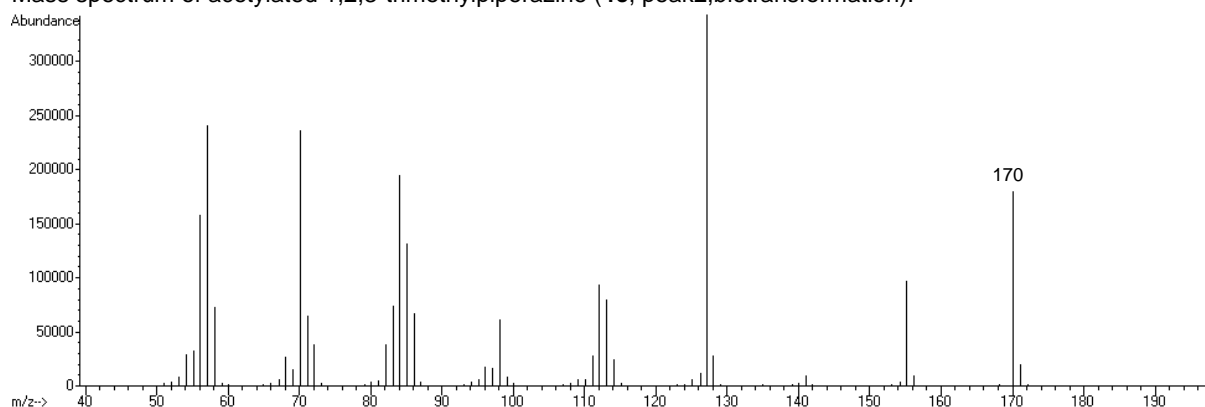
Chromatogram of acetylated 1,2,3-trimethylpiperazine (**4c**, biotransformation):



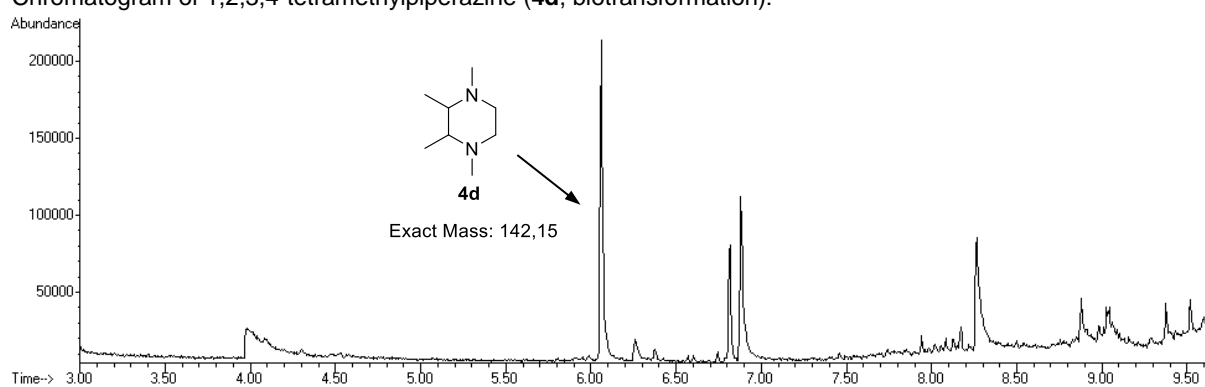
Mass spectrum of acetylated 1,2,3-trimethylpiperazine (**4c**, peak1, biotransformation):



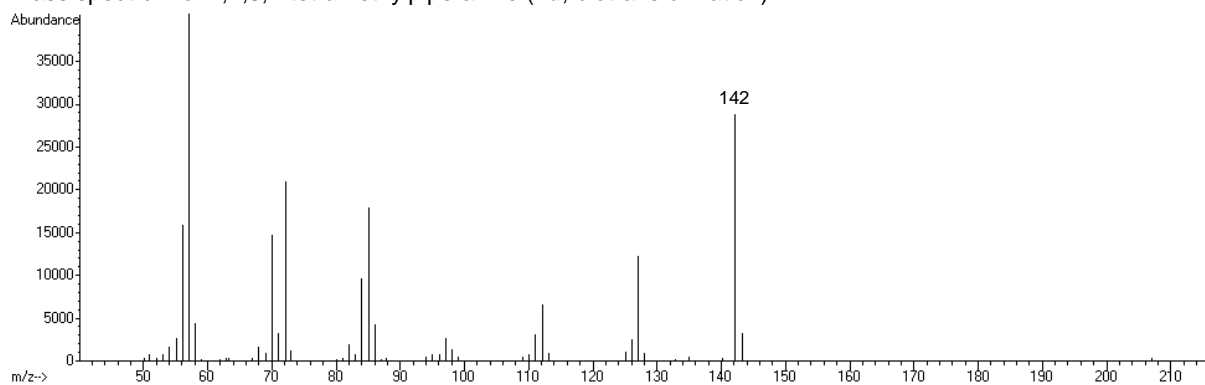
Mass spectrum of acetylated 1,2,3-trimethylpiperazine (**4c**, peak2,biotransformation):



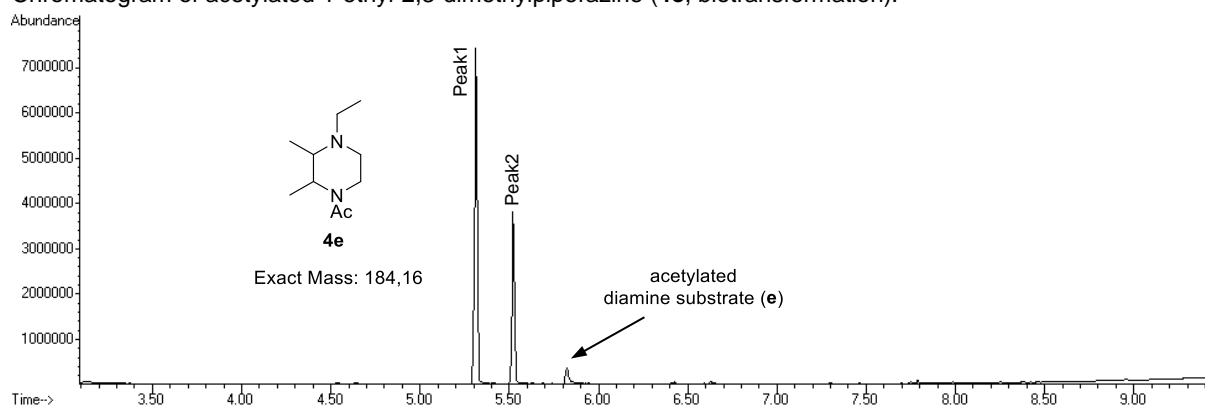
Chromatogram of 1,2,3,4-tetramethylpiperazine (**4d**, biotransformation):



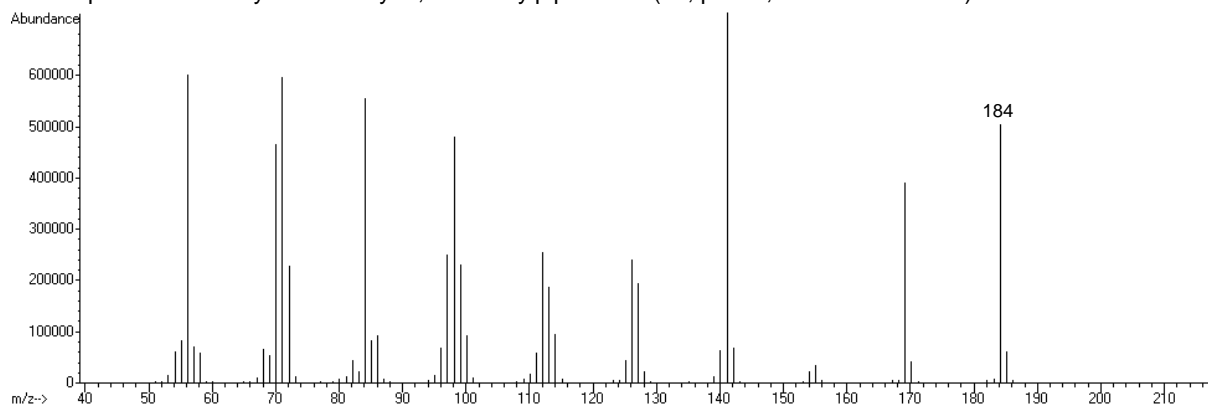
Mass spectrum of 1,2,3,4-tetramethylpiperazine (**4d**, biotransformation):



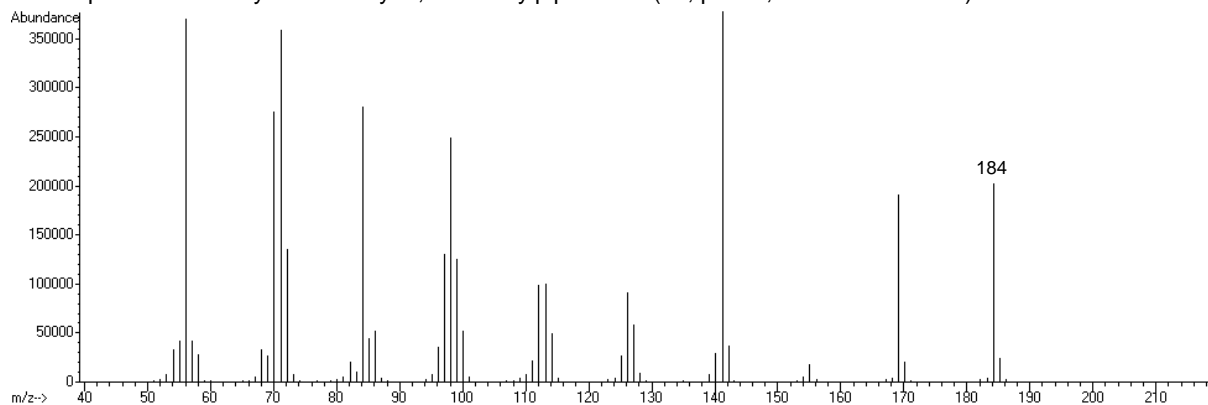
Chromatogram of acetylated 1-ethyl-2,3-dimethylpiperazine (**4e**, biotransformation):



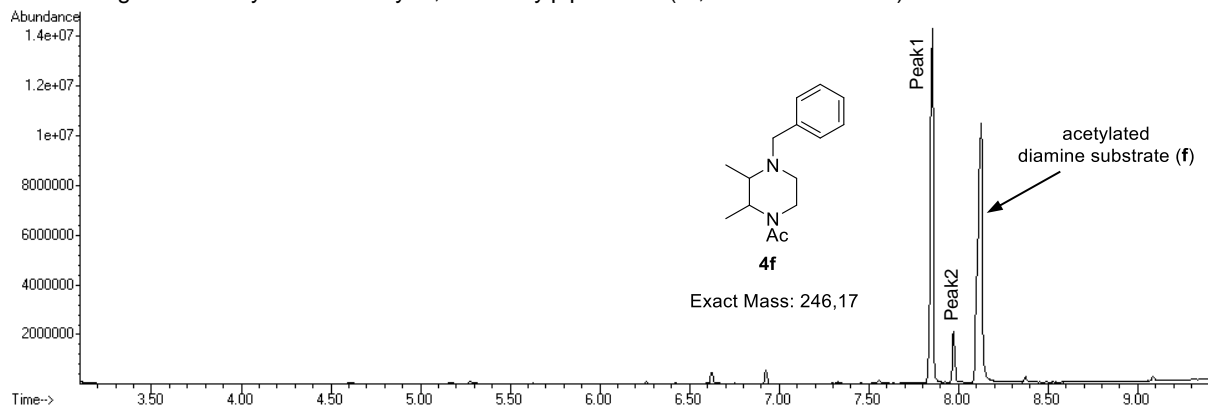
Mass spectrum of acetylated 1-ethyl-2,3-dimethylpiperazine (**4e**, peak1, biotransformation):



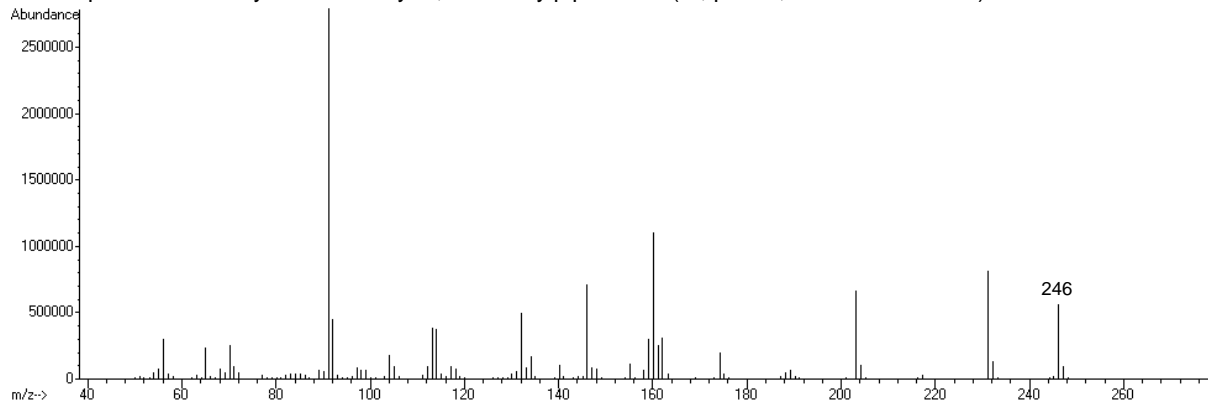
Mass spectrum of acetylated 1-ethyl-2,3-dimethylpiperazine (**4e**, peak2, biotransformation):



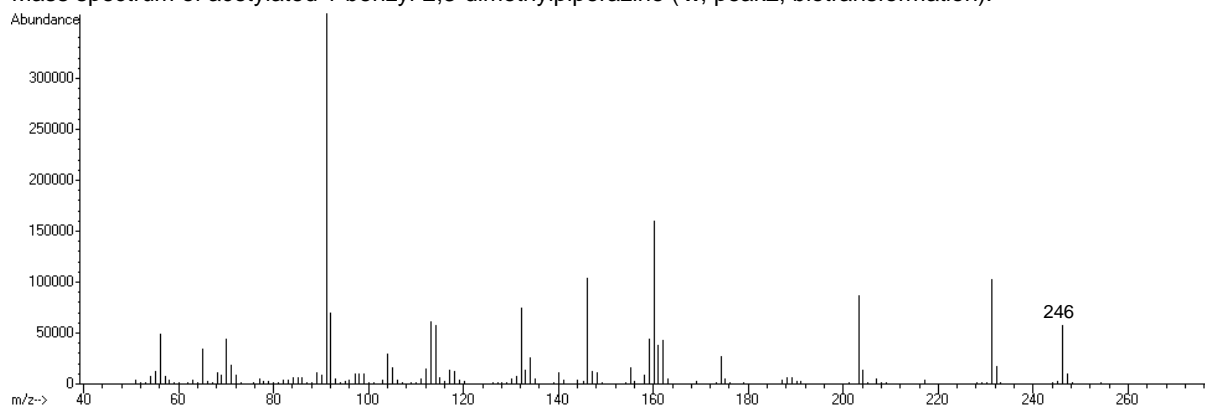
Chromatogram of acetylated 1-benzyl-2,3-dimethylpiperazine (**4f**, biotransformation):



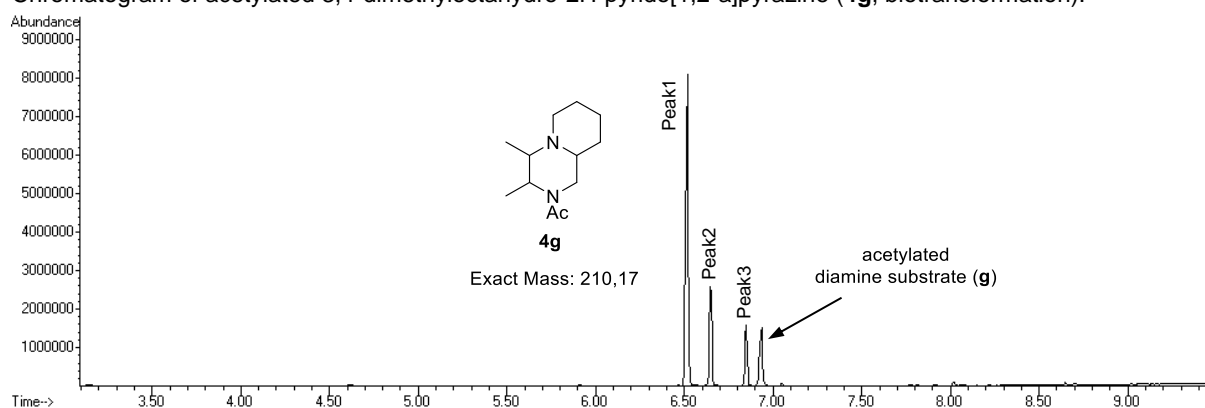
Mass spectrum of acetylated 1-benzyl-2,3-dimethylpiperazine (**4f**, peak1, biotransformation):



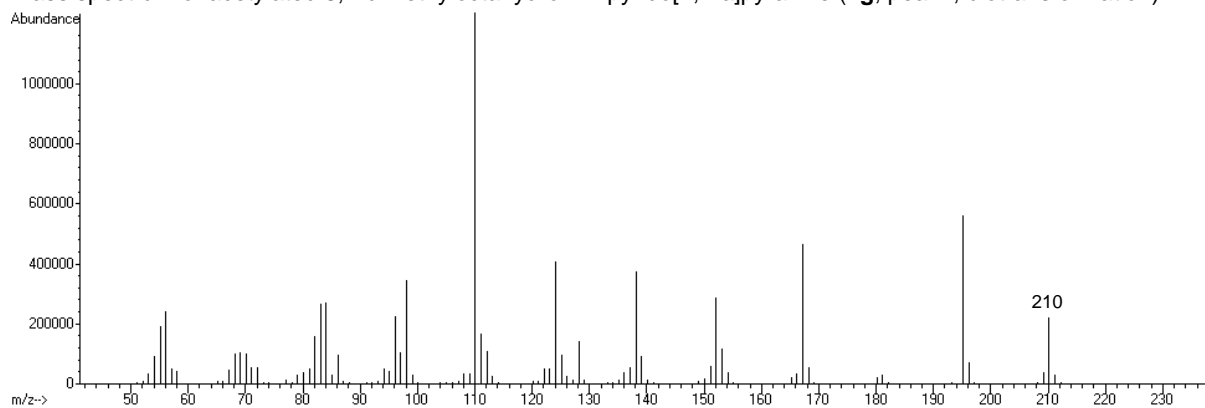
Mass spectrum of acetylated 1-benzyl-2,3-dimethylpiperazine (**4f**, peak2, biotransformation):



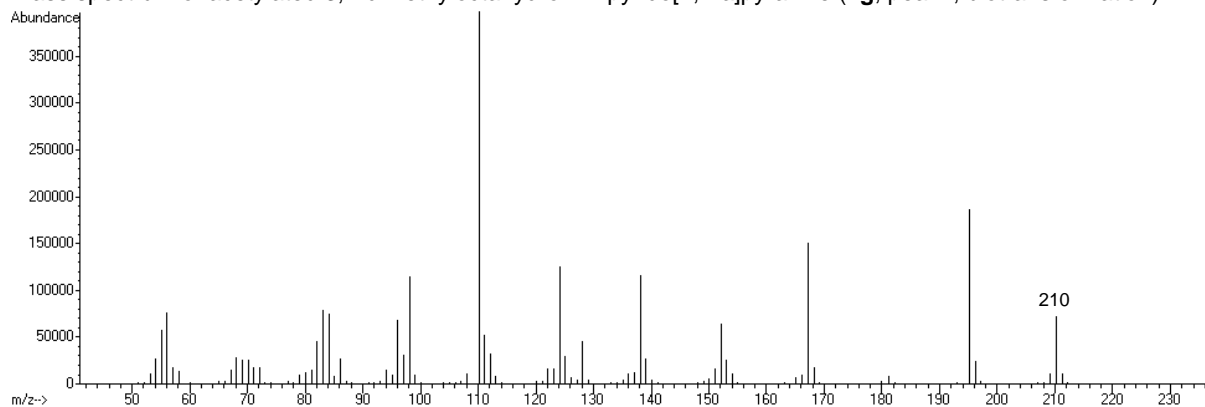
Chromatogram of acetylated 3,4-dimethyloctahydro-2H-pyrido[1,2-a]pyrazine (**4g**, biotransformation):



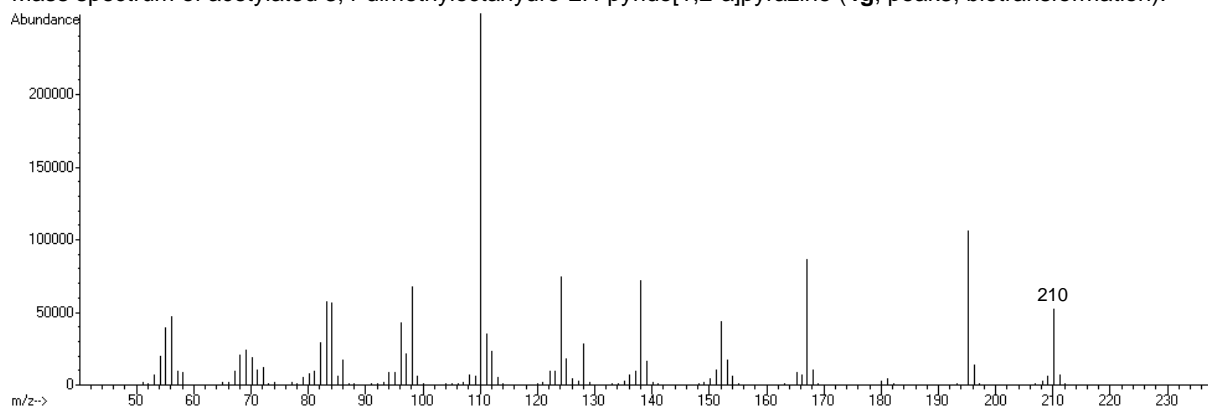
Mass spectrum of acetylated 3,4-dimethyloctahydro-2H-pyrido[1,2-a]pyrazine (**4g**, peak1, biotransformation):



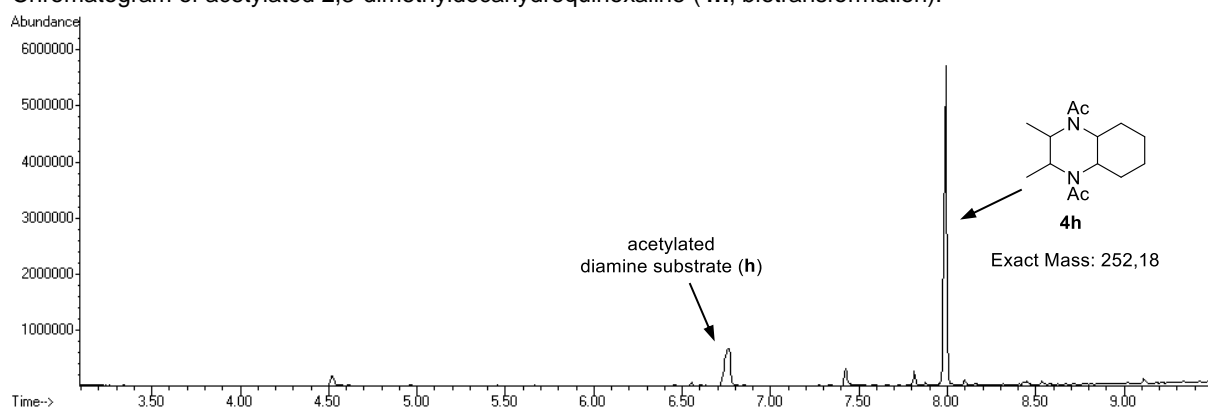
Mass spectrum of acetylated 3,4-dimethyloctahydro-2H-pyrido[1,2-a]pyrazine (**4g**, peak2, biotransformation):



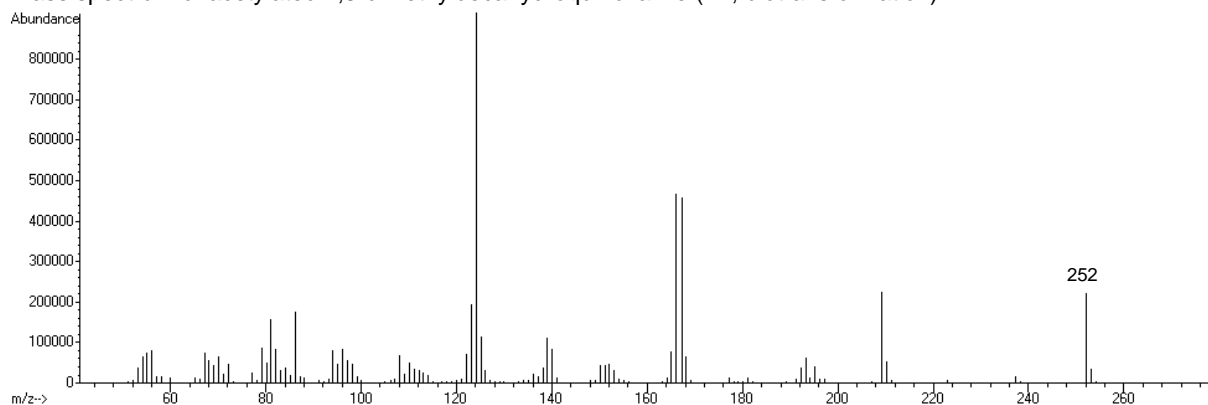
Mass spectrum of acetylated 3,4-dimethyloctahydro-2H-pyrido[1,2-a]pyrazine (**4g**, peak3, biotransformation):



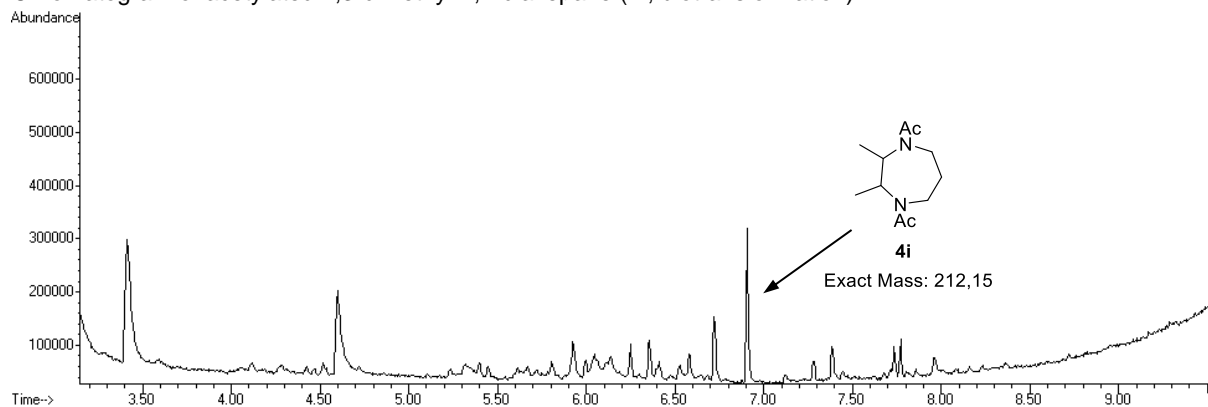
Chromatogram of acetylated 2,3-dimethyldecahydroquinoxaline (**4h**, biotransformation):



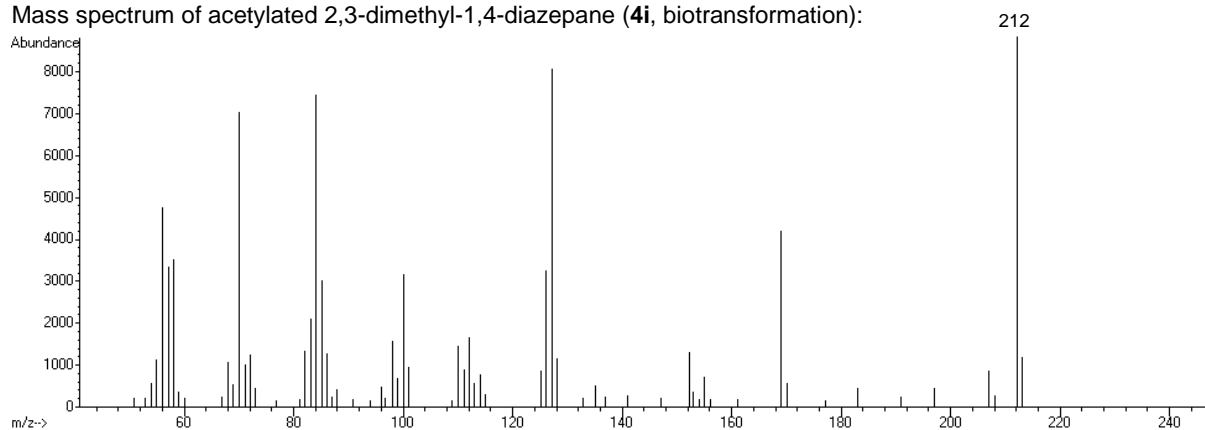
Mass spectrum of acetylated 2,3-dimethyldecahydroquinoxaline (**4h**, biotransformation):



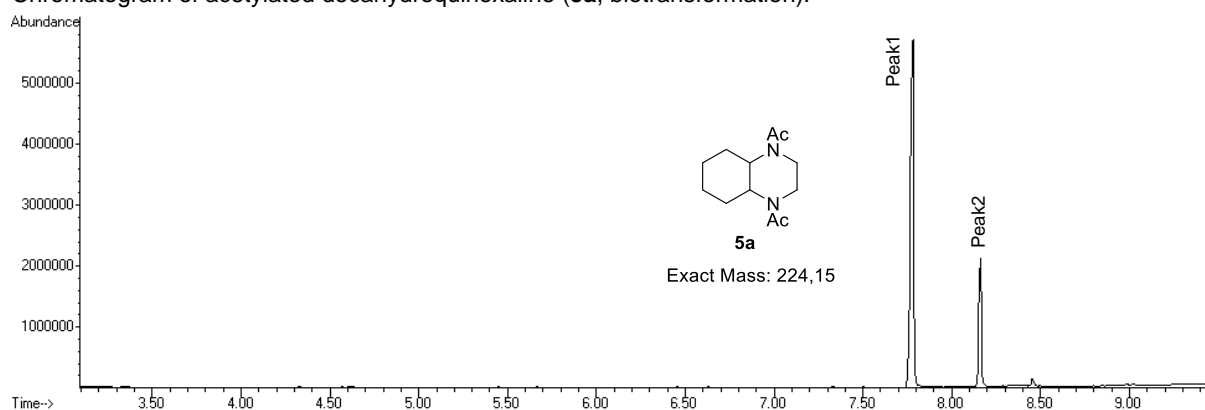
Chromatogram of acetylated 2,3-dimethyl-1,4-diazepane (**4i**, biotransformation):



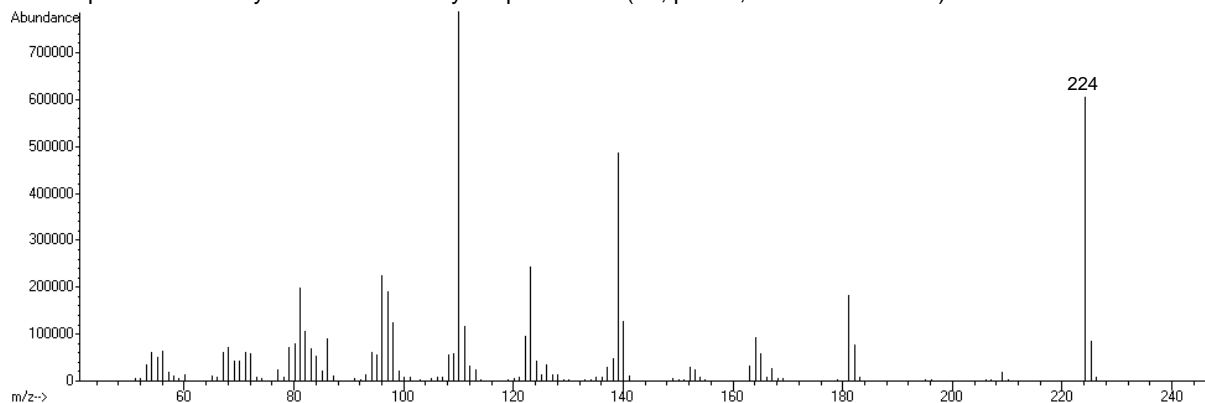
Mass spectrum of acetylated 2,3-dimethyl-1,4-diazepane (**4i**, biotransformation):



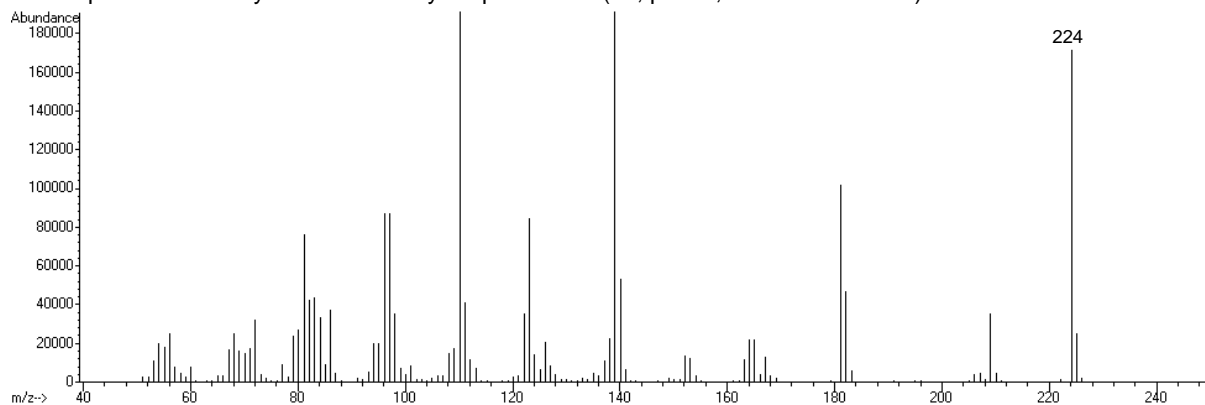
Chromatogram of acetylated decahydroquinoxaline (**5a**, biotransformation):



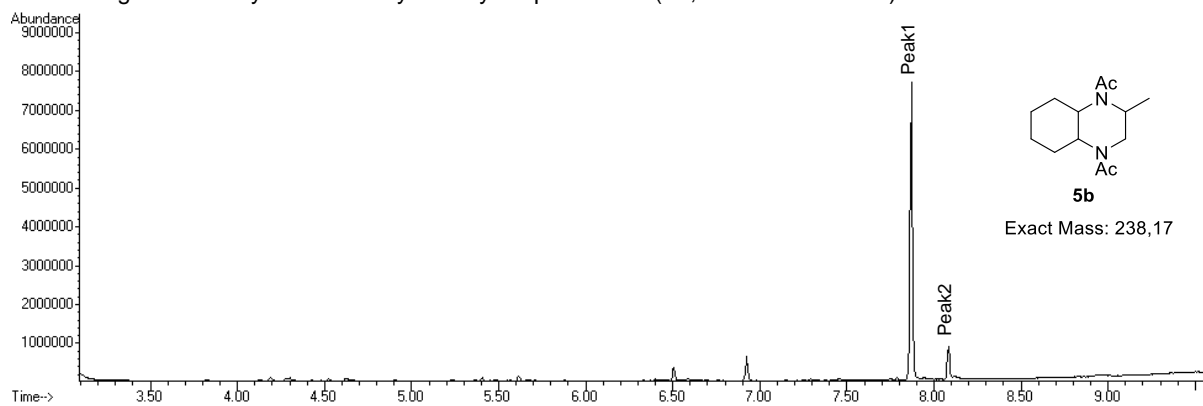
Mass spectrum of acetylated *trans*-decahydroquinoxaline (**5a**, peak1, biotransformation):



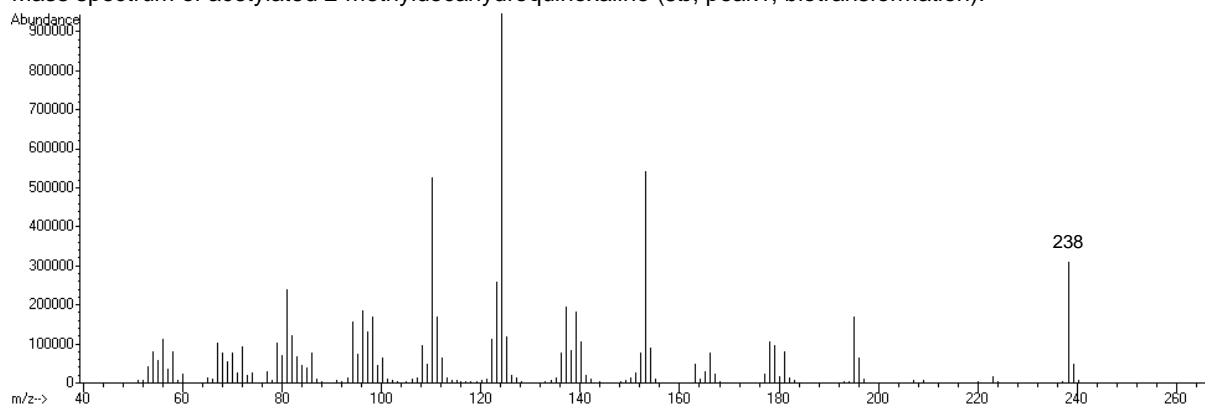
Mass spectrum of acetylated *cis*-decahydroquinoxaline (**5a**, peak2, biotransformation):



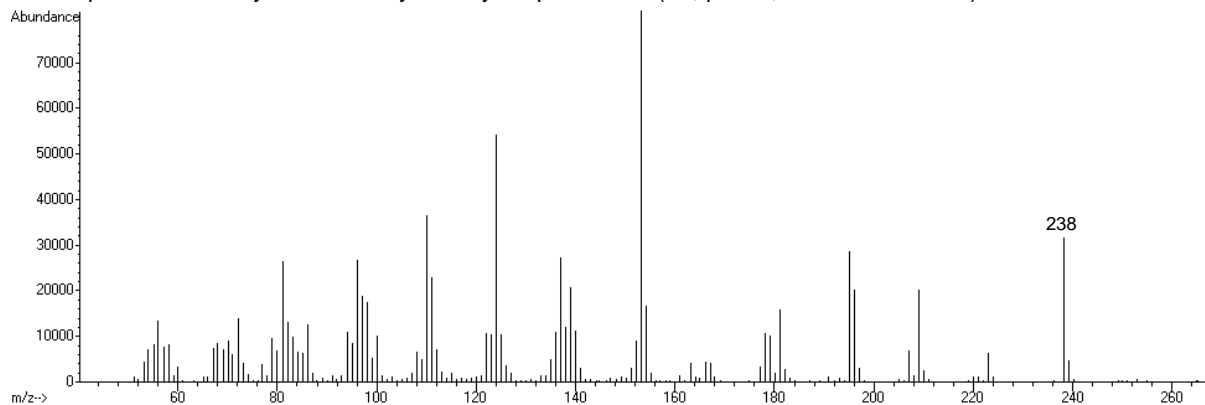
Chromatogram of acetylated 2-methyldecahydroquinoxaline (**5b**, biotransformation):



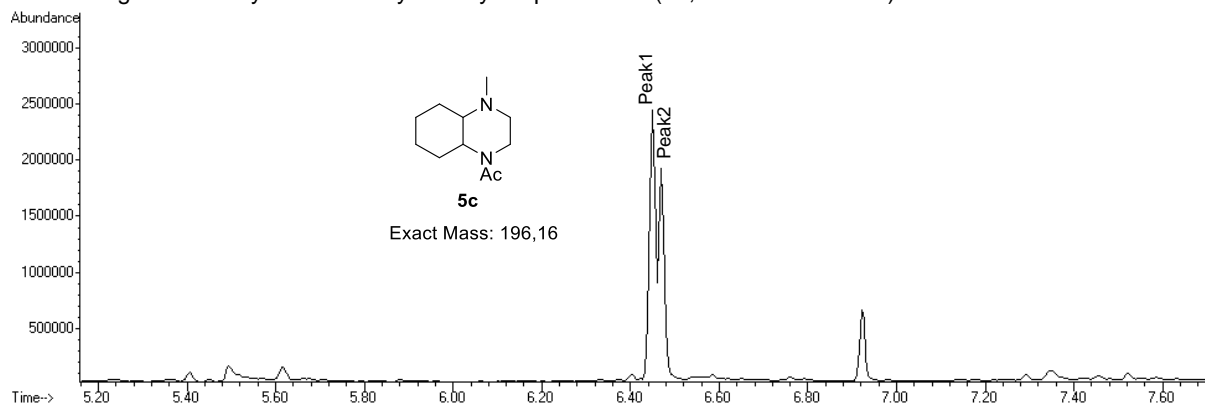
Mass spectrum of acetylated 2-methyldecahydroquinoxaline (**5b**, peak1, biotransformation):



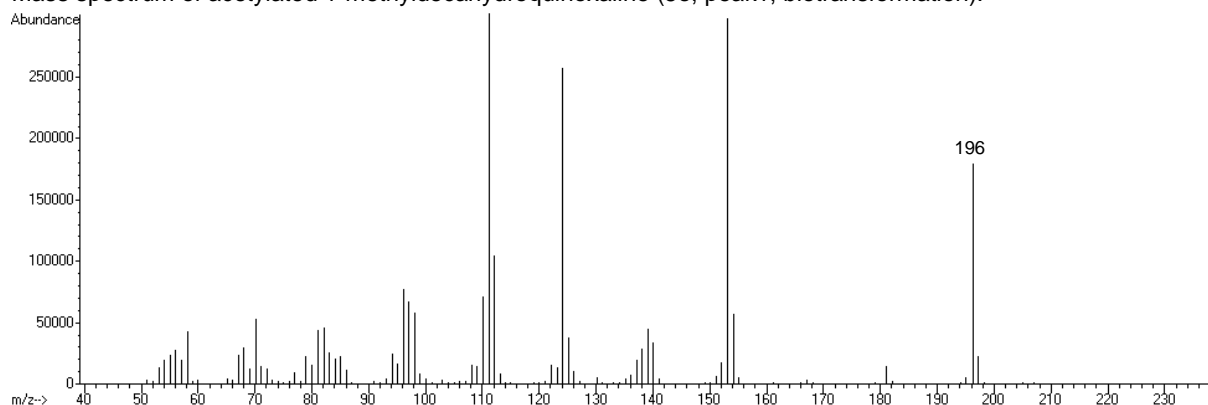
Mass spectrum of acetylated 2-methyldecahydroquinoxaline (**5b**, peak2, biotransformation):



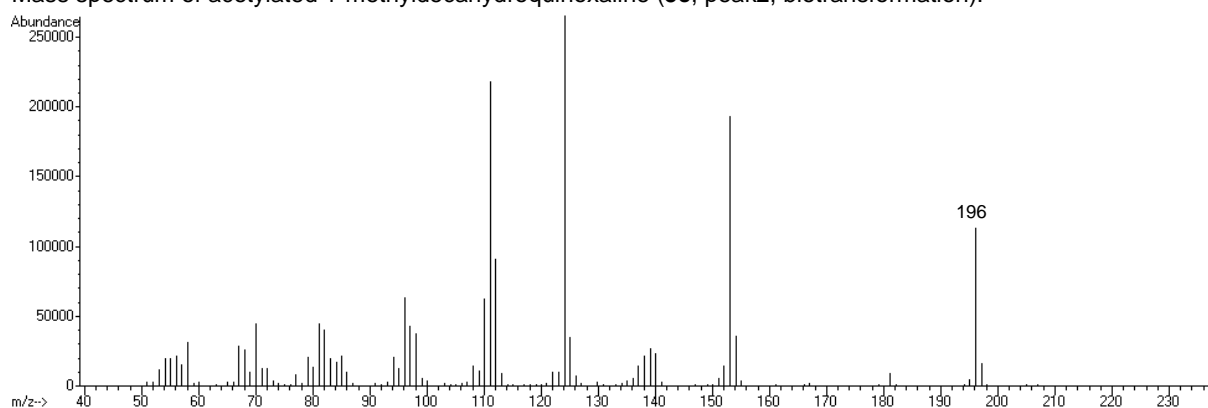
Chromatogram of acetylated 1-methyldecahydroquinoxaline (**5c**, biotransformation):



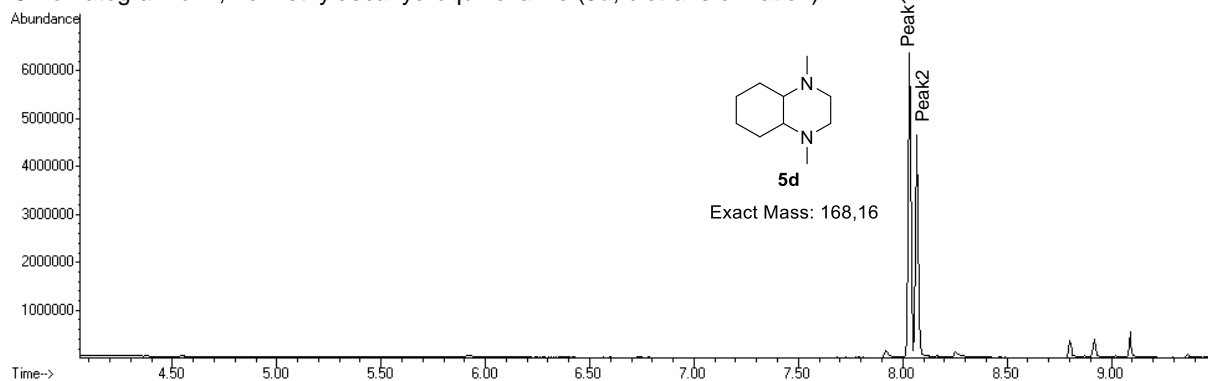
Mass spectrum of acetylated 1-methyldecahydroquinoxaline (**5c**, peak1, biotransformation):



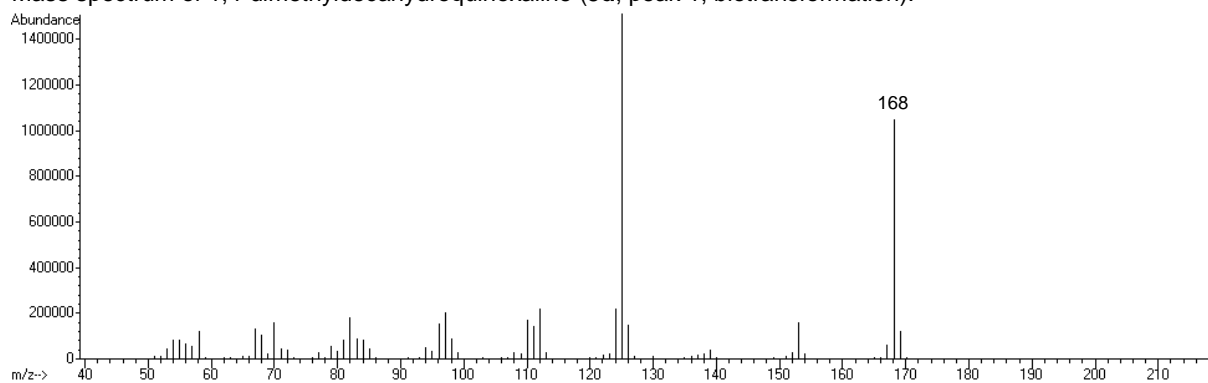
Mass spectrum of acetylated 1-methyldecahydroquinoxaline (**5c**, peak2, biotransformation):



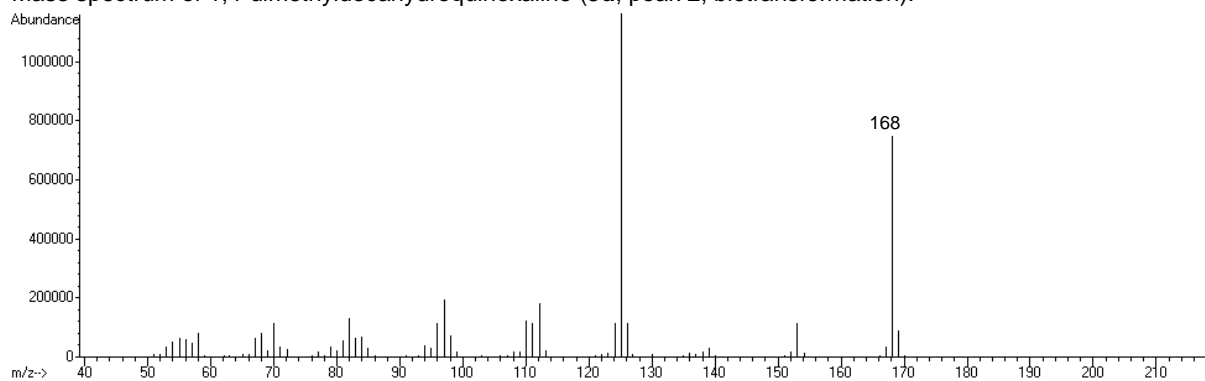
Chromatogram of 1,4-dimethyldecahydroquinoxaline (**5d**, biotransformation):



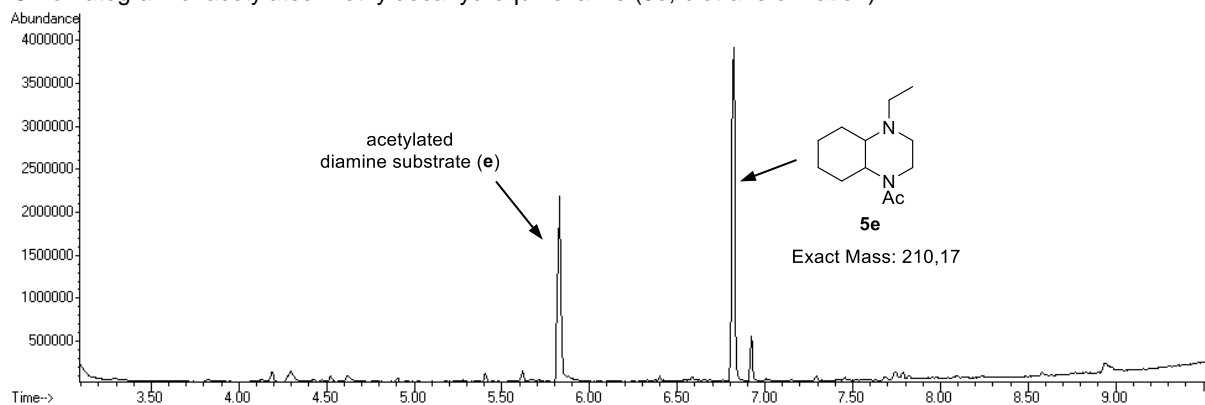
Mass spectrum of 1,4-dimethyldecahydroquinoxaline (**5d**, peak 1, biotransformation):



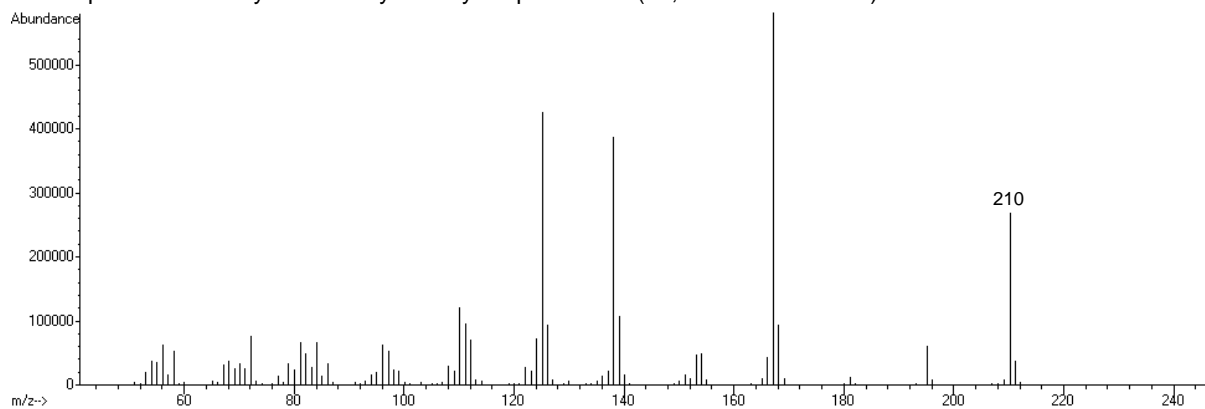
Mass spectrum of 1,4-dimethyldecahydroquinoxaline (**5d**, peak 2, biotransformation):



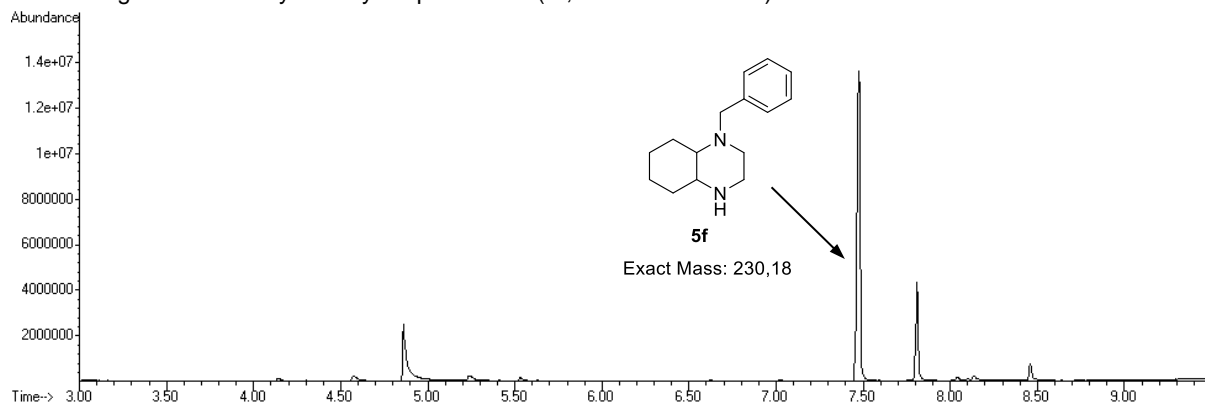
Chromatogram of acetylated 1-ethyldecahydroquinoxaline (**5e**, biotransformation):



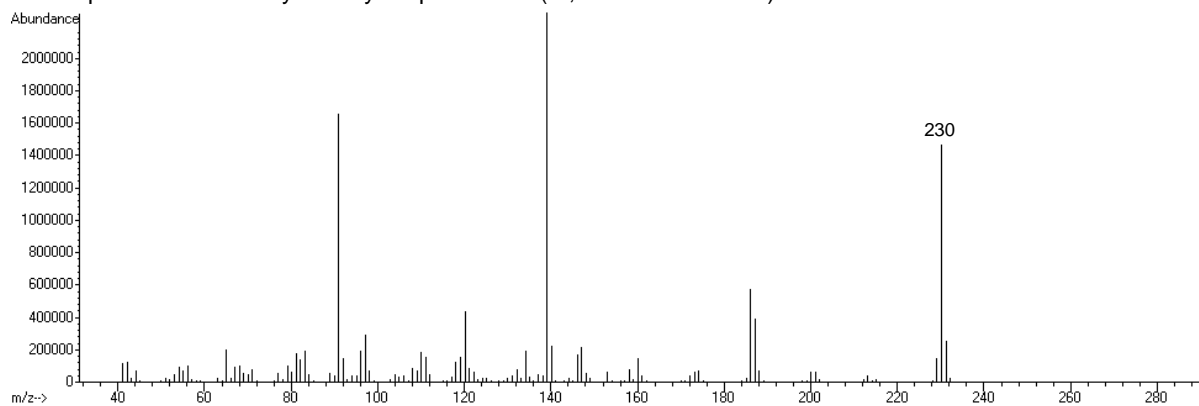
Mass spectrum of acetylated 1-ethyldecahydroquinoxaline (**5e**, biotransformation):



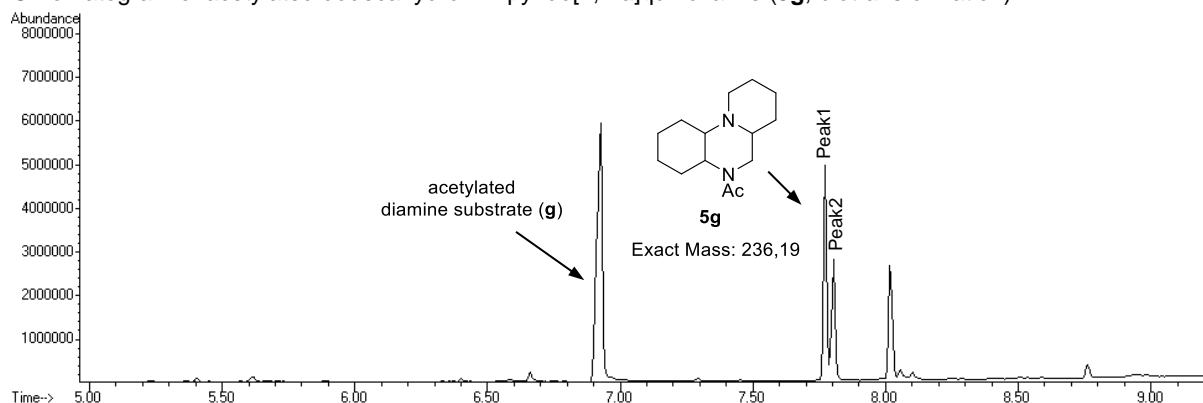
Chromatogram of 1-benzyldecahydroquinoxaline (**5f**, biotransformation):



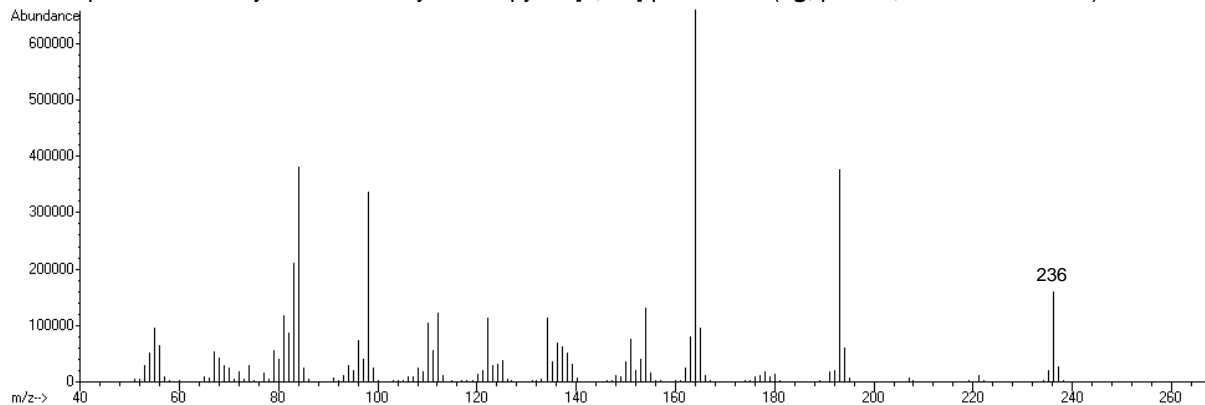
Mass spectrum of 1-benzyldecahydroquinoxaline (**5f**, biotransformation):



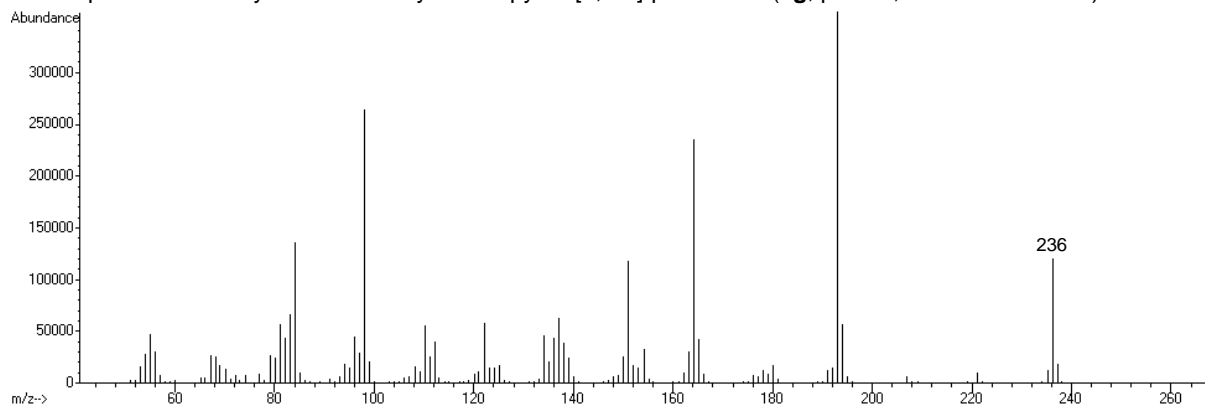
Chromatogram of acetylated dodecahydro-2H-pyrido[1,2-a]quinoxaline (**5g**, biotransformation):



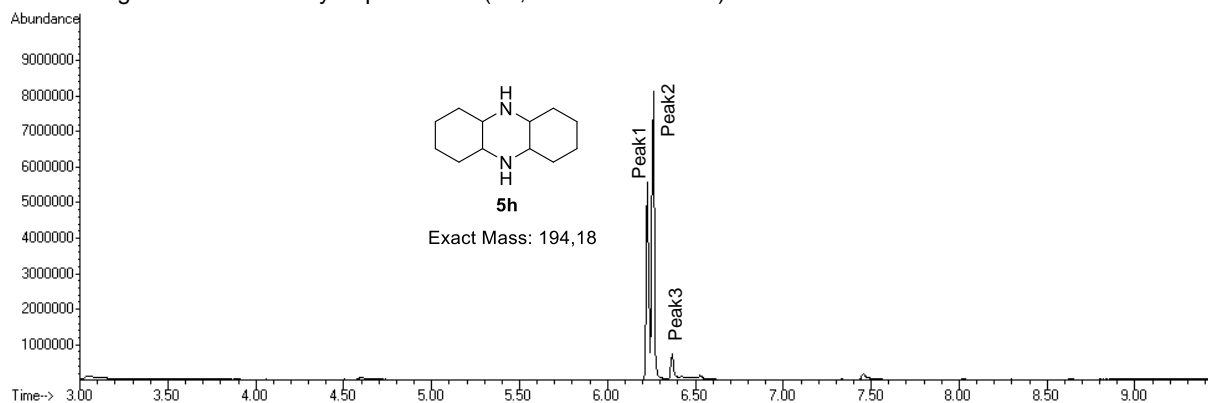
Mass spectrum of acetylated dodecahydro-2H-pyrido[1,2-a]quinoxaline (**5g**, peak 1, biotransformation):



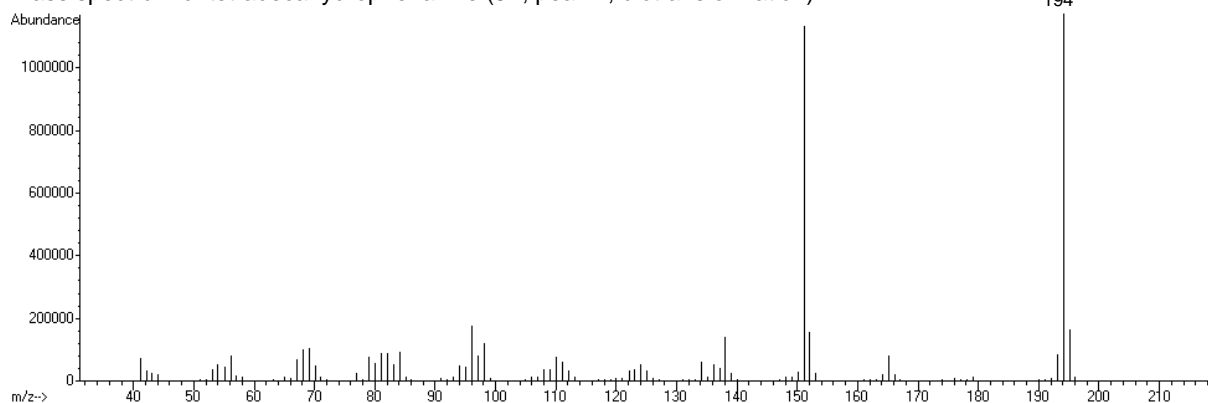
Mass spectrum of acetylated dodecahydro-2H-pyrido[1,2-a]quinoxaline (**5g**, peak 2, biotransformation):



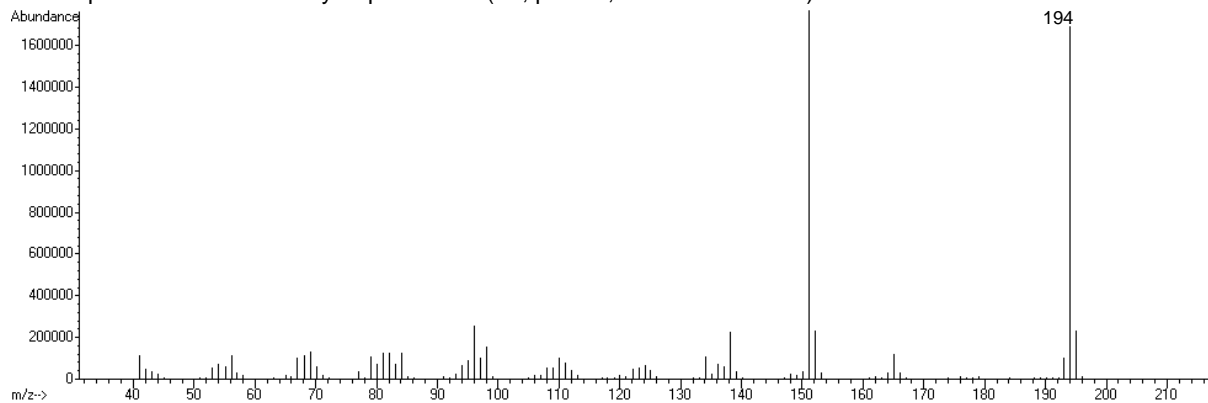
Chromatogram of tetradecahydrophenazine (**5h**, biotransformation):



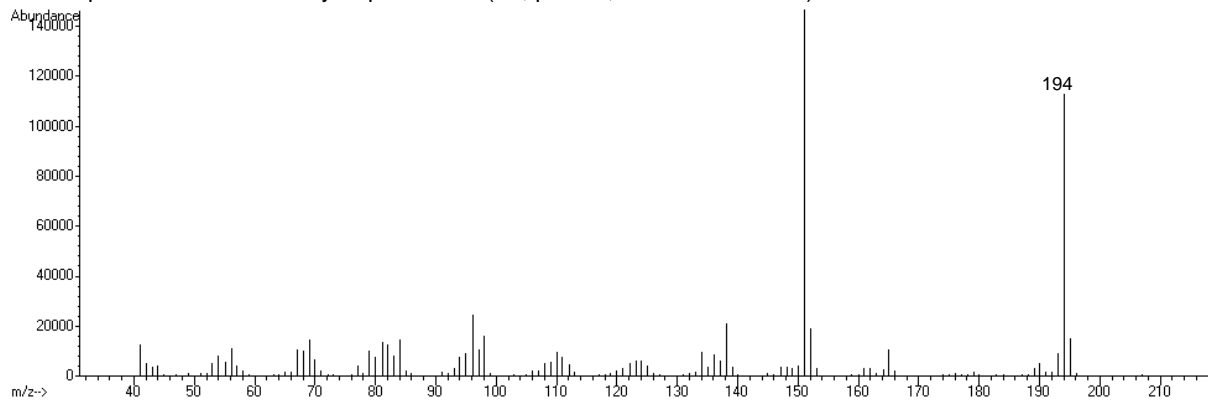
Mass spectrum of tetradecahydrophenazine (**5h**, peak 1, biotransformation):



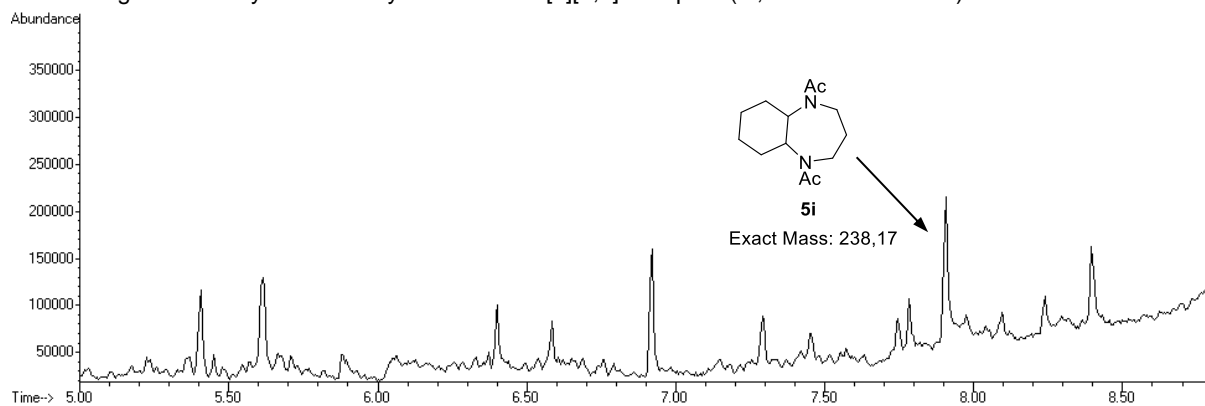
Mass spectrum of tetradecahydrophenazine (**5h**, peak 2, biotransformation):



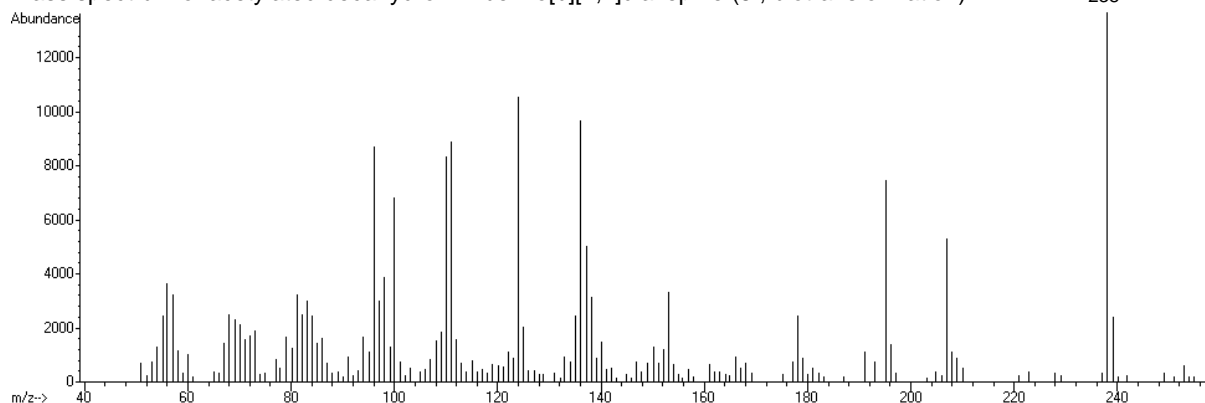
Mass spectrum of tetradecahydrophenazine (**5h**, peak 3, biotransformation):



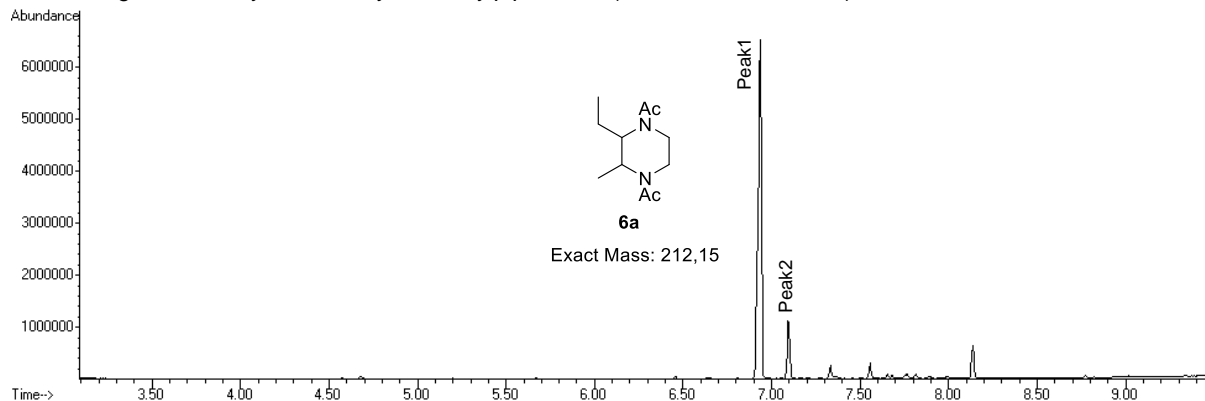
Chromatogram of acetylated decahydro-1H-benzo[b][1,4]diazepine (**5i**, biotransformation):



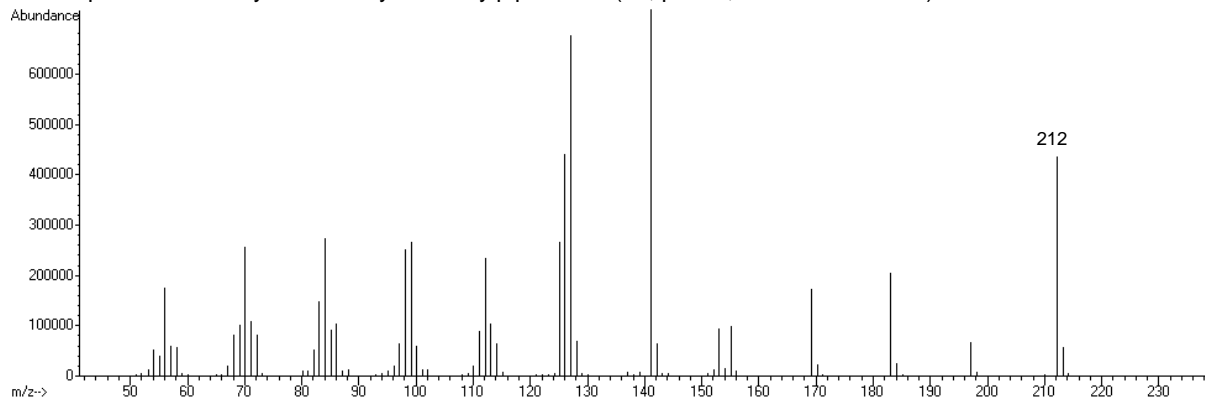
Mass spectrum of acetylated decahydro-1H-benzo[b][1,4]diazepine (**5i**, biotransformation):



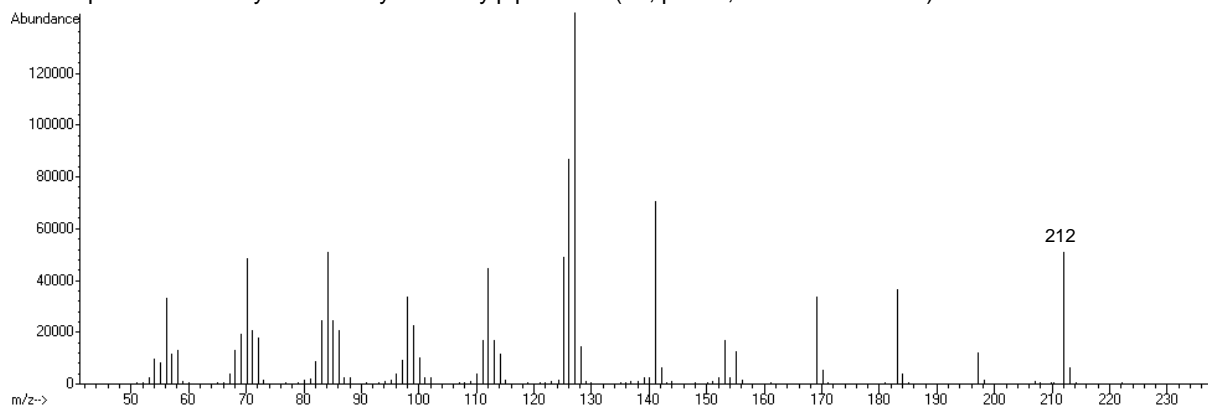
Chromatogram of acetylated 2-ethyl-3-methylpiperazine (**6a**, biotransformation):



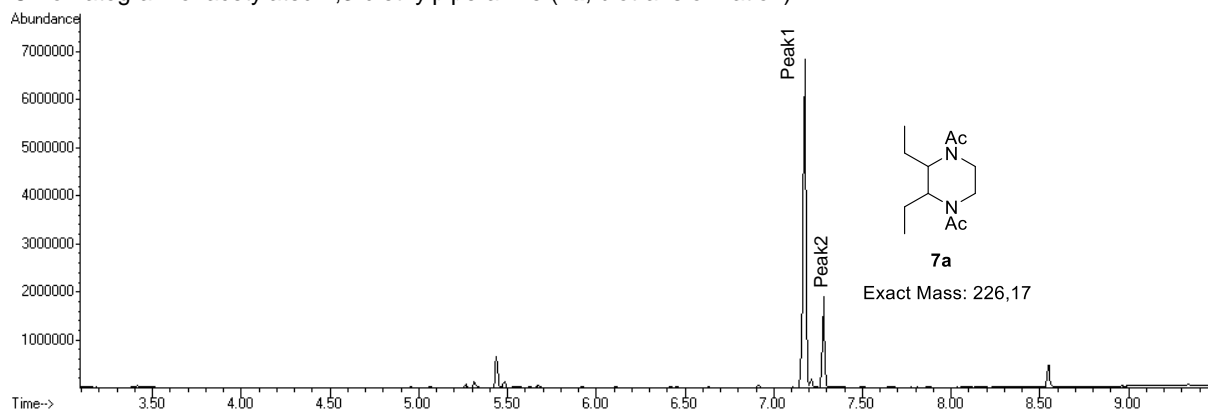
Mass spectrum of acetylated 2-ethyl-3-methylpiperazine (**6a**, peak1, biotransformation):



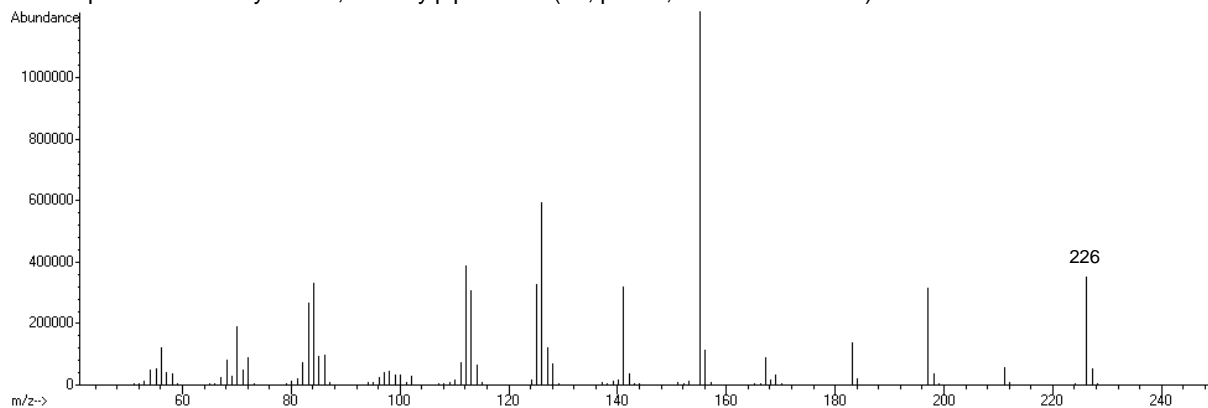
Mass spectrum of acetylated 2-ethyl-3-methylpiperazine (**6a**, peak2, biotransformation):



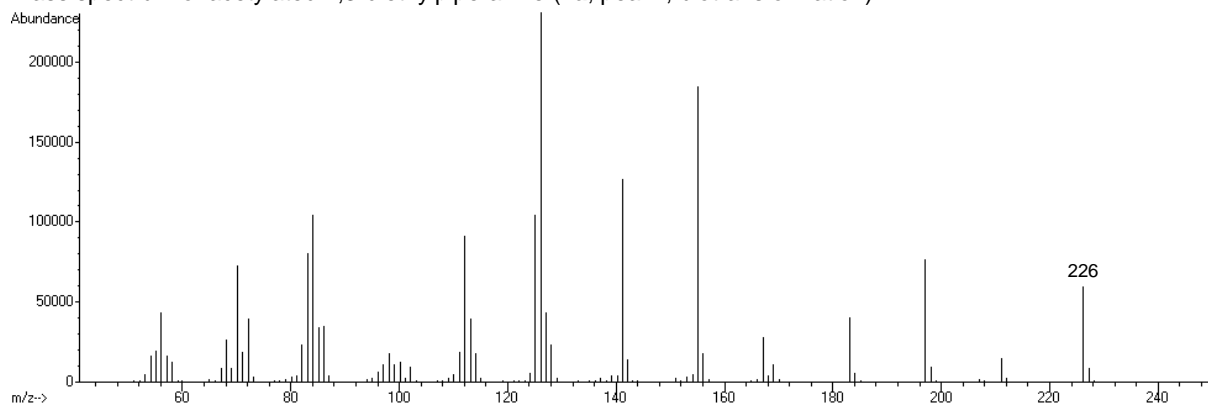
Chromatogram of acetylated 2,3-diethylpiperazine (**7a**, biotransformation):



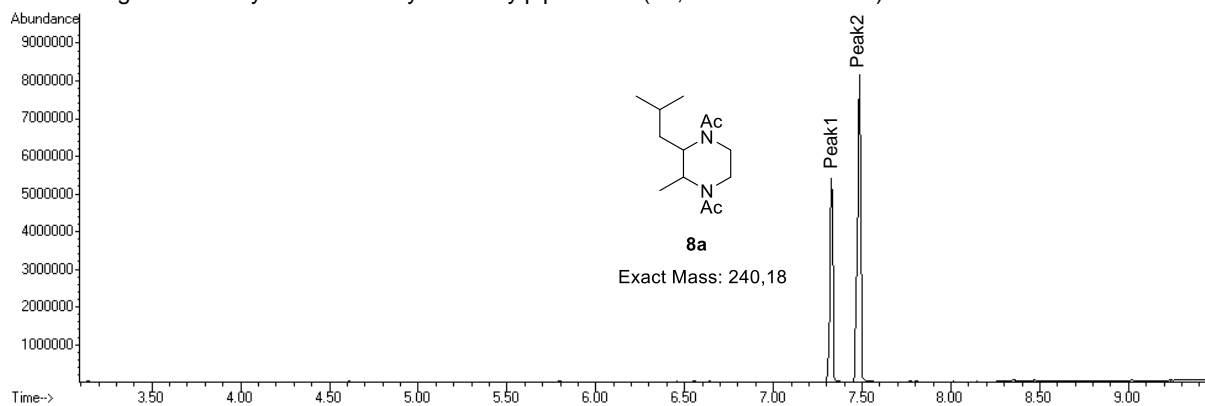
Mass spectrum of acetylated 2,3-diethylpiperazine (**7a**, peak1, biotransformation):



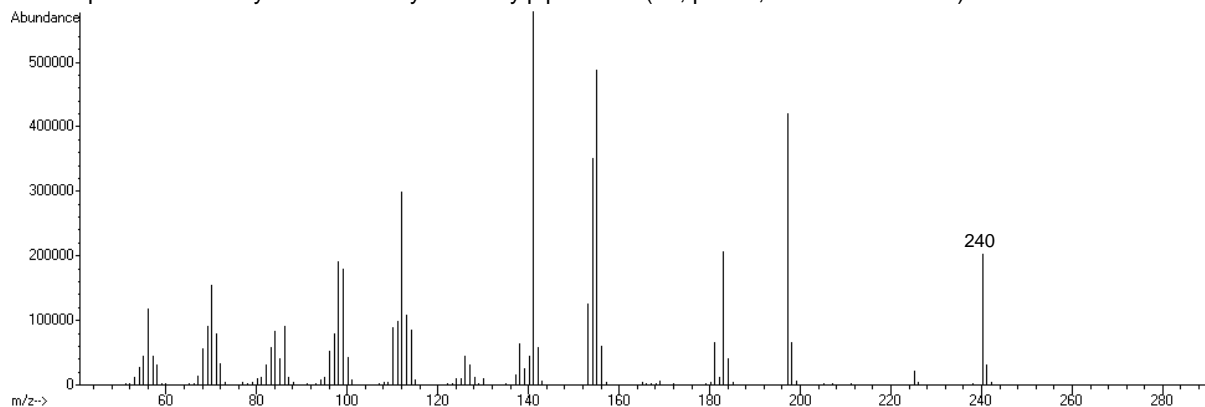
Mass spectrum of acetylated 2,3-diethylpiperazine (**7a**, peak2, biotransformation):



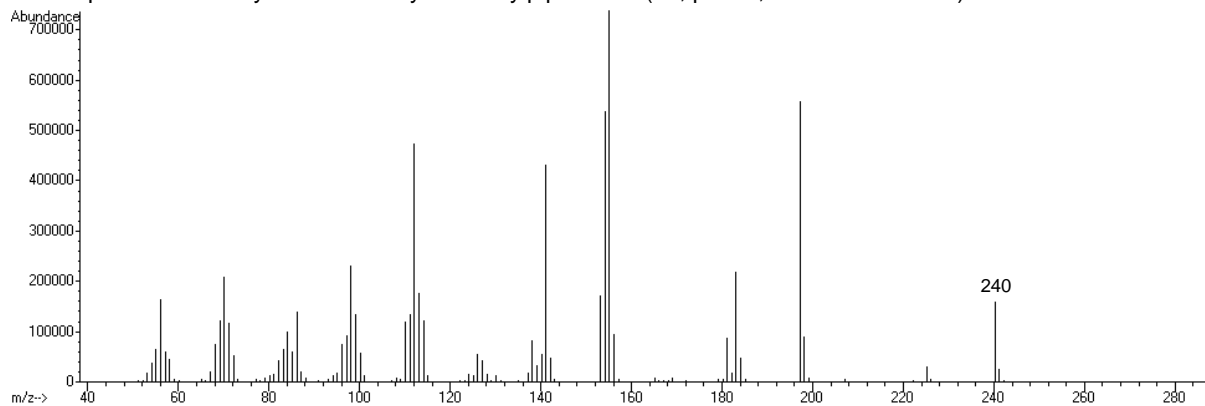
Chromatogram of acetylated 2-isobutyl-3-methylpiperazine (**8a**, biotransformation):



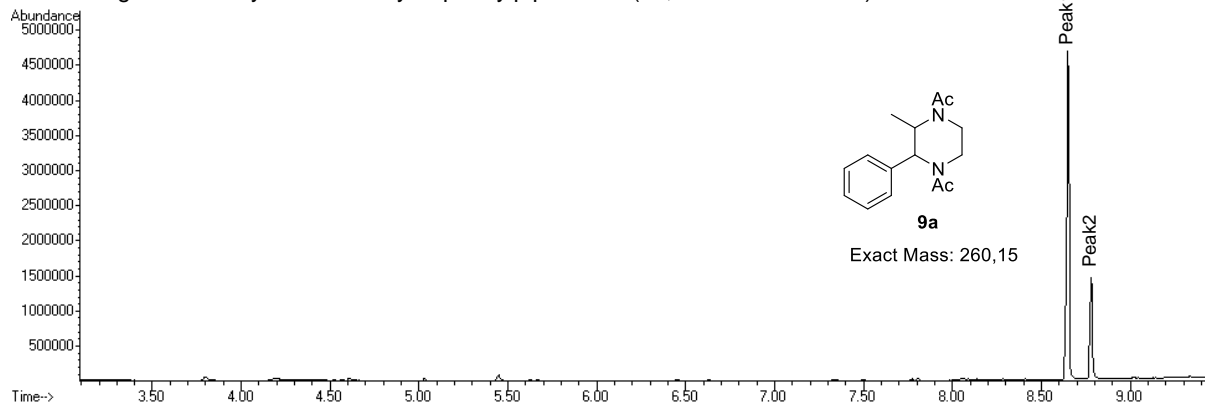
Mass spectrum of acetylated 2-isobutyl-3-methylpiperazine (**8a**, peak1, biotransformation):



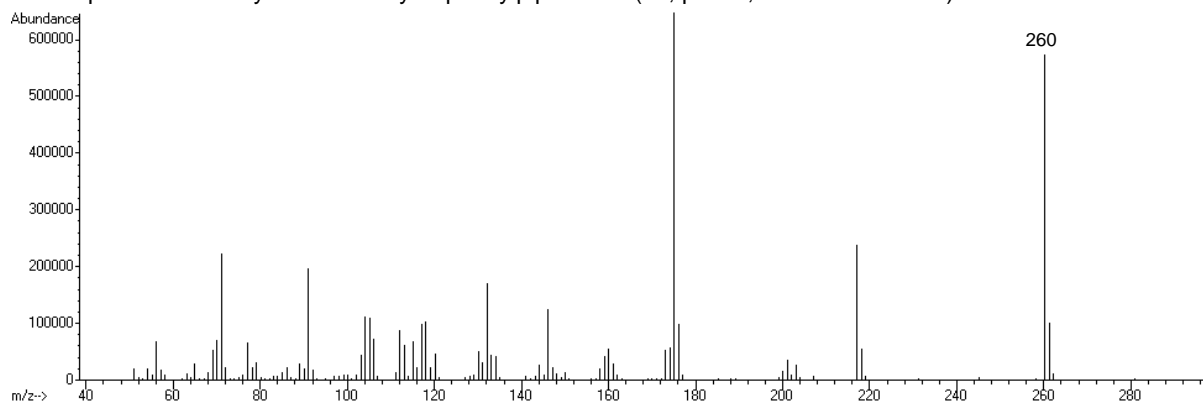
Mass spectrum of acetylated 2-isobutyl-3-methylpiperazine (**8a**, peak2, biotransformation):



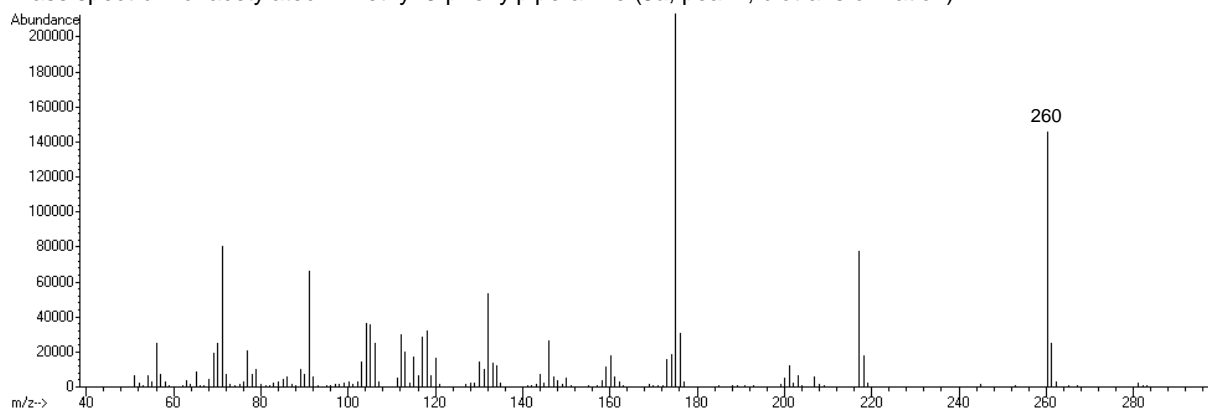
Chromatogram of acetylated 2-methyl-3-phenylpiperazine (**9a**, biotransformation):



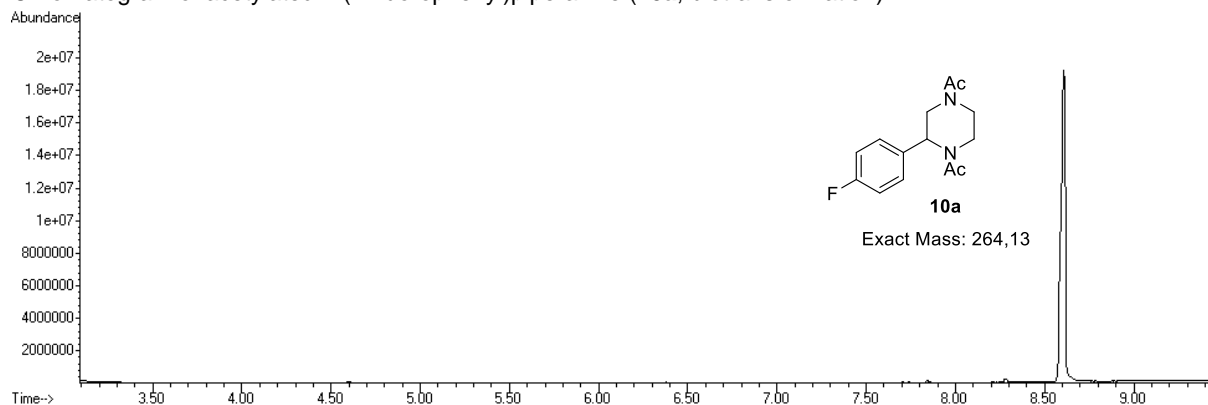
Mass spectrum of acetylated 2-methyl-3-phenylpiperazine (**9a**, peak1, biotransformation):



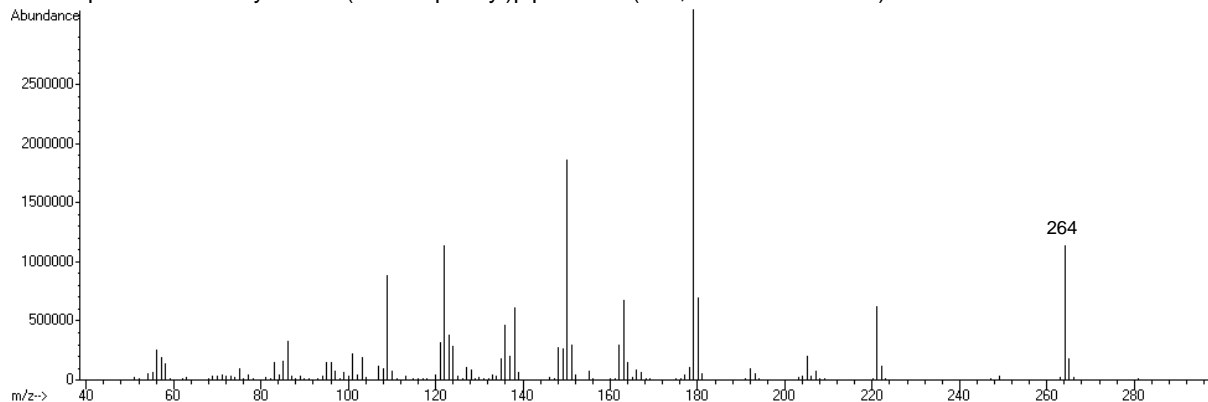
Mass spectrum of acetylated 2-methyl-3-phenylpiperazine (**9a**, peak2, biotransformation):



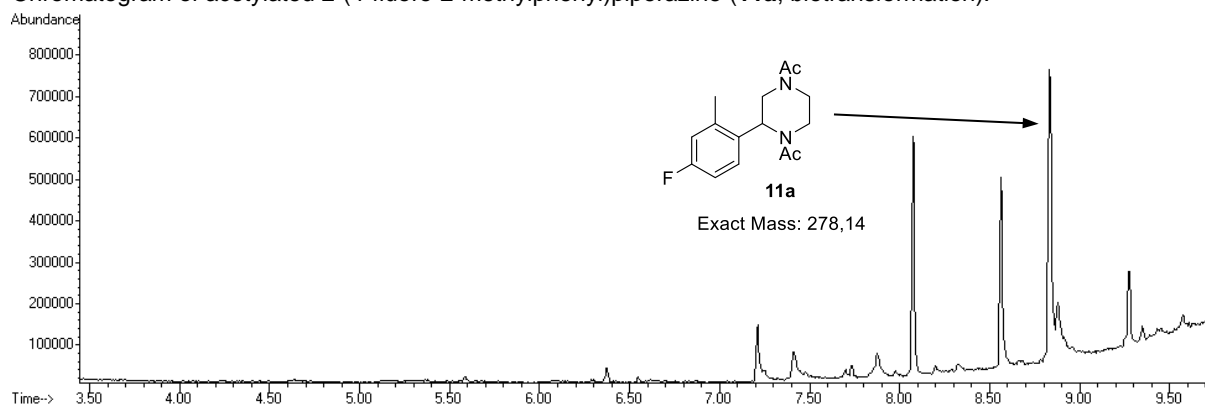
Chromatogram of acetylated 2-(4-fluorophenyl)piperazine (**10a**, biotransformation):



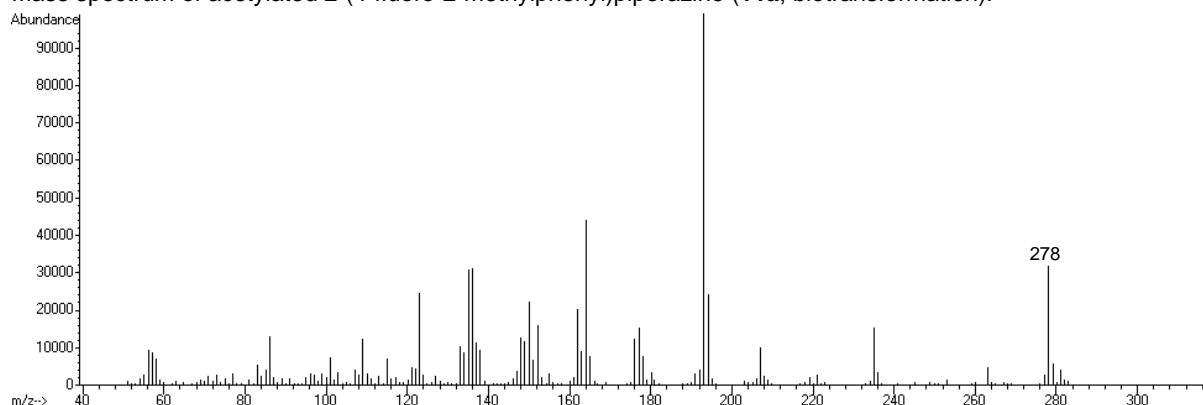
Mass spectrum of acetylated 2-(4-fluorophenyl)piperazine (**10a**, biotransformation):



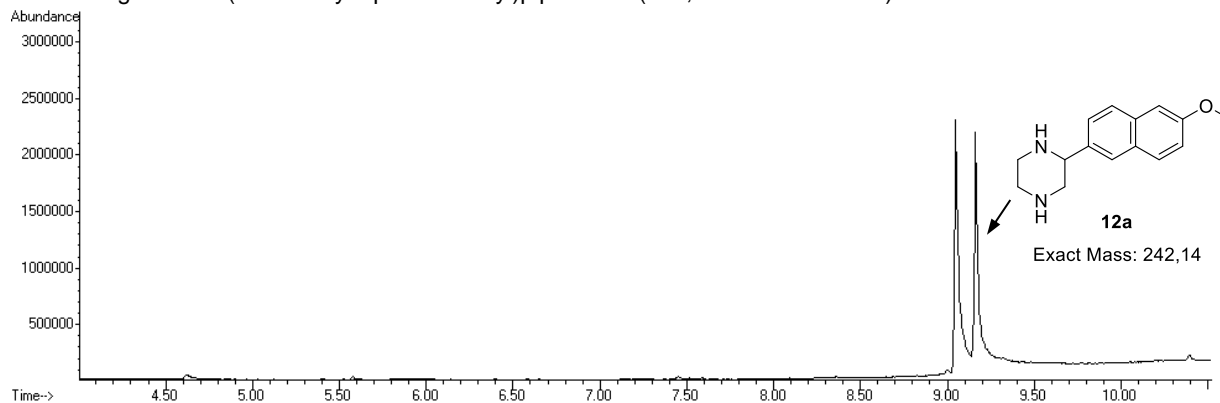
Chromatogram of acetylated 2-(4-fluoro-2-methylphenyl)piperazine (**11a**, biotransformation):



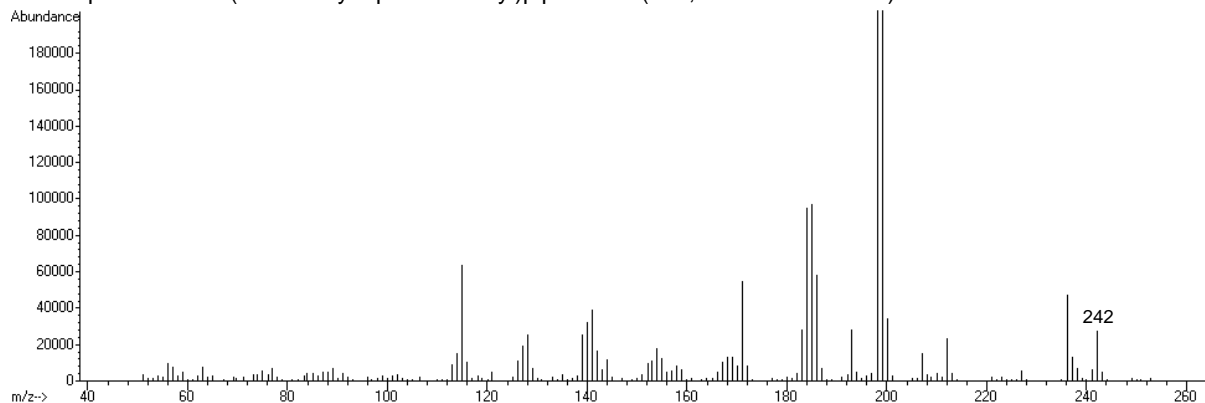
Mass spectrum of acetylated 2-(4-fluoro-2-methylphenyl)piperazine (**11a**, biotransformation):



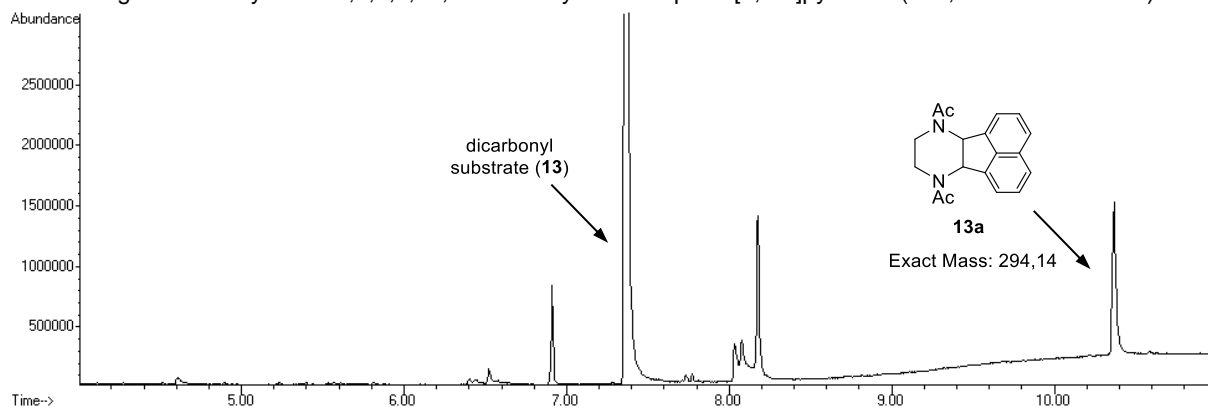
Chromatogram of 2-(6-methoxynaphthalen-2-yl)piperazine (**12a**, biotransformation):



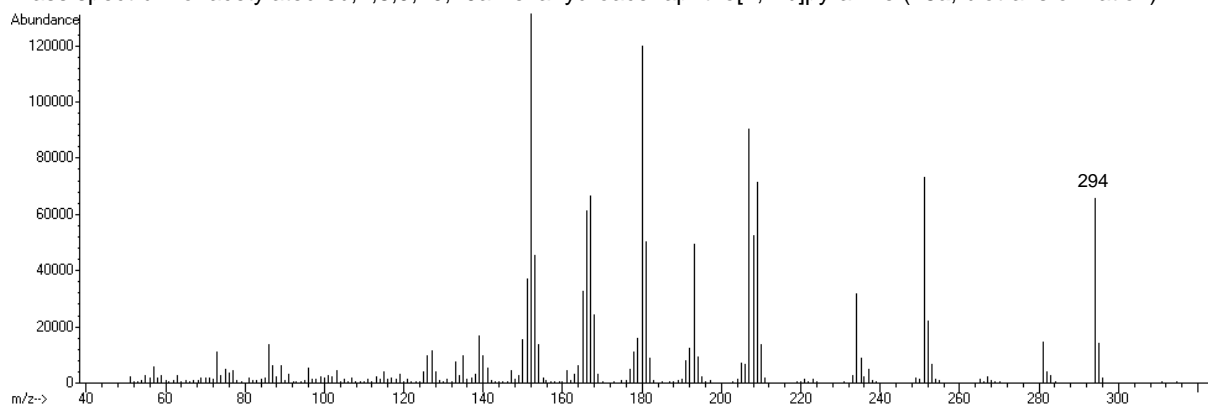
Mass spectrum of 2-(6-methoxynaphthalen-2-yl)piperazine (**12a**, biotransformation):



Chromatogram of acetylated 6b,7,8,9,10,10a-hexahydroacenaphtho[1,2-b]pyrazine (**13a**, biotransformation):



Mass spectrum of acetylated 6b,7,8,9,10,10a-hexahydroacenaphtho[1,2-b]pyrazine (**13a**, biotransformation):



(D) GC-MS chromatograms of selected examples

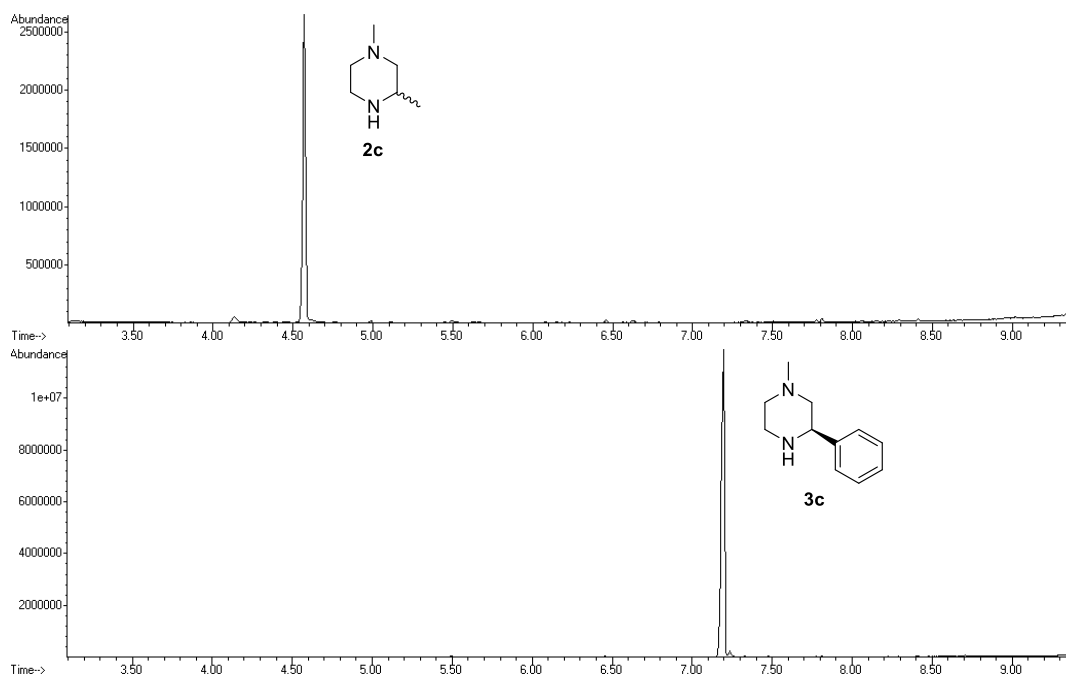


Figure S7: GC-MS chromatograms of **2c** and **3c** (both acetylated) extracted from biotransformation showing the formation of only one of two possible regioisomers.

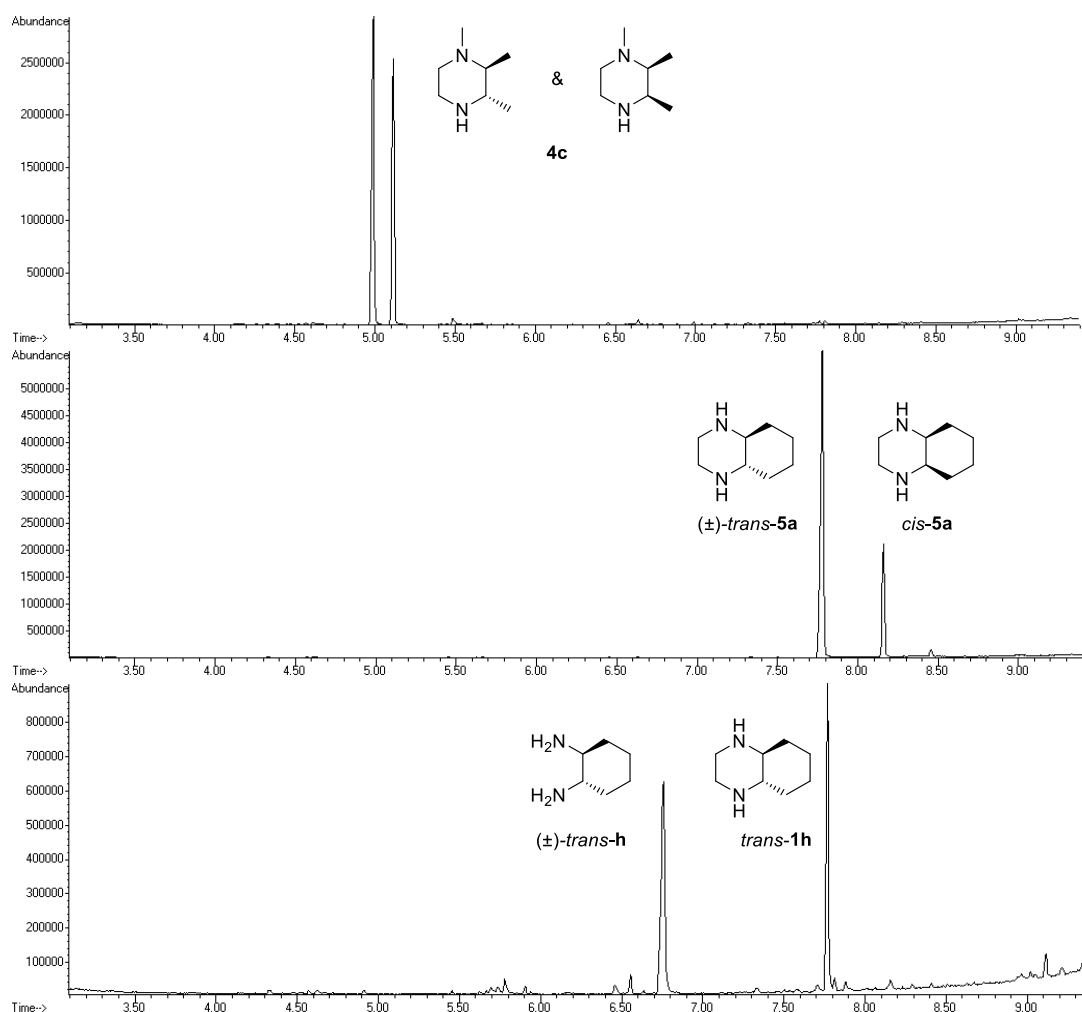


Figure S8: GC-MS chromatograms of **4c** and **5a** (acetylated compounds) extracted from biotransformation. In both cases two possible diastereomers were formed using disubstituted 1,2-dicarbonyls. This might be a result of the already discussed imine-enamine tautomerization of intermediate **III** prior the final reduction step. Due to the reaction of **(±)-trans-1,2-diaminocyclohexane (h)** and glyoxal (**1**) yielding the same compound **5a/1h** on a complementary route (lower chromatogram), it was possible to assign the left signal to be **(±)-trans-5a**.

(E) Chiral GC analysis of 1-methyl-3-phenylpiperazine (3c)

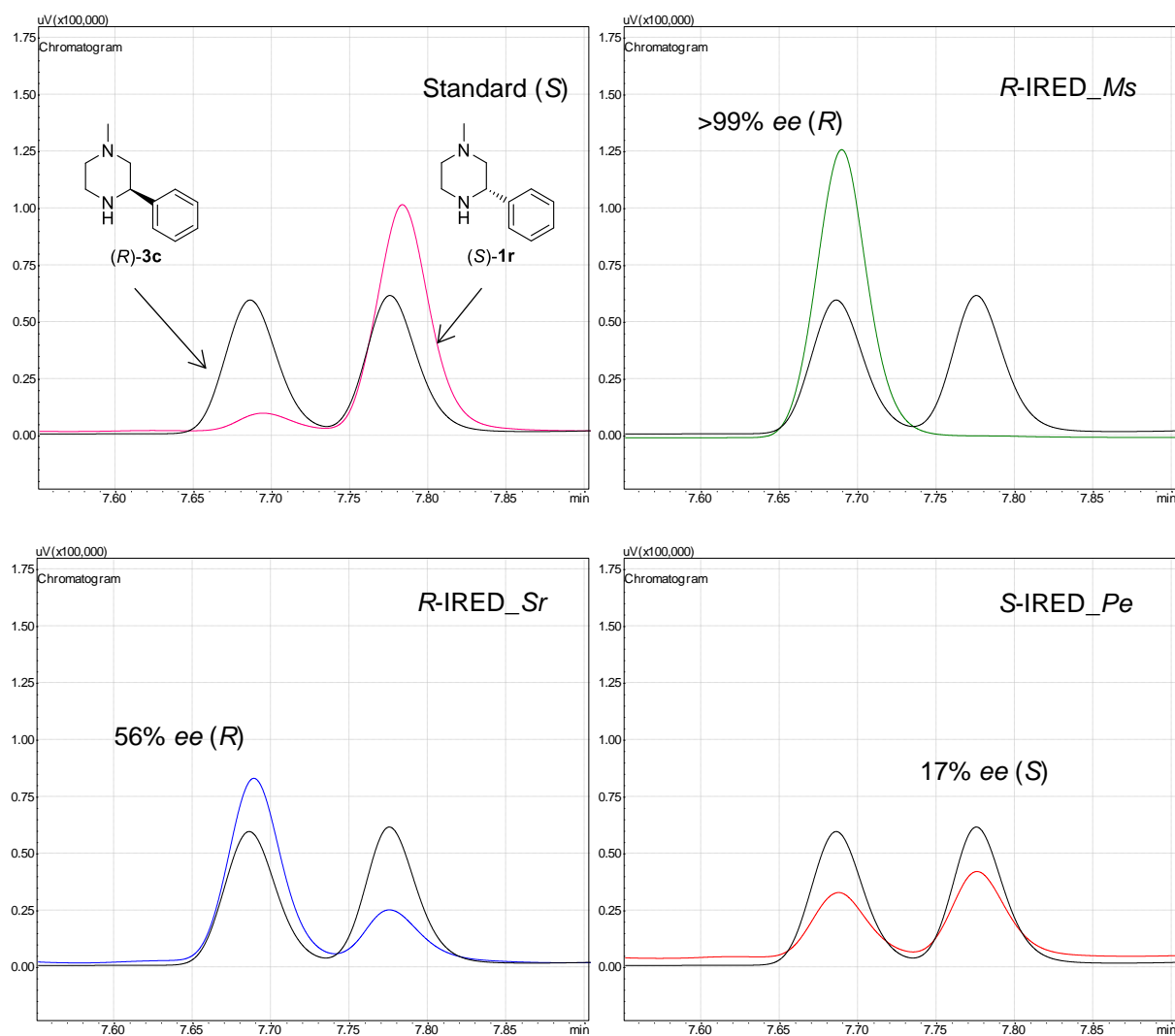


Figure S9: Chiral GC analysis of biotransformations with *R*-IRED_Ms (green), *R*-IRED_Sr (blue) and *S*-IRED_Pe (red). The black chromatogram represents racemic 1-methyl-3-phenylpiperazine (**3c**) compared to synthesized (*S*)-enantiomer standard (depicted in pink). Analytes were detected in their derivatized (acetylated) form, prepared as described in chapter 3(B).

5 HPLC chromatograms

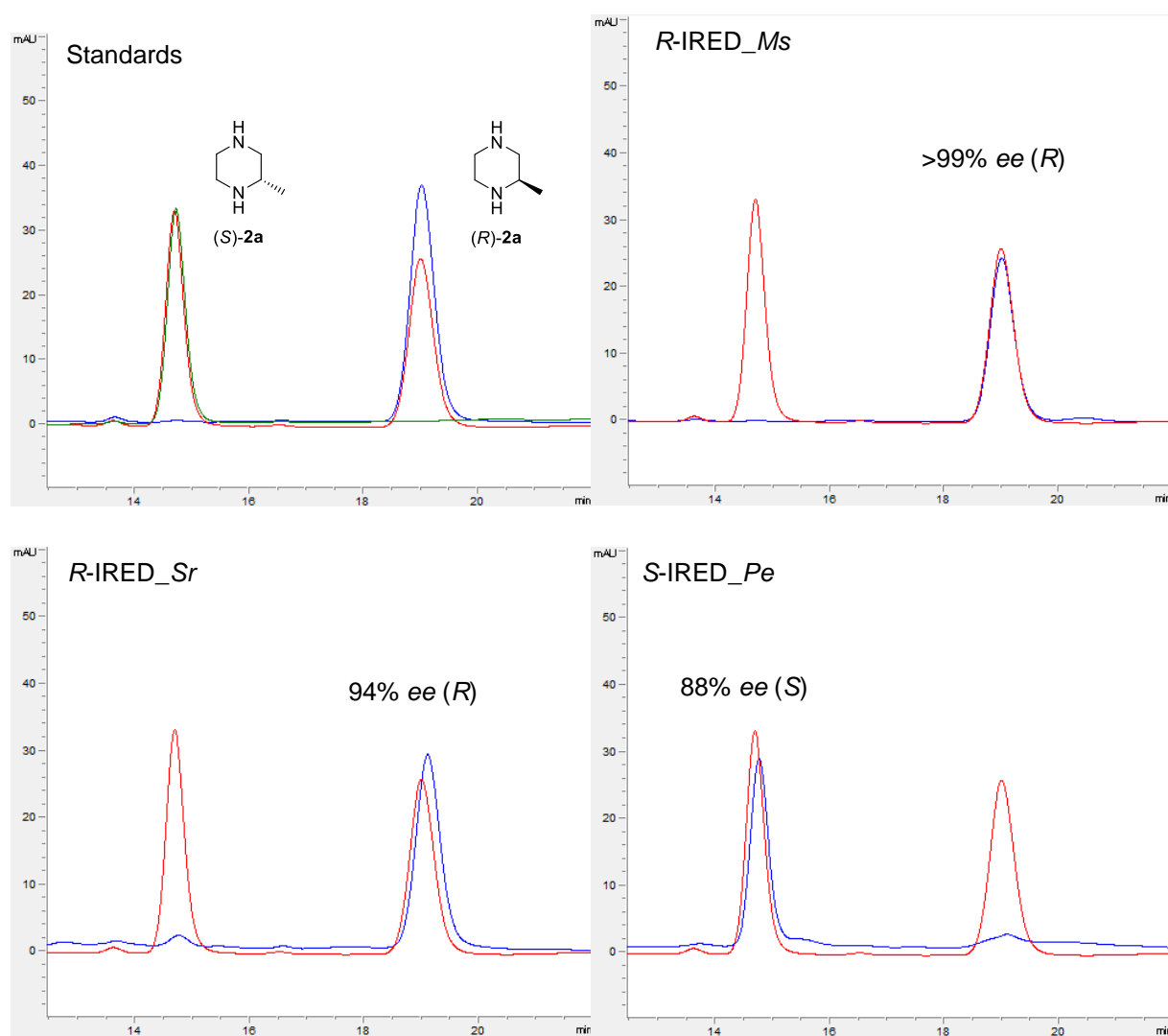


Figure S10: Chiral HPLC analysis of biotransformations with *R*-IRED_Ms (top right), *R*-IRED_Sr (bottom left) and *S*-IRED_Pe (bottom right) using a Daicel Chiralpak IC column. The red chromatogram represents racemic 2-methylpiperazine (**2a**). Analytes were detected in their derivatized form, prepared as described in chapter 3(C).

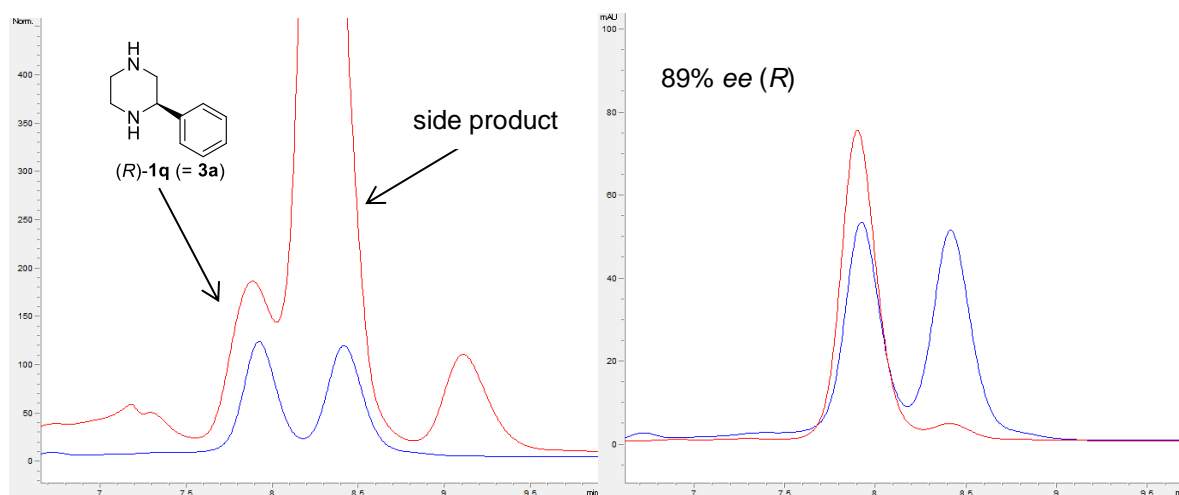
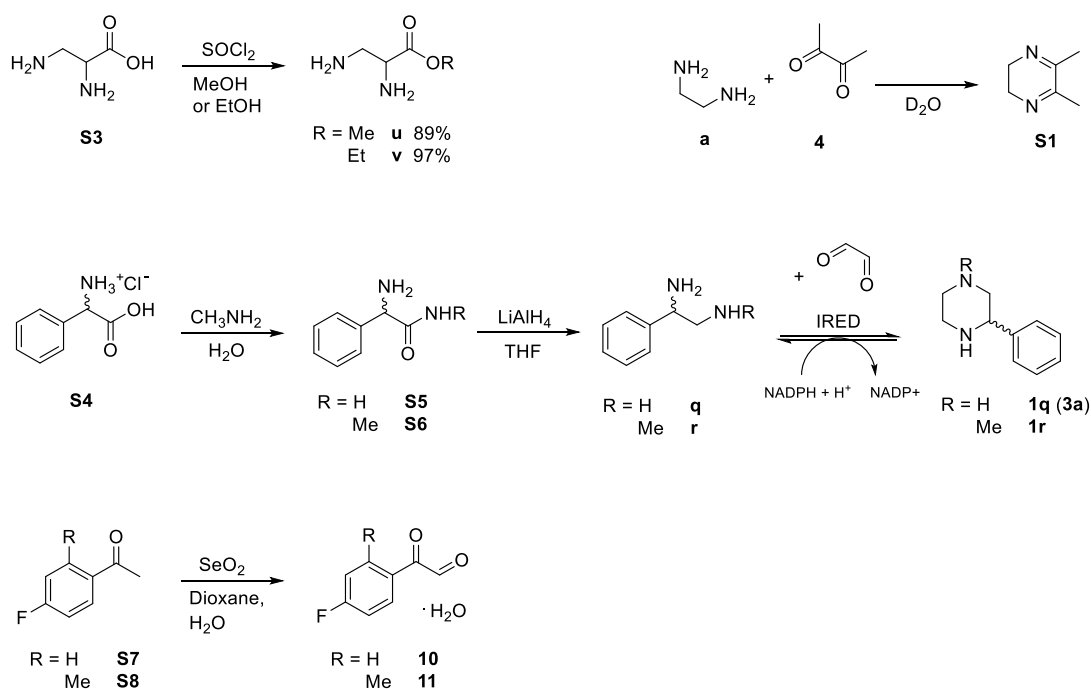


Figure S11: Chiral HPLC analysis (using a Daicel Chiralpak IB column) of biotransformations with *R*-IRED_Ms resulting in 2-phenylpiperazine (**3a**, left, red). The blue chromatogram represents racemic 2-phenylpiperazine (**3a**). The utilization of synthesized (*R*)-enantiomer standard of **1q** (Scheme S1) demonstrates the formation of the enantiopure product (*R*)-**1q** in the biotransformation. Analytes were detected in their derivatized form, prepared as described in chapter 3(C).

6 Chemical syntheses



Scheme S1: Overview of all syntheses carried out, of which all general procedures are listed below.

All products are known compounds and synthesized partially on the basis of instructions published in literature. Generated spectral data are in agreement with reported values.²⁻⁹

Methyl 2,3-diaminopropanoate (u) and **ethyl 2,3-diaminopropanoate (v)**: A solution of 2,3-diaminopropionic acid **S3** (5.00 g, 4.80 mmol) in either methanol (20 mL) or ethanol (20 mL) was prepared and cooled to 0°C before thionyl chloride (1.39 mL, 19.2 mmol, 4 eq.) was added dropwise within a period of 10 min. After heating the reaction mixture at reflux for 4 h, excess thionyl chloride and

solvent were removed under vacuo. Compound **u** (0.50 g, 4.26 mmol, 89%) was obtained as colorless solid without further purification. ^1H NMR (500 MHz, D_2O) δ = 4.48 (dd, J = 5.3, 8.3 Hz, 1H; CH), 3.86 (s, 3H; CH_3), 3.58 (dd, J = 8.2, 13.9 Hz, 1H; CH_2), 3.48 (dd, J = 5.1, 13.9 Hz, 1H; CH_2) ppm. ^{13}C NMR (125 MHz, D_2O) δ = 167.4, 54.3, 49.7, 37.9 ppm. Compound **v** (0.62 g, 4.67 mmol, 97%) was obtained as colorless solid. ^1H NMR (500 MHz, D_2O) δ = 4.46 (m, 1H; CH), 4.37 – 4.28 (m, 2H; CH_2), 3.60 – 3.48 (m, 2H; CH_2), 1.27 (t, J = 7.2 Hz, 3H; CH_3) ppm. ^{13}C NMR (125 MHz, D_2O) δ = 166.9, 64.6, 49.8, 38.0, 13.1 ppm.

5,6-Dimethyl-2,3-dihydropyrazine (S1): Solutions of each ethylenediamine **a** and butanedione **4** in D_2O (100 mM, 250 μL) were combined and let to react for 5 h at room temperature. ^1H NMR analysis verified the quantitative formation of compound **S1** in the corresponding reaction mixture. ^1H NMR (500 MHz, D_2O) δ = 3.23 (s, 4H; CH_2), 2.07 (s, 6H; CH_3) ppm.

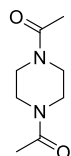
(S)-2-Amino-N-methyl-2-phenylacetamide (S6): (S)-(+)-2-Phenylglycine methyl ester hydrochloride **S4** (2.02 g, 10.0 mmol) was slowly added to an aqueous solution of methylamine (40% *m/v*, 11.7 mL, 150 mmol) under stirring until the solid was dissolved. The reaction mixture was heated to 40°C for 3 h and then extracted with dichloromethane (3 \times 40 mL). After the combined organic extracts were dried over MgSO_4 , the solvent was removed under reduced pressure. The desired compound **S6** (1.44 g, 8.74 mmol, 87%) was obtained as viscous oil without further purification. ^1H NMR (500 MHz, CDCl_3) δ = 7.40 – 7.27 (m, 5H; H_{Ar}), 7.05 (s, 1H; NH), 4.52 (s, 1H, CH), 2.82 (d, J = 5.0 Hz, 3H; CH_3), 1.84 (s, 2H; NH_2) ppm. ^{13}C NMR (125 MHz, CDCl_3) δ = 173.6, 141.1, 128.8, 127.9, 126.9, 59.9, 26.1 ppm.

(S)-N'-Methyl-2-phenylethane-1,2-diamine (r) and **(R)-1-phenylethane-1,2-diamine (q):** Under nitrogen atmosphere, a solution of lithium aluminium hydride in dry THF (1 M, 25.0 mL, 25.0 mmol) was cooled to 0°C. After adding (S)-2-amino-N-methyl-2-phenylacetamide **S5** (0.89 g, 5.41 mmol) or (R)-2-amino-2-phenylacetamide **S6** (0.75 g, 5.00 mmol) dissolved in THF (25.0 mL) over a period of 30 min, the reaction mixture was heated at reflux for 6 h. Excess of LiAlH_4 was quenched by adding dH_2O (2.50 mL) under ice cooling. The precipitate was filtered off over celite and washed with diethyl ether (20 mL), following a washing step of the filtrate with brine (2 \times 10 mL). The organic phase was dried over MgSO_4 and concentrated under reduced pressure. Further purification steps were omitted, since the compounds **r** and **q** were needed only for analytical purposes. Therefore considerable amounts of educt were still present in the corresponding product mixture. Compound **r** was obtained as slightly yellow liquid. ^1H NMR (500 MHz, CDCl_3) δ = 7.35 – 7.33 (m, 4H; H_{Ar}), 7.28 – 7.24 (m, 1H; H_{Ar}), 4.04 (dd, J = 5.0, 7.9 Hz, 1H; CH) 2.79 – 2.71 (m, 2H; CH_2), 2.44 (s, 3H; CH_3), 1.62 (s, 3H; NH, NH_2) ppm. ^{13}C NMR (125 MHz, CDCl_3) δ = 144.7, 128.6, 127.2, 126.4, 59.9, 55.4, 36.4 ppm. Compound **q** was obtained as yellow oil. ^1H NMR (500 MHz, CDCl_3) δ = 7.35 – 7.31 (m, 5H; H_{Ar}), 3.91 (dd, J = 5.7, 6.9 Hz, 1H; CH) 2.93 – 2.79 (m, 2H; CH_2) ppm. ^{13}C NMR (125 MHz, CDCl_3) δ = 144.3, 128.5, 127.2, 126.5, 58.4, 50.0 ppm.

4-Fluorophenylglyoxal hydrate (10) and **4-fluoro-2-methylphenylglyoxal hydrate (11):** Selenium dioxide (2.22 g, 20.1 mmol) was dissolved in a mixture of dioxane (5.50 mL) and water (0.34 mL). After addition of 4'-fluoroacetophenone **S7** (1.53 g, 11.1 mmol) or 4'-fluoro-2'-methylacetophenone **S8** (1.69 g, 11.1 mmol) the reaction mixture was heated for 4 h at 80°C and afterwards filtered through a pad of celite. The solvent was removed under reduced pressure and the crude product was purified via flash chromatography on silica gel (*n*-heptane/EtOAc, 1:1 *v/v*). The resulting yellow oil (partially anhydrous arylglyoxal) was dissolved in hot water (5 mL) and crystallized in order to obtain the corresponding hydrates. Compound **10** (1.39 g, 8.17 mmol, 74%) was obtained as colorless solid. ^1H NMR (500 MHz, DMSO-d_6) δ = 8.16 – 8.00 (m, 2H, H_{Ar}), 7.42 – 7.35 (m, 2H, H_{Ar}), 6.83 (s, 2H, OH), 5.63 (s, 1H, CH) ppm. Compound **11** (1.21 g, 6.57 mmol, 59%) was obtained as slightly red solid. ^1H NMR (500 MHz, DMSO-d_6) δ = 8.07 – 8.04 (m, 1H, H_{Ar}), 7.19 – 7.12 (m, 2H, H_{Ar}), 6.66 (s, J = 7.4 Hz, 2H, OH), 5.56 (t, J = 7.4 Hz, 1H, CH), 2.43 (s, 3H, CH_3) ppm.

7 NMR analysis of acetylated and extracted products from up-scaled biotransformations

1,1'-(Piperazine-1,4-diyl)bis(ethan-1-one)

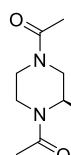


1a
(acetylated)

$^1\text{H-NMR}$ (500 MHz; CDCl_3): δ = 2.13 (s, 6H, CH_3), 3.58 (m, 8H, CH_2) ppm.

Obtained spectroscopic data for the acetylated product extracted from biotransformations are consistent with those of the product standard

(*R*)-1,1'-(2-Methylpiperazin-1,4-diyl)bis(ethan-1-on)

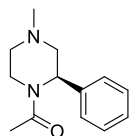


2a
(acetylated)

$^1\text{H-NMR}$ (500 MHz; CDCl_3): δ = 1.13 – 1.18 (m, 3H, CHCH_3 , A), 1.21 – 1.29 (m, 3H, CHCH_3 , B), 2.10 (s, 3H, CH_3), 2.11 (s, 3H, CH_3), 2.14 (s, 3H, CH_3), 2.16 (s, 3H, CH_3), 2.63 – 2.75 (m, 1H, CH_2 , A), 2.87 – 2.95 (m, 2H, CH_2 , B), 3.16 – 3.25 (m, 1H, CH_2 , B), 3.31 – 3.41 (m, 2H, CH_2 , A), 3.57 – 3.63 (m, 2H, CH_2 , A), 3.77 (m, 1H, CH_2 , B), 4.06 (m, 1H, CH, B), 4.36 – 4.47 (m, 2H, CH_2 , B), 4.56 (m, 1H, CH_2 , A), 4.84 (m, 1H, CH, A) ppm.

A double set of signals in the ^1H NMR spectrum suggests that two conformational isomers are present at room temperature in the ratio 1:1. Significantly broadened signals also indicate a slower structural fluctuation, which is explained by a low-frequency inversion of the chiral nitrogen center.^{10–12} Signal assignment was enabled by COSY and HSQC spectroscopy on acetylated product standards. Signals corresponding to each conformational isomer are marked with the letters A and B.

(*R*)-1-(4-Methyl-2-phenylpiperazin-1-yl)ethan-1-on



3c
(acetylated)

$^1\text{H-NMR}$ (500 MHz; CDCl_3): δ = 2.08 (m, 2H, CH_2 , B), 2.16 (s, 6H, CH_3), 2.30 (s, 6H, CH_3), 2.37 – 2.42 (m, 2H, CH_2 , A), 2.81 (m, 2H, CH_2 , B), 2.95 (m, 1H, CH_2 , A), 3.31 (m, 1H, CH_2 , B), 3.40 (m, 2H, CH_2 , A), 3.55 (m, 1H, CH_2 , B), 4.53 (m, 1H, CH_2 , A), 4.97 (m, 1H, CH, B), 5.86 (m, 1H, CH, A), 7.25 – 7.44 (m, 10H, H_{Ar} , A, B), ppm.

At room temperature, two conformational isomers are present in a 1:1 ratio.¹⁰ The signal assignment was based on COSY and HSQC spectroscopy for an acetylated product standard. Signals pertaining to the particular isomer are indicated by the letters A and B.

8 NMR spectra

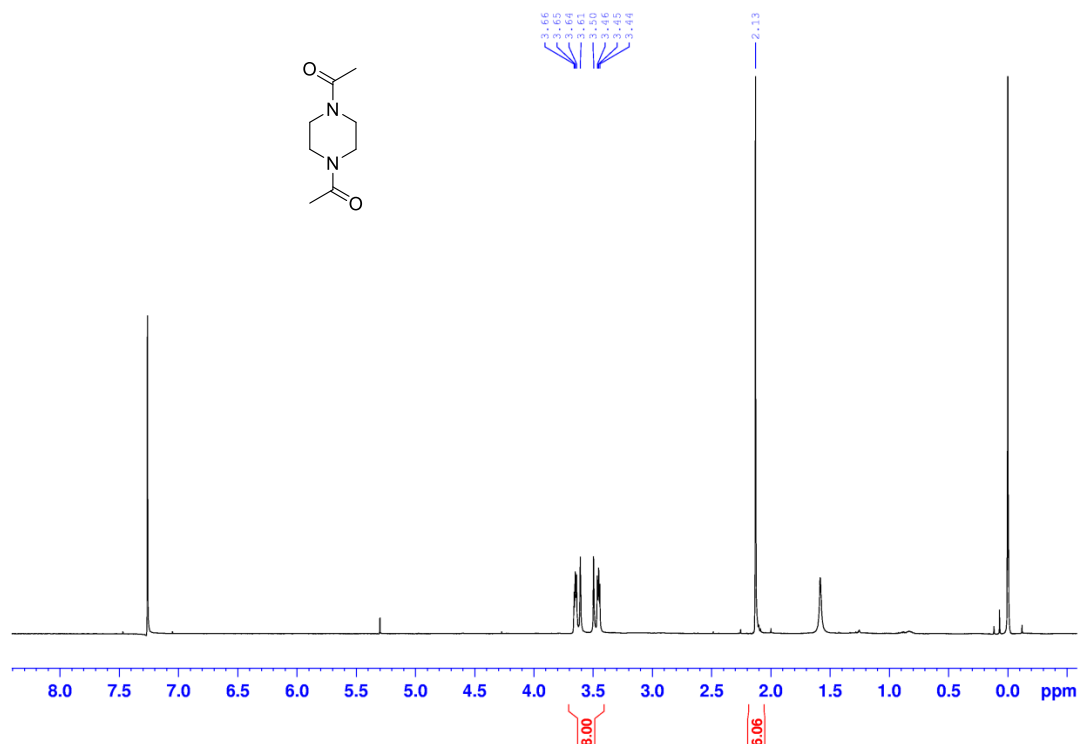


Figure S12: ¹H NMR spectrum of acetylated piperazine **1a** extracted with CDCl₃ from up-scaled biotransformation.

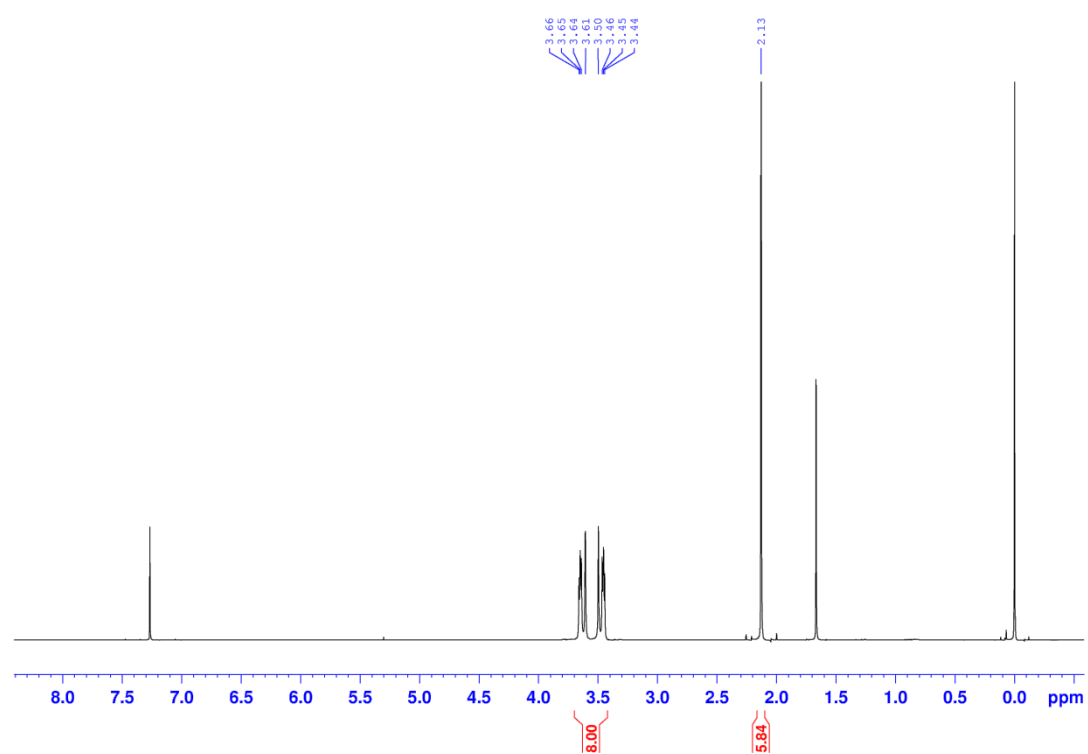


Figure S13: ¹H NMR spectrum of an acetylated product standard (piperazine **1a**) extracted with CDCl₃.

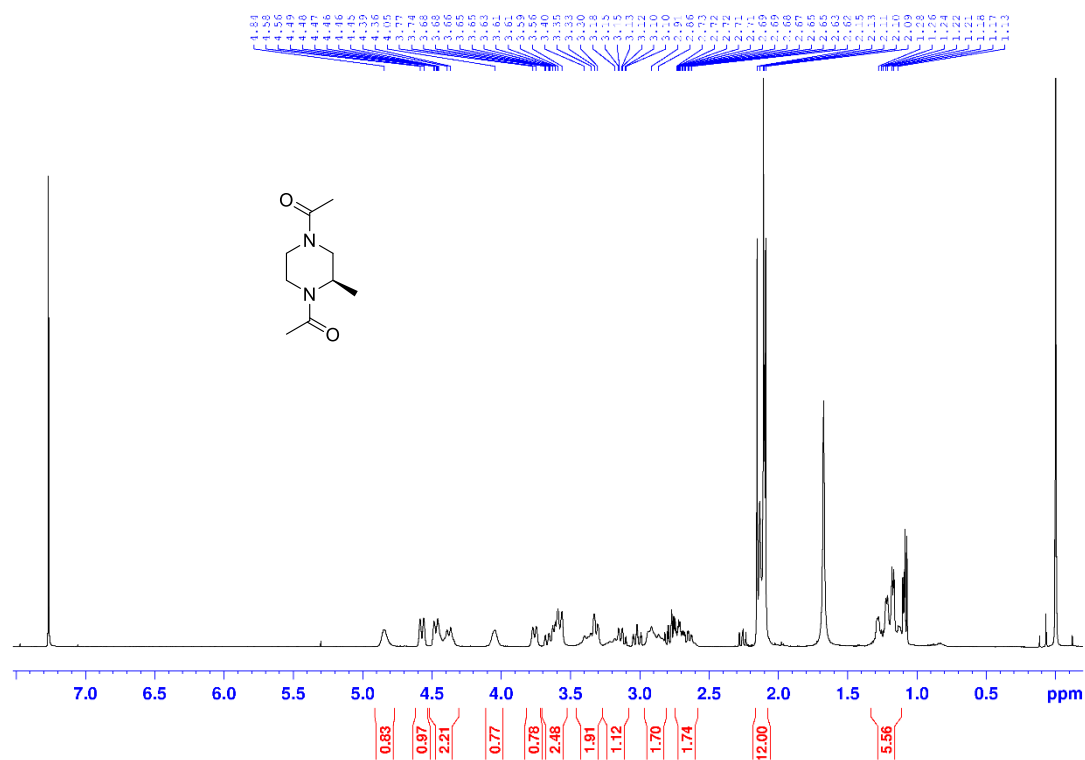


Figure S14: ¹H NMR spectrum of acetylated (*R*)-2-methylpiperazine **2a** extracted with CDCl₃ from up-scaled biotransformation.

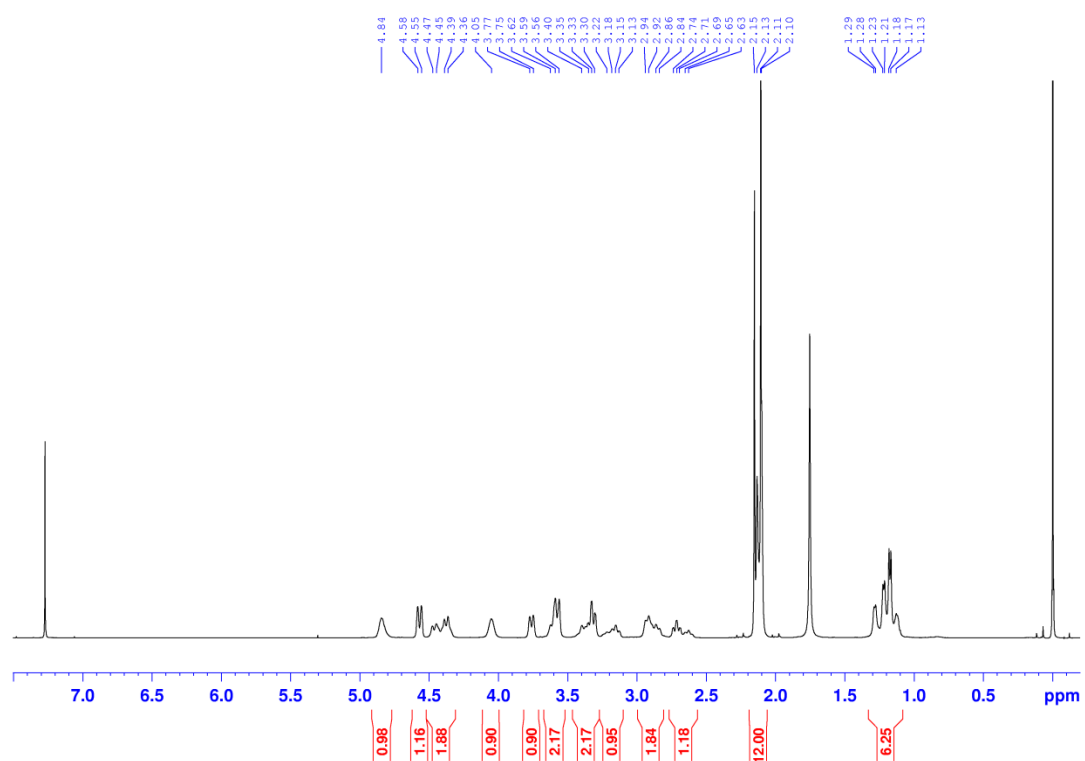


Figure S15: ¹H NMR spectrum of an acetylated product standard (2-methylpiperazine **2a**) extracted with CDCl₃.

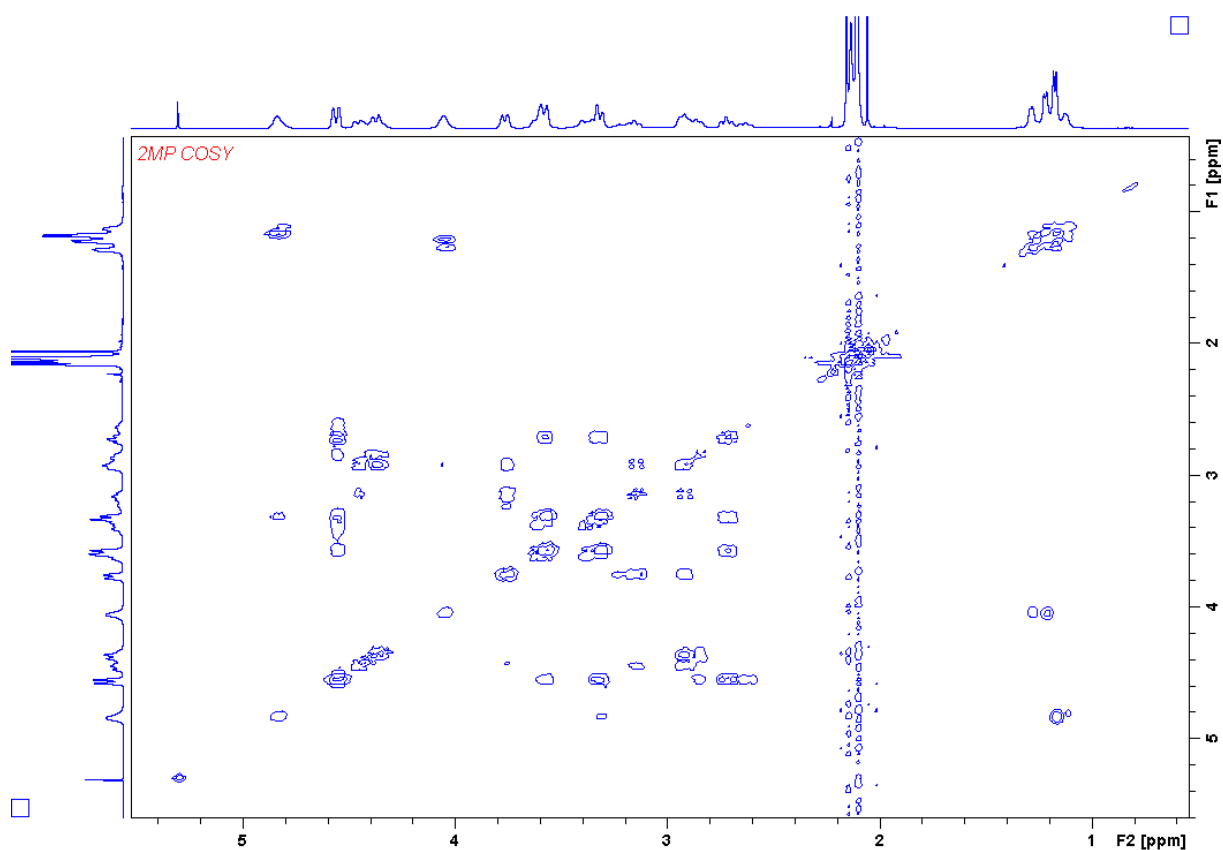


Figure S16: ^1H COSY spectrum of an acetylated product standard (2-methylpiperazine **2a**) extracted with CDCl_3 .

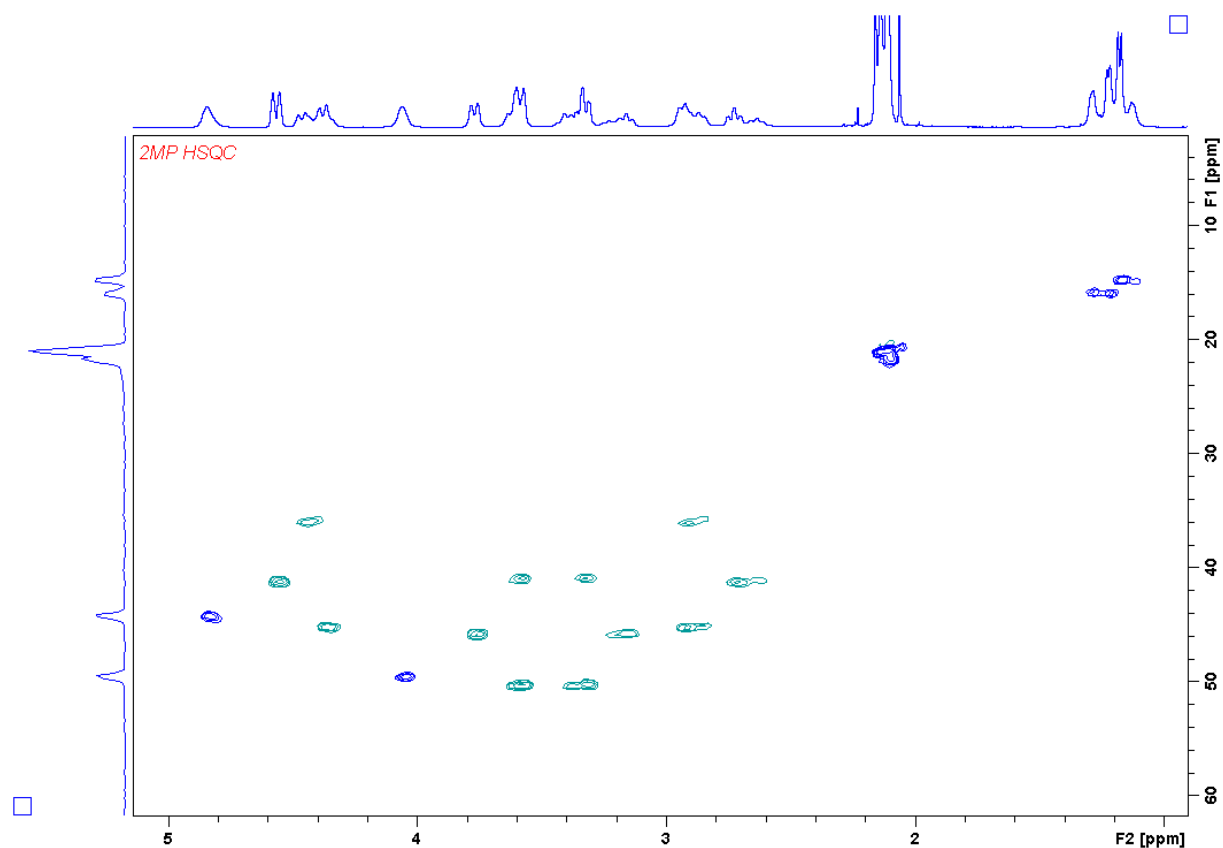


Figure S17: ^1H - ^{13}C HSQC spectrum of an acetylated product standard (2-methylpiperazine **2a**) extracted with CDCl_3 .

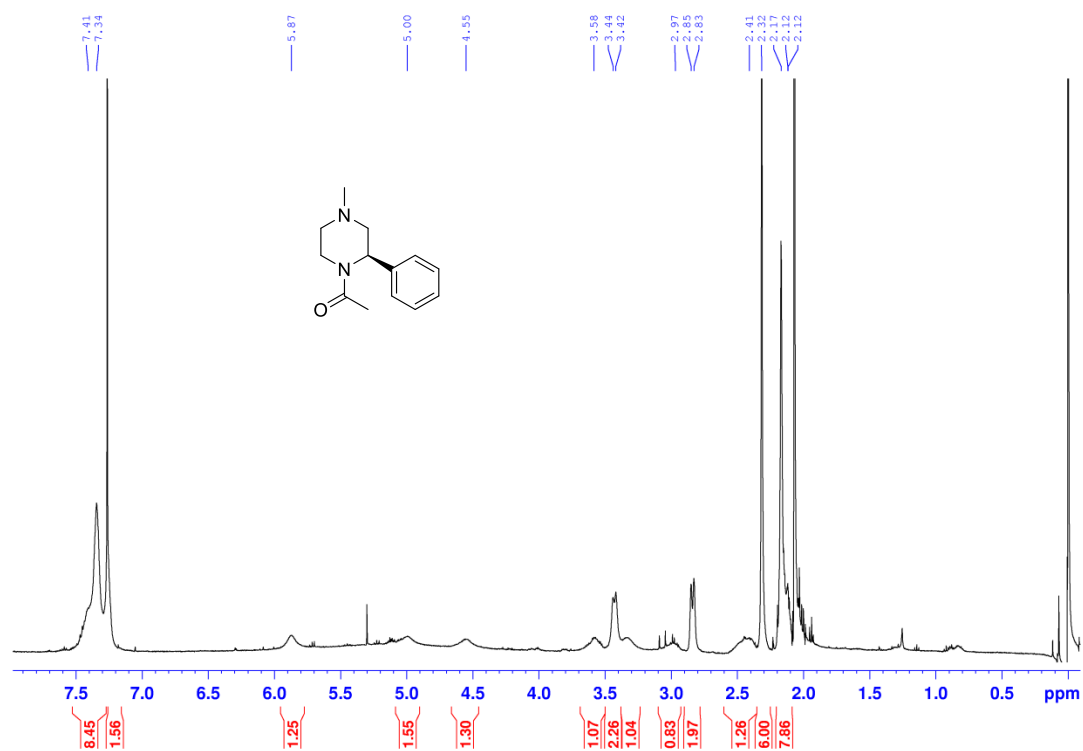


Figure S18: ^1H NMR spectrum of acetylated (*R*)-1-methyl-3-phenylpiperazine **3c** extracted with CDCl_3 from up-scaled biotransformation.

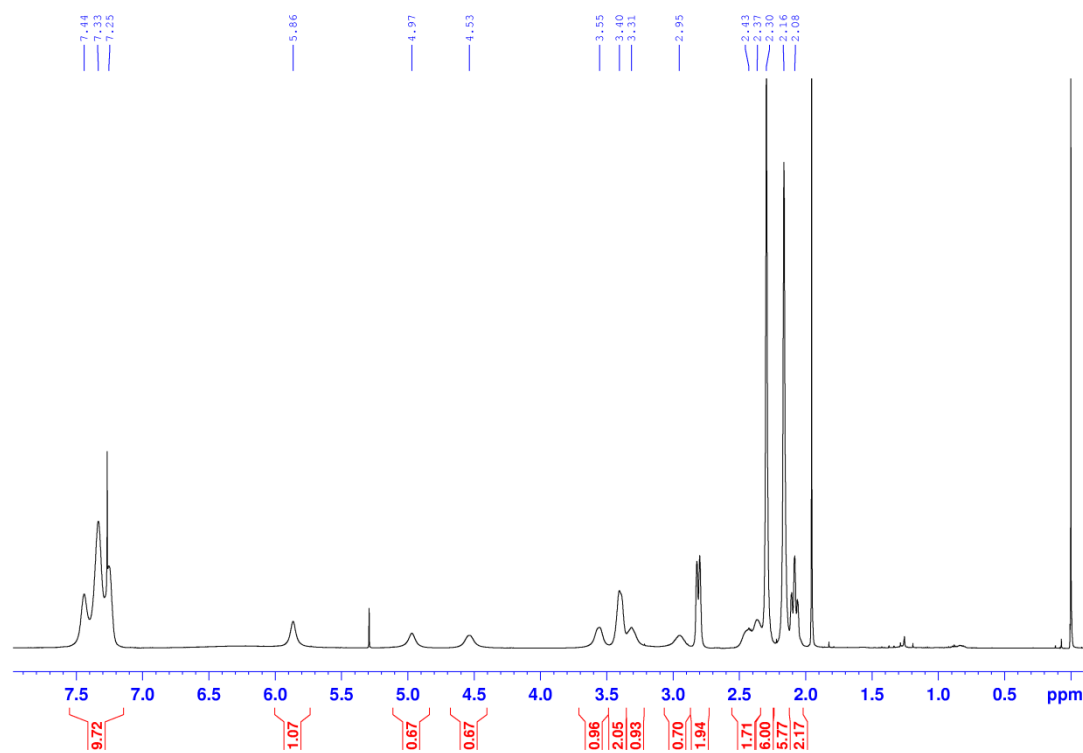


Figure S19: ^1H NMR spectrum of an acetylated product standard (1-methyl-3-phenylpiperazine **3c**) extracted with CDCl_3 .

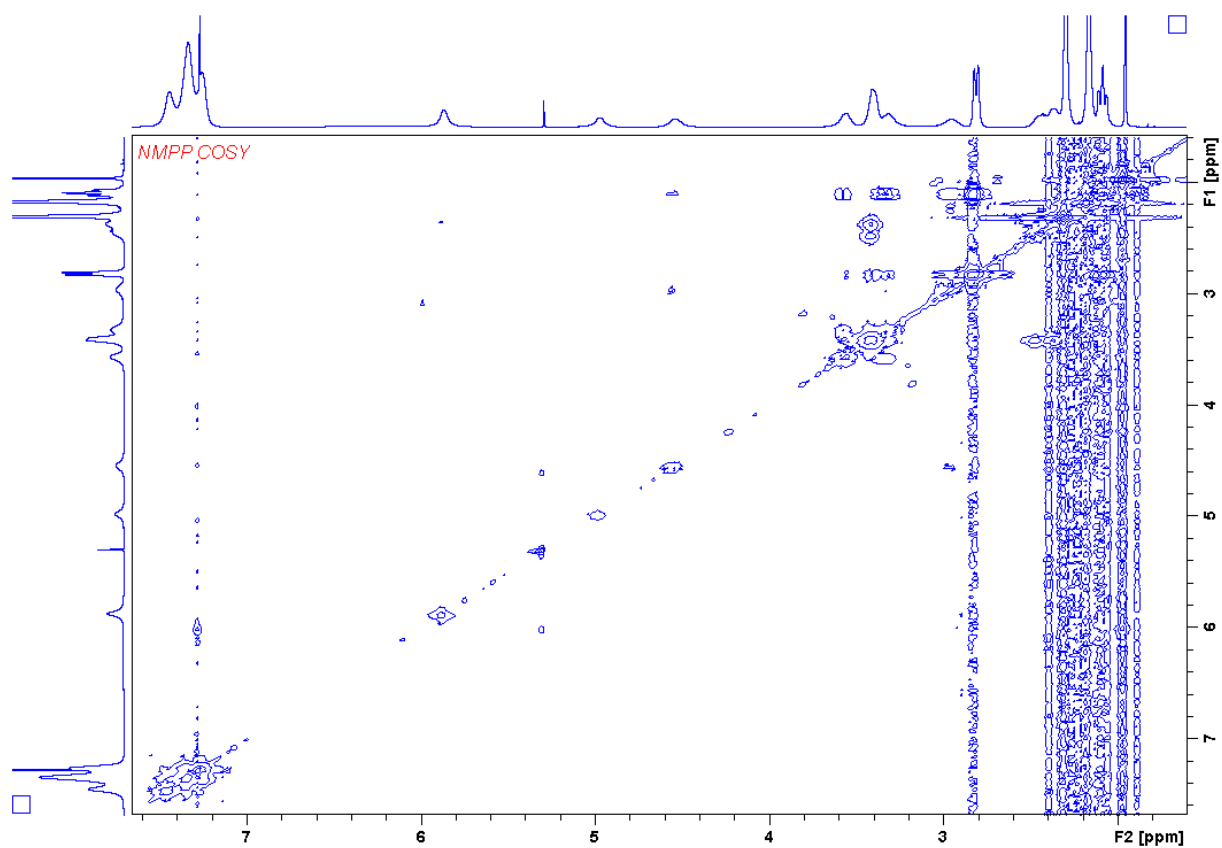


Figure S20: ^1H COSY spectrum of an acetylated product standard (1-methyl-3-phenylpiperazine **3c**) extracted with CDCl_3 .

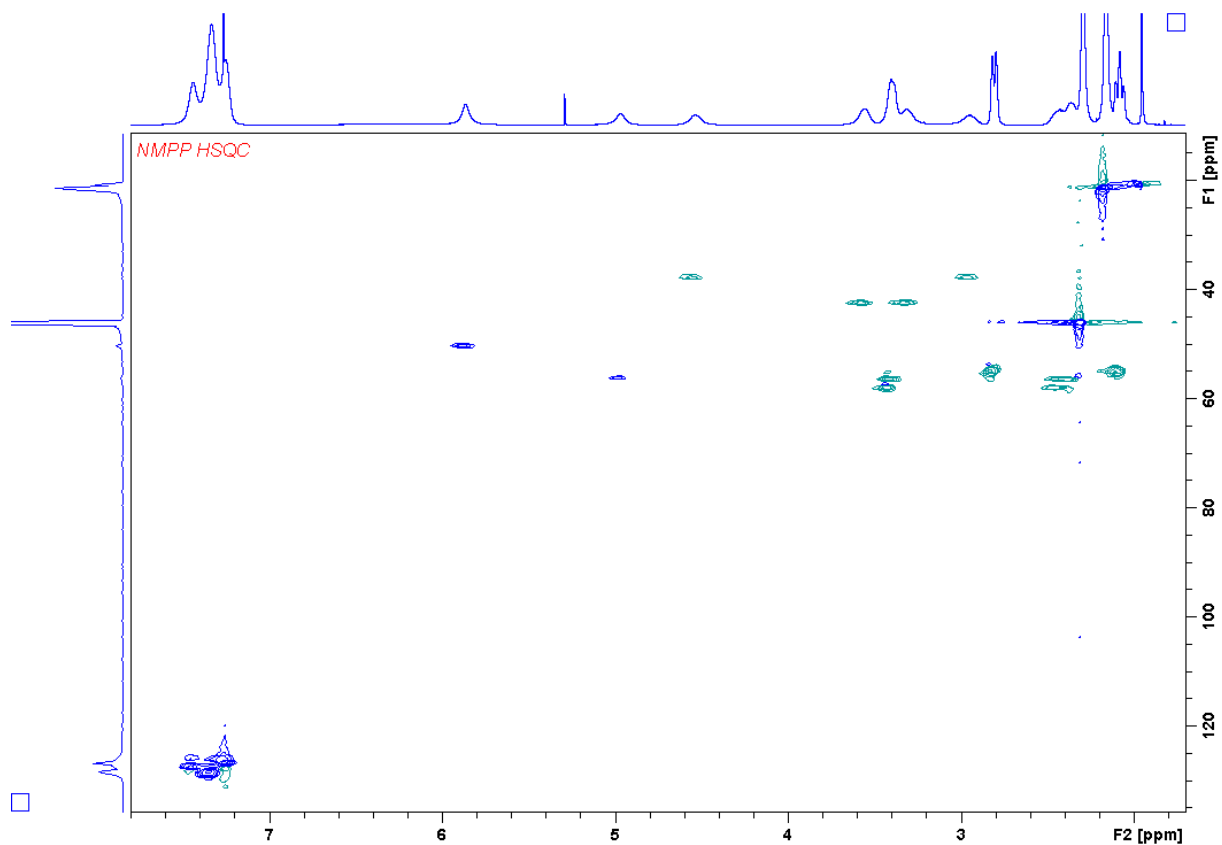


Figure S21: ^1H - ^{13}C HSQC spectrum of an acetylated product standard (1-methyl-3-phenylpiperazine **3c**) extracted with CDCl_3 .

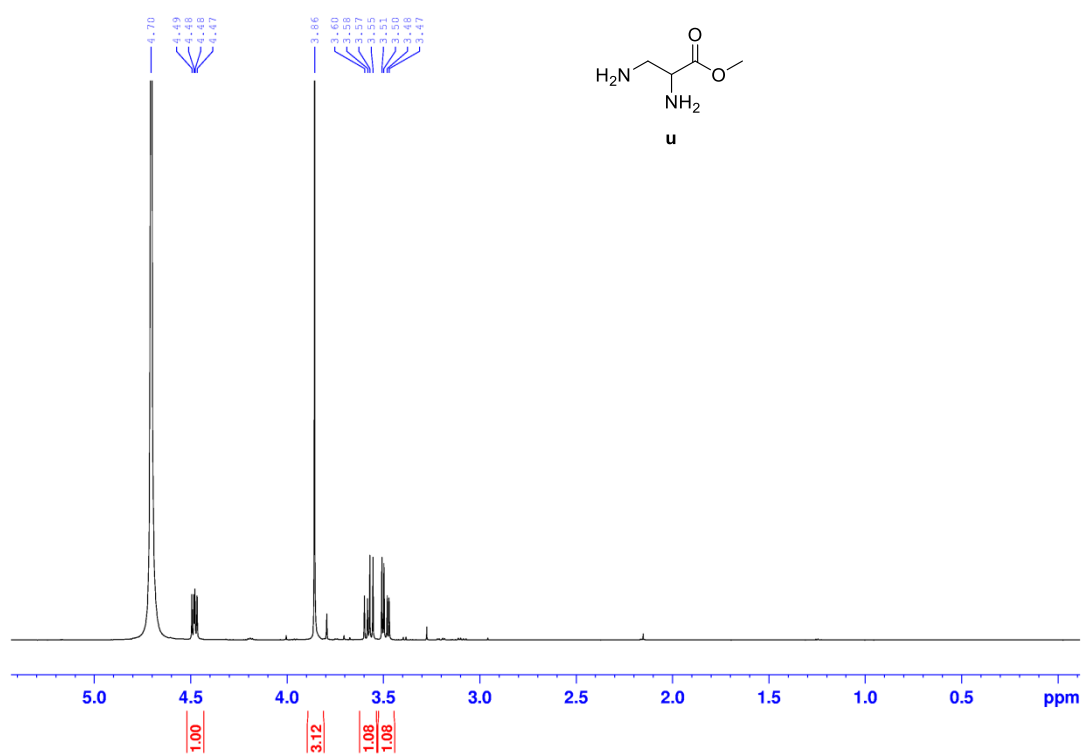


Figure S22: ¹H NMR spectrum of methyl 2,3-diaminopropanoate **u**.

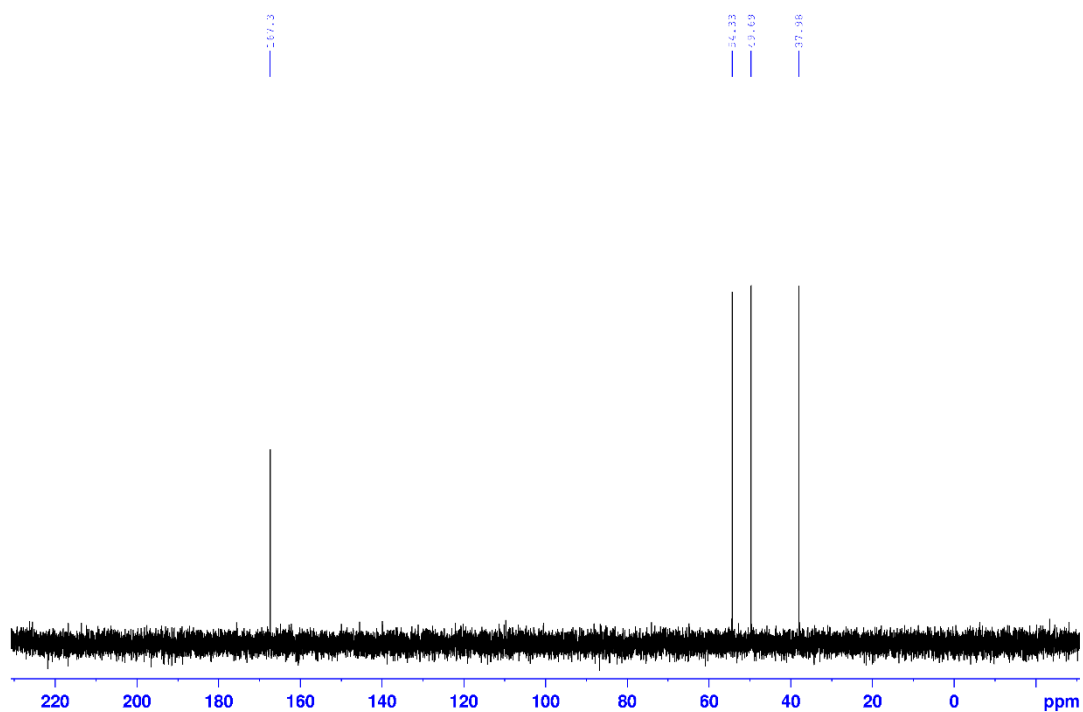


Figure S23: ¹³C NMR spectrum of methyl 2,3-diaminopropanoate **u**.

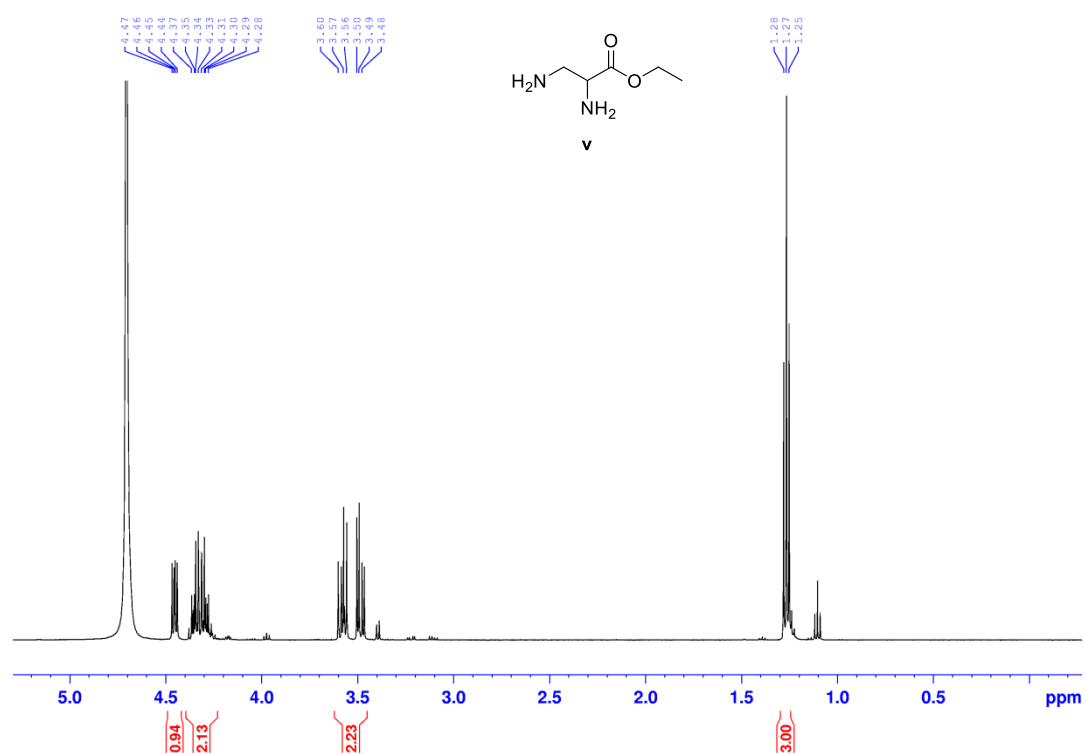


Figure S24: ¹H NMR spectrum of ethyl 2,3-diaminopropanoate **v**.

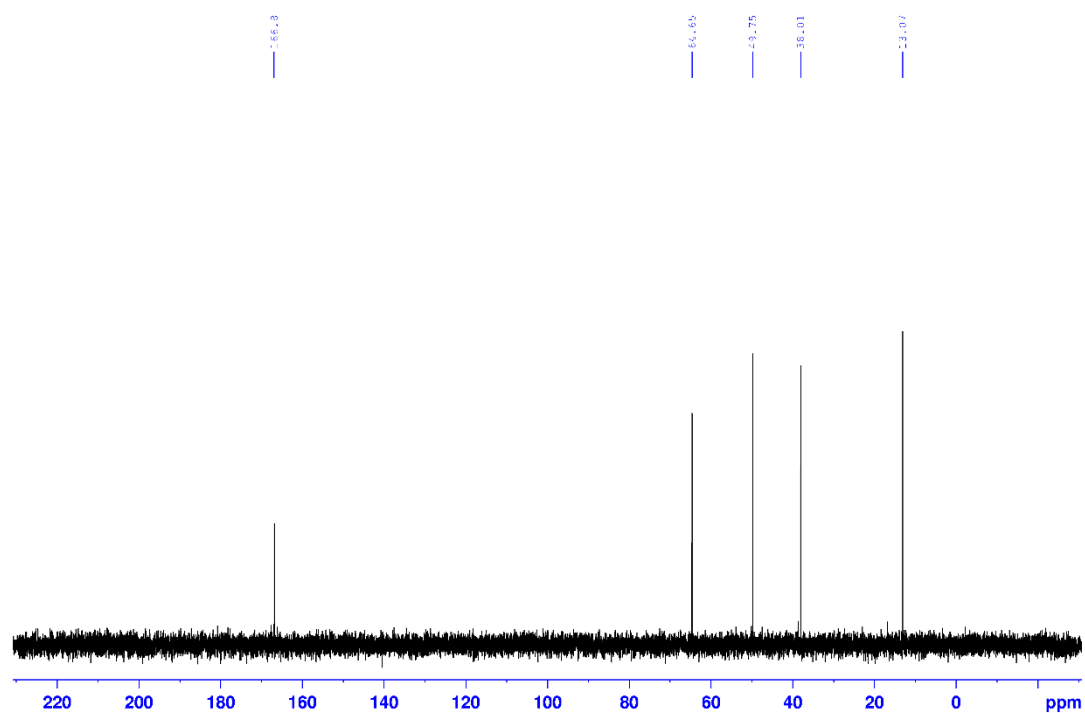


Figure S25: ¹³C NMR spectrum of ethyl 2,3-diaminopropanoate **v**.

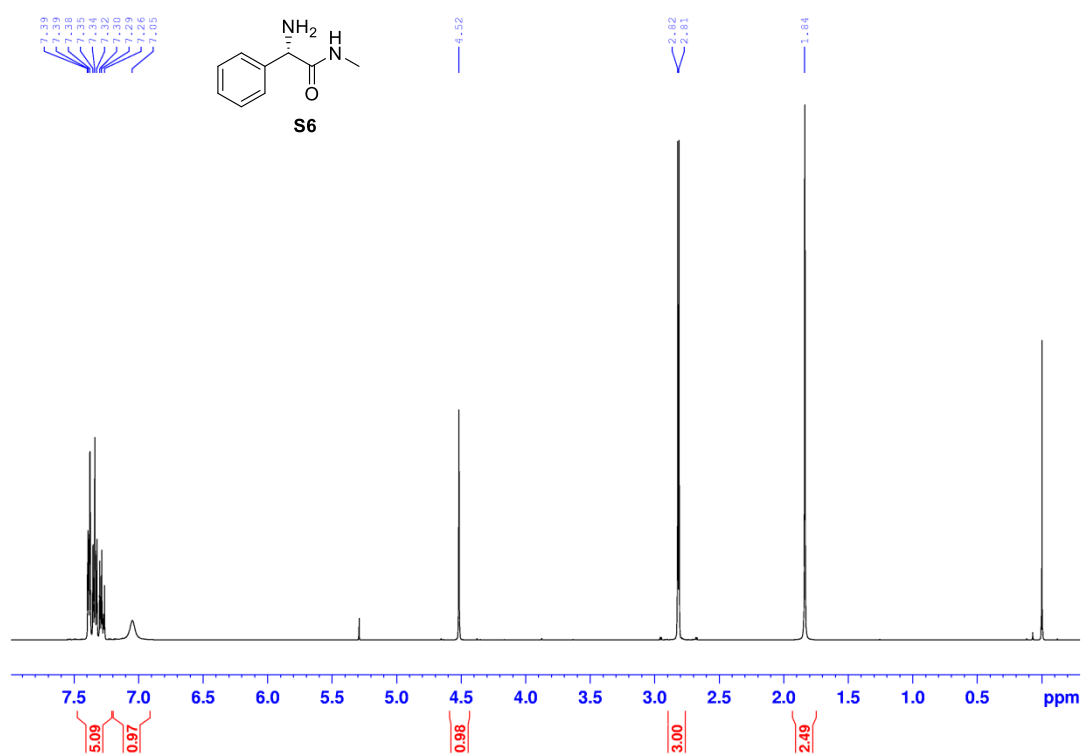


Figure S26: ¹H NMR spectrum of (S)-2-amino-N-methyl-2-phenylacetamide **S6**.

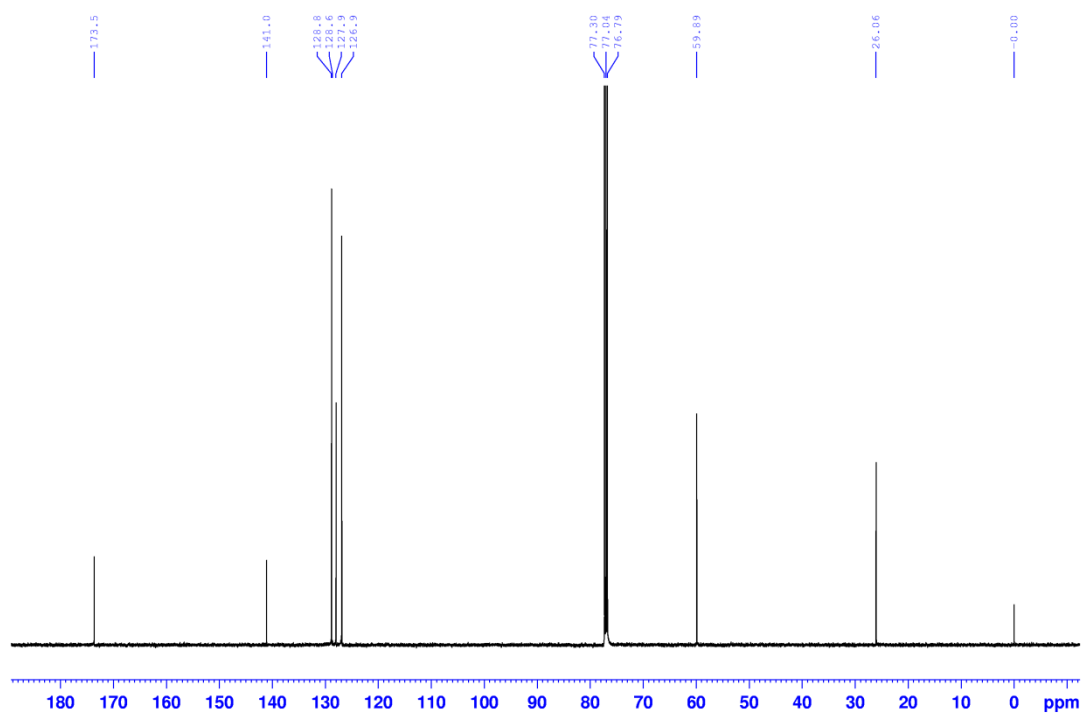


Figure S27: ¹³C NMR spectrum of (S)-2-amino-N-methyl-2-phenylacetamide **S6**.

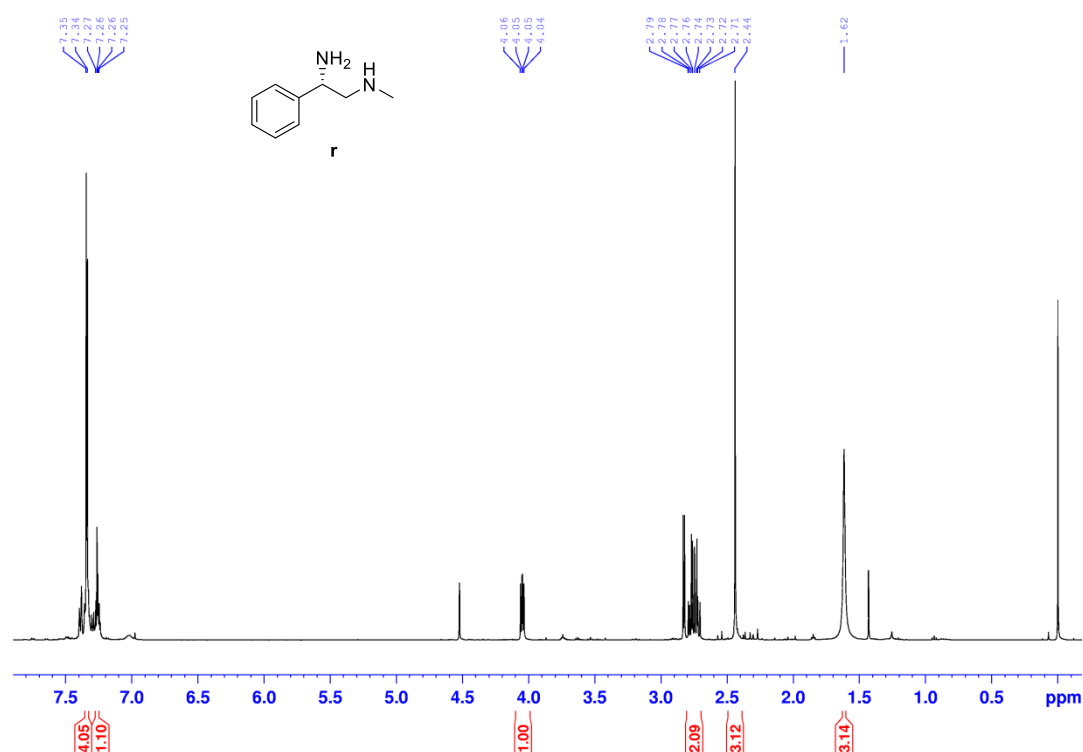


Figure S28: ¹H NMR spectrum of (S)-N¹-methyl-2-phenylethane-1,2-diamine **r** (containing impurities of (S)-2-amino-N-methyl-2-phenylacetamide **S6**).

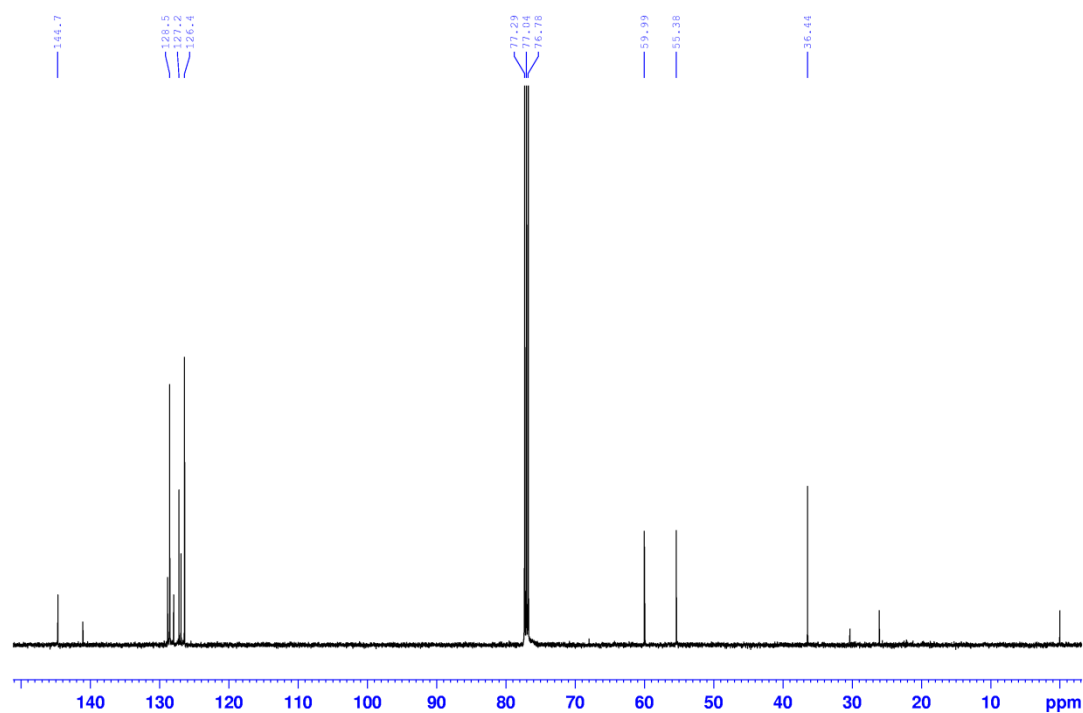


Figure S29: ¹³C NMR spectrum of (S)-N¹-methyl-2-phenylethane-1,2-diamine **r** (containing impurities of (S)-2-amino-N-methyl-2-phenylacetamide **S6**).

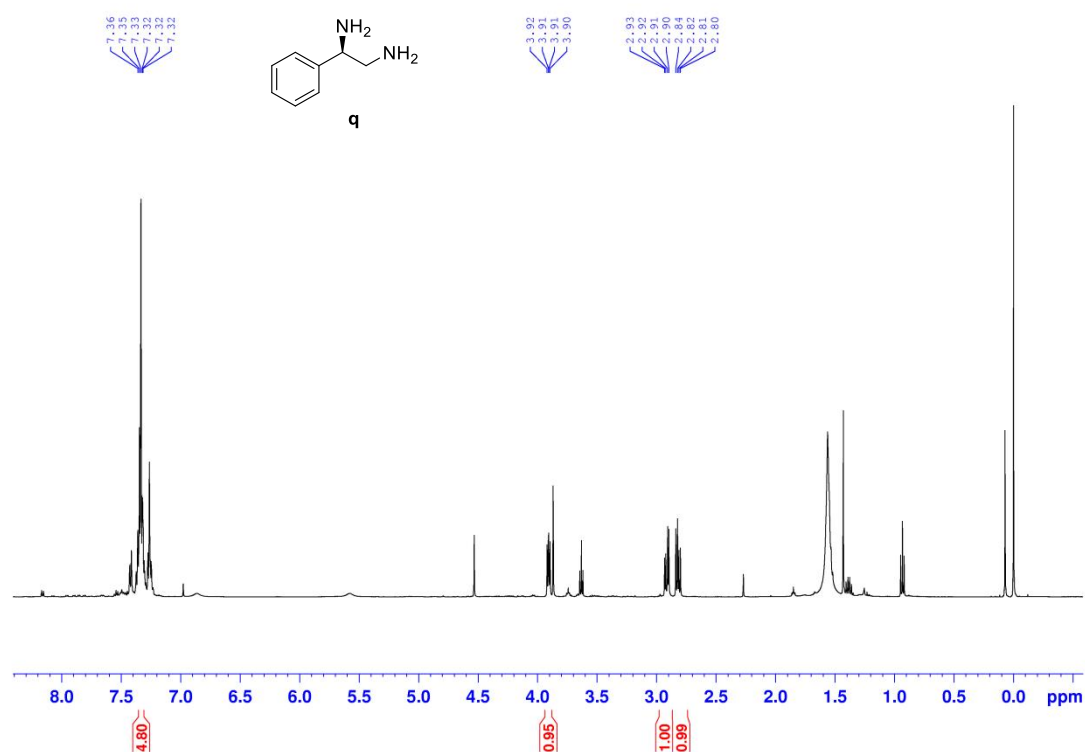


Figure S30: ¹H NMR spectrum of (*R*)-1-phenylethane-1,2-diamine **q** (containing impurities of (*R*)-2-amino-2-phenylacetamide **S5**).

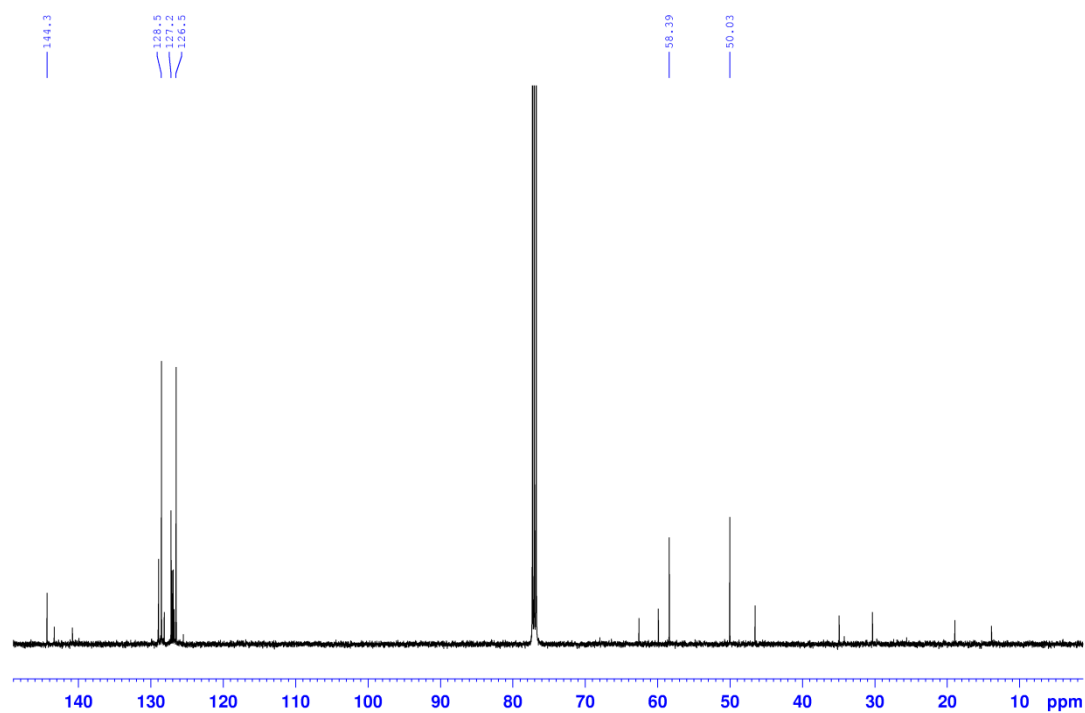


Figure S31: ¹³C NMR spectrum of (*R*)-1-phenylethane-1,2-diamine **q** (containing impurities of (*R*)-2-amino-2-phenylacetamide **S5**).

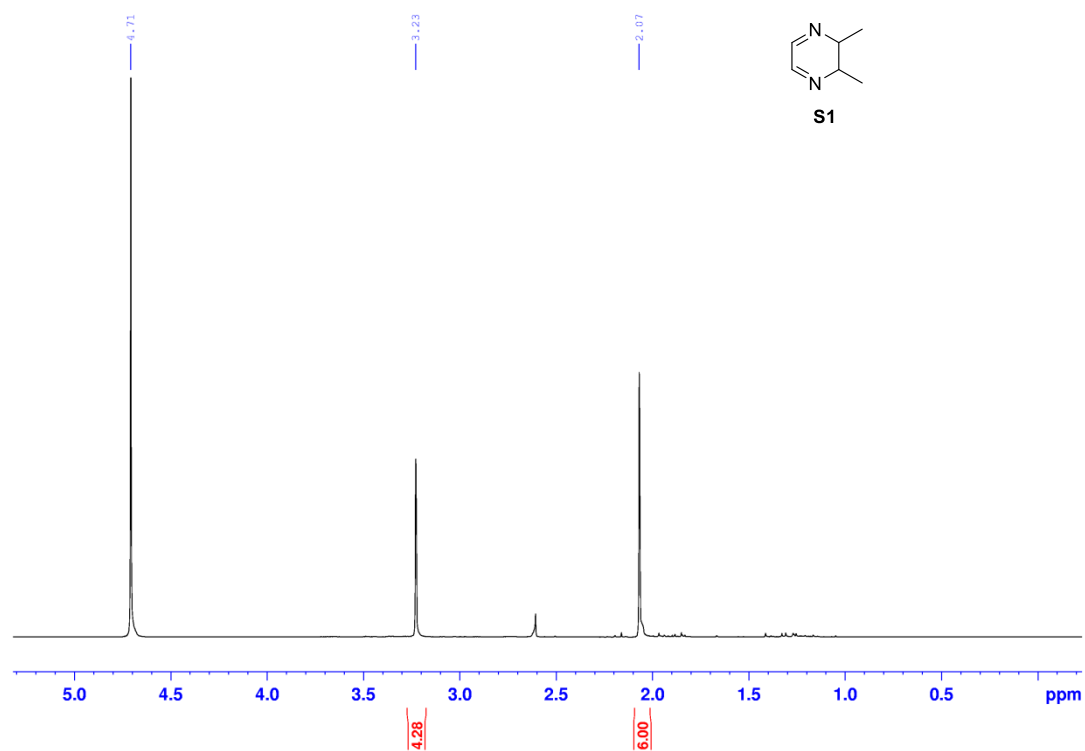


Figure S32: ¹H NMR spectrum of 5,6-dimethyl-2,3-dihydropyrazine **S1**.

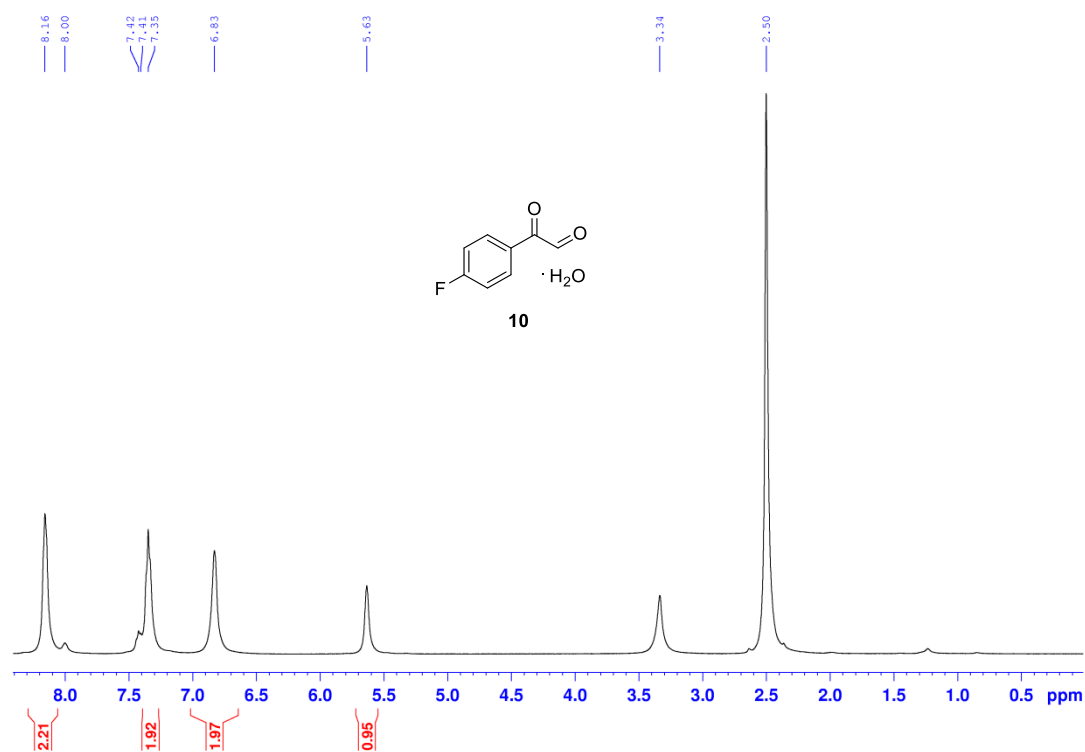


Figure S33: ¹H NMR spectrum of 4-fluorophenylglyoxal hydrate (**10**).

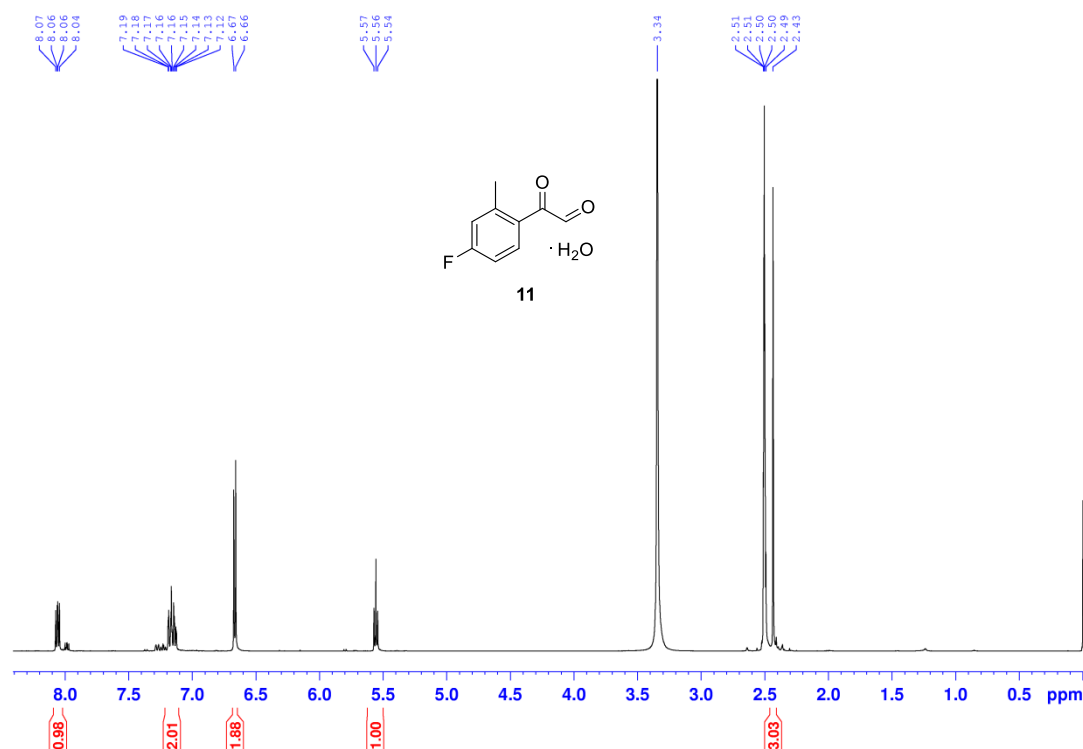


Figure S34: ¹H NMR spectrum of 4-fluoro-2-methylphenylglyoxal hydrate (11).

9 References

- (1) Li, C.; Lei, Y.; Jiang, Q. Enantioseparation of 2-Methylpiperazine by Chiral Stationary Phase with Pre-Column Derivatization. *Huaxue Shiji* **2013**, 35, 68–70.
- (2) Egbertson, M. S.; Homnick, C. F.; Hartman, G. D. A Selective Protection of 2,3-Diaminopropionic Acid. *Synth. Commun.* **1993**, 23, 703–709.
- (3) Lemp, E.; Zanocco, A. L.; Günther, G.; Pizarro, N. Solvent Effect on the Sensitized Photooxygenation of Cyclic and Acyclic α -Diimines. *Tetrahedron* **2006**, 62, 10734–10746.
- (4) Kametani, T.; Umezawa, O. A Novel Dehydrazination Reaction. V. The Formation of Various Amides from Aliphatic and Aromatic Carboxylic Acid Hydrazides in the Presence of Chloral. *Chem. Pharm. Bull. (Tokyo)*. **1966**, 14, 369–375.
- (5) Cortes, S.; Liao, Z. K.; Watson, D.; Kohn, H. Effect of Structural Modification of the Hydantoin Ring on Anticonvulsant Activity. *J. Med. Chem.* **1985**, 28, 601–606.
- (6) Malkov, A. V.; Stewart-Liddon, A. J. P.; McGeoch, G. D.; Ramírez-López, P.; Kočovský, P. Catalyst Development for Organocatalytic Hydrosilylation of Aromatic Ketones and Ketimines. *Org. Biomol. Chem.* **2012**, 10, 4864.
- (7) Sheshenev, A. E.; Boltukhina, E. V.; White, A. J. P.; Hii, K. K. Methylene-Bridged Bis(imidazoline)-Derived 2-Oxopyrimidinium Salts as Catalysts for Asymmetric Michael Reactions. *Angew. Chem. Int. Ed.* **2013**, 52, 6988–6991.
- (8) Belokon', Y. N.; Pritula, L. K.; Tararov, V. I.; Bakhmutov, V. I.; Struchkov, Y. T.; Timofeeva, T. V.; Belikov, V. M. Synthesis of Chiral Atropoisomeric Square-Planar nickel(II) and copper(II) Complexes Formed by Macrocyclic Ligands Containing Pendant Polyether Groups and a Quaternary Ammonium Group. *J. Chem. Soc. Dalt. Trans.* **1990**, 1867.

- (9) Baranac-Stojanović, M.; Marković, R.; Stojanović, M. Catalytic Oxidations of Enolizable Ketones Using 2-Alkylidene-4-Oxothiazolidine Vinyl Bromide. *Tetrahedron* **2011**, 67, 8000–8008.
- (10) Fujita, T.; Makishima, D.; Akiyama, K.; Hayashi, H. New Convulsive Compounds, Brasilamides A and B, from *Penicillium Brasilianum* Batista JV-379. *Bioscie. Biotechnol. Biochem.* **2002**, 66, 1697–1705.
- (11) Harris, R. K.; Spragg, R. A. Nuclear Magnetic Resonance Studies of Six-Membered Rings. Part I. Rings Inversion in Heterocyclic Compounds. *J. Chem. Soc. B Phys. Org.* **1968**, 684.
- (12) Spragg, R. A. Nuclear Magnetic Resonance Studies of Six-Membered Rings. Part II. Chemical Shifts and Coupling Constants in Morpholine and Piperazine Derivatives. *J. Chem. Soc. B Phys. Org.* **1968**, 1128.